The Role of HOP in Emerin-Mediated Nuclear Structure

A thesis submitted in fulfillment of the requirements for the degree of

Doctor of Philosophy in Biochemistry

of

Rhodes University

by

Sarah Naulikha Kituyi

14K0005

Department of Biochemistry and Microbiology

Biomedical Biotechnology Research Unit (BioBRU)

Science Faculty

Rhodes University, Grahamstown, South Africa

April 2017

ABSTRACT

A vital component of the integral nuclear membrane is emerin, a Lamin Emerin and Man1 (LEM) domain protein whose concentration determines the levels of partner proteins that together constitute the structure of the nuclear envelope. Deficiencies in any of these proteins causes the failure of the structure and assembly and disassembly of the nuclear envelope, which disrupts chromosome segregation and nuclear compartmentalization that are both associated with disease. Emerin also localizes in the cytoplasm where it is implicated in the structure of the cytoskeleton via interaction with tubulin and actin and thus its deficiency may equally contribute to the collapse of the cytoskeleton. The Hsp70-Hsp90 organising protein (Hop) functions as a co-chaperone for entry of client proteins into the Hsp90 folding cycle. Hop is upregulated in cancer and regulates a number of cell biology processes via interactions with proteins independently of Hsp90. In a previous study using global whole cell mass spectrometry, emerin was shown to be the most significantly down regulated protein in Hop depleted cell lysates. In this current study, it was postulated that emerin interacts with Hop, and this interaction regulates the stability, and level of emerin in the nucleus which impacts on the structure of the nuclear envelope**.** We used HEK293T cell lines stably expressing shRNA against Hop, emerin and a non-targeting control alongside the over expression of Hop in HEK293 cells to determine the effect of Hop levels on emerin expression and vice versa via Western blotting. The effect of Hop on the localization of emerin was assessed via subcellullar fractionation and confocal microscopy, while the impact on the structure of the nucleus was determined by transmission electron microscopy (TEM). We established that the depletion of Hop using shRNA and the over expression of Hop both result in the proteasomal and lysosomal degradation of emerin. Co-immunoprecipitation assays confirmed that Hop and emerin are in a common complex, which was not dependent on the presence of

Hsp90. Loss of Hop or emerin led to a deformation of nuclear structure and a statistically significant decrease in nuclear size compared to control cells and was associated with an increase in the levels of nuclear protein, lamin A-C. Loss of emerin and Hop resulted in increased long term cell survival, but only after restriction of the nucleus when the cells had migrated across a transwell membrane. Taken together, the results obtained suggest that Hop acts as a scaffold for the stabilization of emerin and that the effects of Hop depletion on the structure of the nucleus and long term survival are mediated via the depletion of emerin.

DECLARATION

I declare that this thesis is my own unaided work and its being submitted for the award of the degree of Doctor of Philosophy at Rhodes University and has not been submitted for the award of any other degree at any other university.

sarah kituyi

.....

Sarah Naulikha Kituyi

April 2017

Grahamstown

TABLE OF CONTENTS

LIST OF FIGURES

LIST OF TABLES

LIST OF ABBREVIATIONS

ADP	Adenosine diphosphate
Aha1	Activator of Hsp90 ATPase homologue 1
ATCC	American type culture collection
ATP	Adenosine triphosphate
ATPase	Adenosine triphosphatase
BAF	Barrier to auto integration factor
Btf	BCL2 associated transcription factor
BSA	Bovine serum albumin
C-terminal	Carboxy terminal
CDK	Cyclin dependent kinase
CK1/2	Casein kinase 1 or 2
CT	Cytoplasmic fraction
CST	Cell signaling technology
DMEM	Dulbecco's modified eagle's medium
DNA	Deoxyribonucleic acid
ECL	Enhanced chemiluminescence
EDTA	Ethylenediaminetetraacetic acid
EEVD	Glutamic acid-glutamic acid-valine-aspartic acid
EGFP	Enhanced green fluorescent protein
EMD	Emerin
EDMD	Emery dreifuss muscular dystrophy
ER	Endoplasmic reticulum

ESCRT iii	Endosomal sorting complex required for transport iii
FG	Phenylalanine glycine repeats
FBS	Foetal bovine serum
GAPDH	Glyceraldehyde 3-phosphate dehydrogenase
GCL	Germ cell less
GFP	Green fluorescent protein
Grp94	Glucose-regulated protein 94
HA	Hemagglutinin
H2/H3	Histone
HER2	Human epidermal growth factor receptor 2
Hop	Hsp70/Hsp90 organising protein
HRP	Horseradish peroxidase
Hsp	Heat shock protein
IF	Immunoflourescence
IP	Immunoprecipitation
INM	Inner nuclear membrane
LB	Luria broth
LAP	Lamina associated protein
LBR	Lamin B receptor
LEM	Lap emerin and MAN 1
MAF	Maturation promoting factor
MAPK	Mitogen activated protein kinase
MEM	Minimum essential medium

mRNA	Messenger RNA
MS	Mass spectrometry
MW	Molecular weight
MKL1	Megakaryoblastic leukaemia 1
N-terminal	Amino terminal
NC	Nuclear fraction
NE	Nuclear envelope
NEBD	Nuclear envelope break down
NLS	Nuclear localization signal
NPC	Nuclear pore complex
NM	Nuclear membrane
Nups	Nucleosporins
ONM	Outer nuclear membrane
PAP	Papanicolauou
PKC	Protein kinase C
p23	Prostaglandin-E synthase
PBS	Phosphate-buffered saline
PDM	Product of the differences from the mean
PMSF	Phenylmethylsulfonyl fluoride
PPI	Protein-protein interaction
PP1/2A	Protein phosphatase 1/2-alpha
PP5	Protein phosphatase 5
PrPc	Cellular prion protein

PSA	Penicillin, streptomycin, amphotericin
PML	Promyelocytic leukemia
RNA	Ribonucleic acid
RB	Retinoblastoma
RNAi	RNA interference
ROI	Region of interest
Rho	Ras homologue
RhoA	Ras homologous A protein
RhoB	Ras homologous B protein
RhoC	Ras homologous C protein
rRNA	Ribosomal RNA
Rr value	Pearson's correlation coefficient
R value	Manders overlap coefficient
SDS	Sodium dodecyl sulphate
SDS-PAGE	SDS-polyacrylamide gel electrophoresis
Ser	Serine
shRNA	Short hairpin RNA
shNT	Short hairpin RNA against a non targeting sequence
shEMD	Short hairpin RNA against emerin
shHop	Short hairpin RNA against Hop
siRNA	Short interfering RNA
STIP1	Stress-induced phosphoprotein 1
TEM	Transmission electron microscopy

TBS	Tris-buffered saline
TBS-T	TBS-Tween®-20
TGF	Transforming growth factor
Thr	Threonine
TPR	Tetratricopeptide repeat
TRAP-1	Tumour necrosis factor receptor-associated protein-1
WB	Western blot

LIST OF SYMBOLS

α	Alpha
β	Beta
°C	Degree celsius
%	Percent or g/100 mL
U	Units
V	Volts
A	Ampere
rpm	Revolutions per minute
M	Molar
mM	Millimolar
µM	Micromolar
nM	Nanomolar
g	Grams
mg	Milligrams
µg	Micrograms
ng	Nanograms
L	Litres
ml	Millilitres
µl	Microlitres
cm	Centimetres
µm	Micrometres
nm	Nanometres

kDa	Kilodaltons
mol	Mole
v/v	Volume per volume
w/v	Weight per volume

ACKNOWLEDGEMENTS

I wish to extend my sincere gratitude to my supervisor Prof Adrienne Edkins for support, supervision and critical review of the dissertation. This study was conducted in her laboratory that offered immense financial, technical and intellectual support required to execute this project. Prof Edkins's mentorship and encouragement was invaluable and enabled me to balance a highly demanding study schedule. Thank you very much for believing in me.

I am heavily indebted to the National Research Foundation of South Africa for funding my research and providing me with an opportunity to present my research findings at an international conference in Seeon- Bayern Germany. Long live NRF.

I also wish to offer my sincere gratitude and appreciation to my beloved family the Naulikhas especially my dad Gabriel Paul Naulikha and my siblings Sammy, Theophilus, Augustine and Teresa for all their support during this work. This work is a special dedication to my mother Beatrice whose love for me I can never replace, through her life my character was shaped and her dream to see me become an academic is hereby fulfilled. I hope I have made you proud of me mum. A special thank you to all my friends especially members of BioBRU for supporting me through this course. Natasha Boel and Ianthe Wingate took time to teach me how to carry out SDS-PAGE gels and perform immunoblotting, Dr Jason Sterrenberg taught me how to perform endo-toxin free plasmid preparations and instructed me on the development of a lentiviral based shRNA stable cell line. May God bless them.

In addition, I would wish to thank my spiritual mentors Rev. Fr. Lance Nadeau of Christ the Teacher Kenyatta University Catholic Church (Kenya) and Rev. Fr. Peter Wilson of St Patrick's

Catholic church Grahamstown (South Africa) for their guidance and spiritual nourishment. Above all, I highly acknowledge that all things were made possible through Jesus Christ, my Lord and giver of all good and perfect gifts. Glory be to his name.

OUTPUTS

Conference outputs (oral presentation):

Kituyi, S.N and Edkins, A.L. The Role of Hop in Emerin-Mediated Structure of the Nuclear Envelope, **The 25TH South African Society of Biochemistry Congress (SASBMB 2016) East London, South Africa (10-14 July 2016)**

Kituyi, S.N and Edkins, A.L. The Role of Hop in the Nuclear Envelope. **The 8TH International Conference on the Hsp90 Chaperone Machine, Seeon, Bayern, Germany (2-6 Nov 2016)**

Chapter 1: Literature review

The nuclear envelope

In higher organisms, the contents of the nucleus are normally enclosed by a nuclear envelope which separates the nuclear genome from the cytoplasm (Hatch and Hetzer, 2014). When cells undergo division via mitosis, the nuclear envelope (NE) dissociates at prometaphase to allow for chromosome segregation and later reassembles during late telophase resulting in the formation of two distinct daughter cells (Webster *et al.*, 2009). The disassembly and assembly of the NE is vital to the process of cell division and is highly determined by the composition of the nuclear envelope (Hirano *et al.*, 2005), which consists of an outer and inner membrane alongside an embedded nuclear pore complex (NPC) (Figure 1).

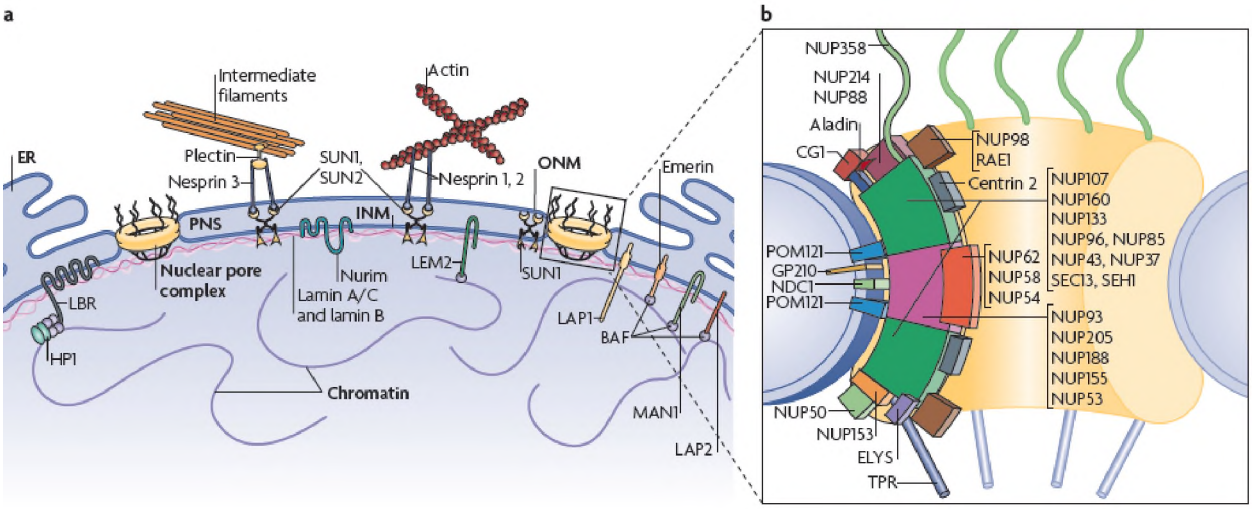

Figure 1: Structure of the nuclear envelope illustrating the two membranes
(a) The outer (ONM) and inner (INM) nuclear membranes alongside the nuclear lamina beneath the nucleoplasmic space are depicted. The Lap2, emerin, and Man1 (LEM) domain proteins tethering the inner nuclear membrane to the nuclear lamina and chromatin are illustrated. (b) The structure of the nuclear pore complex and the cytoplasmic filaments are illustrated (Guttinger *et al.*, 2009).

The outer (ONM) and inner (INM) nuclear membranes are composed of distinct groups of proteins that interact with each other to enhance the structure of the NE (Hatch and Hetzer, 2014). Unlike the inner nuclear membrane (INM), the outer nuclear membrane (ONM) is continuous with the endoplasmic reticulum (ER) and has been shown to contain ribosomes (Burke *et al.*, 2005; Katta *et al.*, 2014). Among the proteins that constitute the outer nuclear membrane are members that directly interact with inner nuclear membrane proteins and have been shown to exhibit a Klarsicht, ANC-1, Syne Homology (KASH) domain (Katta *et al.*, 2014). These proteins include spectrin repeat family members such as nesprin 1 and nesprin 2 which have been shown to be involved in shaping nuclear structure dynamics via linking the NE to the cytoskeleton (Hetzer, 2010). Although the outer and inner nuclear membranes have distinct protein compositions and are normally separated by a periplasmic space (Hetzer, 2010), they have been shown to exhibit similarities in protein composition on merging at the nuclear pore complex (Fichtman *et al.*, 2010; Katta *et al.*, 2014).

The nuclear pore complex traverses the outer and the inner nuclear membrane and is structurally composed of proteins called nucleoporins (Nups) that are thought to be enriched with phenylalanine-glycine (FG) repeats forming channels that allow for the selective passage of molecules in and out of the nucleus (Figure 1) (Fichtman *et al.*, 2010; Hetzer, 2010; Katta *et al.*, 2014; Hagen *et al.*, 2015). The Nups are composed of various polypeptides, such as Nup107-160 and Nup 205, which form a scaffold structure that supports the pore membrane, and peripheral Nups that contain FG repeats which dictate the permeability of the NPC (Hetzer, 2010) to a size that is not more than 60 kDa (Katta *et al.*, 2014). Molecules that exceed the size limit of the NPC, such as ribonucleoproteins, require unfolding before passing through the NPC (Hatch and Hetzer, 2014). However, studies indicate that various organisms have developed alternative

processes such as NE budding via vesicle formation to allow for the trafficking of large size molecules in and out of the nucleus (Hatch and Hetzer, 2014). It is thought that the NPC exhibits a double phase of formation where the number of NPCs have been shown to increase prior to mitosis and later during NE assembly after mitosis (Fichtman *et al.*, 2010).

The inner nuclear membrane (INM) is connected to the nuclear lamina which is a dense network of filamentous fibers that tethers the NPC and subsequently connects to the chromatin (Webster *et al.*, 2009). The integral INM proteins are normally synthesized in a similar manner to the ONM proteins in the rough endoplasmic reticulum before reaching their destination at the INM via lateral diffusion (Worman, 2005). Retention of their position at the inner nuclear membrane is enhanced by oligomerization among transmembrane domains and studies indicate that the association of INM proteins to the nuclear lamina and chromatin also serves to enhance their retention (Worman, 2005; Katta *et al.*, 2014). Among the proteins that constitute the INM are the lamin B receptor (LBR) protein (Haraguchi *et al.*, 2000; Worman, 2005) and what are commonly referred to as the LEM (Lap2, emerin and MAN1) domain containing proteins such as emerin (EMD), LEM domain containing 3 (MAN1) (Berk *et al.*, 2013) and the lamina associated polypeptide2 (Lap2) (Haraguchi *et al.*, 2000). The LEM domain refers to a 40 amino acid residue domain within the N-terminal of these proteins that serves to connect these proteins to the chromatin (Berk *et al.*, 2013).

The nuclear lamina consists of filamentous lamin proteins (lamin A and B) characterized by a C-terminal domain that promotes their interaction with the inner nuclear membrane (Webster *et al.*, 2009). Mammals have been shown to exhibit two isoforms of lamin A (Lamin A and C) which originate from the *LMNA* gene following alternative splicing (Hutchison *et al.*, 2001). However,

unlike lamin A and B, lamin C is deficient in the C-terminal domain (Webster *et al.*, 2009). The nuclear lamina is connected to lamina-associated proteins such as the barrier to auto integration factor (BAF), a DNA bridging protein and LEM domain proteins such as emerin (Lee *et al.*, 2001). Lamins can thus be found in both the nucleoplasm and the INM (Webster *et al.*, 2009). The structure and function of the nuclear lamina is highly determined by the interaction between the lamin proteins and the lamina-associated proteins (Webster *et al.*, 2009) and the concentration of each of these proteins has an effect on the concentration of the other (Berk *et al.*, 2013) and the overall structure of the nuclear lamina which determines the architecture of the NE (Liu, 2003). In *Caenorhabditis elegans*, a reduction in the levels of either of the proteins has been shown to result in an abnormal nuclear structure and poor chromosome segregation (Liu, 2003; Berk *et al.*, 2013), but the expression levels may vary from one type of cell to the other as determined by the type of chromatin organization and the cell's demand for mechanical strength (Hatch and Hetzer, 2014).

Nuclear envelope disassembly

During NE disassembly, the nuclear envelope breaks down and so does the nuclear lamina, the NPC and the INM, resulting in the exportation of nucleoporins and INM proteins to the endoplasmic reticulum (ER) membrane (Marshall and Wilson, 1997) and the cytoplasm (Terasaki *et al.*, 2001). The mechanisms that trigger the dissociation of the nuclear lamina, the NPC and the INM proteins during nuclear disassembly have been associated to an increase in phosphorylation events at the onset of mitosis (Marshall and Wilson, 1997; Zink *et al.*, 2004; Hirano *et al.*, 2005; Guttinger *et al.*, 2009). Activation of various kinases in mitosis triggers the depolymerization of the components of the NE, and inhibition of phosphorylation via inactivation of kinases or the absence of phosphorylation sites on mutated nuclear membrane

proteins (Guttinger *et al.*, 2009) has been shown to delay the disassembly of the NE and subsequently arrest mitosis (Guttinger *et al.*, 2009). This possibly explains the increase in the activation and accumulation of kinases in the nucleus at the onset of mitosis (Pfaller and Newport, 1995; Terasaki *et al.*, 2001; Hirano *et al.*, 2005). In particular, the process of nuclear envelope disassembly is initiated by the rapid accumulation of the maturation-promoting factor (MPF) in the nucleus (Terasaki *et al.*, 2001). The MPF is thought to be a complex of various kinases including the cyclin dependent kinases (CDK1) (Guttinger *et al.*, 2009) and cyclin B, and has been shown to trigger the depolymerization of various nuclear proteins such as the lamins, LBR and Lap2 via phosphorylation (Terasaki *et al.*, 2001; Guttinger *et al.*, 2009). Other kinases such as protein kinase C (PKC) have also been shown to accumulate in the nucleus at the onset of mitosis to trigger the phosphorylation of lamins (Guttinger *et al.*, 2009) leading to their dissociation from the chromatin.

Before the NE breaks down in prometaphase, the structure of the NPC is destabilized following phosphorylation of nucleoporins resulting into the loss of the ability of the NPC to restrict exit of molecules (Terasaki *et al.*, 2001; Guttinger *et al.*, 2009), which marks the first phase of nuclear envelope breakdown (NEBD) (Terasaki *et al.*, 2001). This is then followed by a second phase characterized by the loss of the membrane barrier following the dissociation of the nuclear lamina and the INM proteins from the chromatin, resulting in their diffusion to the outer membrane and subsequently onto the ER membrane and the cytoplasm (Marshall and Wilson, 1997; Terasaki *et al.*, 2001). The entire process is essential for cell division because it allows for chromosome segregation (Guttinger *et al.*, 2009; Hatch and Hetzer, 2014).

Nuclear envelope assembly

The assembly of the nuclear membrane in mitosis ensues upon the binding of vesicles derived from the nucleus onto the chromatin surface coupled with subsequent fusion and flattening (Lu *et al.*, 2011). The latter process results in the formation of the outer and inner nuclear membranes characterized by distinct membrane proteins (Marshall and Wilson, 1997). The recruitment of NPC constituents triggers the closure of the NE which is then followed by the importation of lamin and lamina-associated proteins to constitute the nuclear lamina (Marshall and Wilson, 1997; Guttinger *et al.*, 2009). The return of proteins into the nucleus requires their desphosphorylation at various sites in a cell cycle dependent manner (Hirano *et al.*, 2005) which occurs via the inhibition of various associated kinases (Webster *et al.*, 2009), such as protein kinase C (PKC) and cyclin dependent kinase 1 (CDK1) (Guttinger *et al.*, 2009) by phosphatases. These proteins are normally dissociated from the chromatin and the nuclear lamina via phosphorylation which triggers their exportation and dispersal onto the ER membrane (Marshall and Wilson, 1997; Hirano *et al.*, 2005; Webster *et al.*, 2009) and the cytoplasm (Guo *et al.*, 2014). Dephosphorylation serves to dissociate the proteins from the ER membrane and enhance their return into the INM for the reconstitution of the nuclear lamina allowing for growth of the nucleus (Marshall and Wilson, 1997; Guttinger *et al.*, 2009; Hatch and Hetzer, 2014). This is characterized by proper localization of deoxyribonucleic acids (DNA) replication centers, decondensation of chromosomes with a proper configuration of the nuclear matrix and lamina, which is essential for correct DNA replication and subsequent gene transcription (Marshall and Wilson, 1997). The latter demonstrates the importance of the nuclear lamina and lamin-associated proteins in the assembly of the NE and it is supported by the fact that lamin and INM protein deprived cells are characterized by the presence of a fragile NE (Marshall and Wilson,

1997; Guttinger *et al.*, 2009; Hatch and Hetzer, 2014) and mitotic arrest (Hatch and Hetzer, 2014).

Emerin

Unlike the other proteins implicated in the nuclear lamina and the INM, emerin has been shown to bind directly to both the lamin proteins and BAF, and subsequently influences the concentration of both proteins (Holaska *et al.*, 2004; Hirano *et al.*, 2005). The binding of emerin to BAF tethers the NE to the chromatin providing a mechanism for membrane migration (Lu *et al.*, 2011), which is vital for cell processes. In humans, the LEM domain protein emerin is a 254 serine-rich protein with a mass as revealed by SDS-PAGE of 34 kDa (Haraguchi *et al.*, 2001; Lee *et al.*, 2001; Wolff *et al.*, 2001; Hirano *et al.*, 2005). It is a product of the *EMD* gene on the X chromosome, in which mutations have been linked to the Emery-Dreifuss muscular dystrophy (EDMD) condition (Hirano *et al.*, 2005). Emerin contains an N-terminal domain made up of 50 amino acid residues, a hydrophobic region containing an estimated 100 amino acid residues which also hosts the nuclear localization signal (NLS) (Hirano *et al.*, 2005), and the C terminal domain (Berk *et al.*, 2013). The LEM domain located within the N-terminal mediates binding to the DNA bridging protein BAF, while binding to lamin A-C occurs via an active domain in the central region which doubles as a NM retention signal (Lee *et al.*, 2001). It is believed that emerin does not interact with lamin B (Hutchison *et al.*, 2001). Previous studies indicated that emerin mainly localizes within the INM (Cartegni *et al.*, 1997) following synthesis in the cytoplasm and subsequent packaging into the endoplasmic reticulum membrane (Berk *et al.*, 2013). However, the entry of emerin into the INM via the NPC does not rely on a nuclear localization signal (Tsuchiya *et al.*, 1999) because of its small size and hence it just slides through the NPC (Berk *et al.*, 2013).

The role of the hydrophobic domains is vital for the localization of emerin in the INM (Cartegni *et al.*, 1997). However, this localization is not enough to enhance its stability and may require an interaction with BAF (Berk *et al.*, 2013) which has been shown to actively recruit emerin onto the core region of the NE lacking a NPC mechanism (Haraguchi *et al.*, 2001; Berk *et al.*, 2013). It is assumed that emerin is first recruited into the core region (Lee *et al.*, 2001) before the assembly of an efficient nuclear import machinery in the NPC, but localization to target regions in the INM is evident on the assembly of the NPC machinery (Haraguchi *et al.*, 2000). The implicated localization in the INM depends on the presence of lamin proteins (Vaughan *et al.*, 2001; Melcon *et al.*, 2006) and it is likely that the retention of emerin in the INM is enhanced via interaction with lamin A (Melcon *et al.*, 2006). It is therefore thought that emerin may possibly exhibit a double phase of distribution which shifts from the core region at the proximal end of the chromosomes guided by recruitment by BAF (Lee *et al.*, 2001; Hirano *et al.*, 2005), to a uniform distribution in the entire chromosome (Lu *et al.*, 2011) guided by lamins (Vaughan *et al.*, 2001; Melcon *et al.*, 2006; Guo *et al.*, 2014). However, in disease conditions characterized by deficiencies in emerin, the mutated region has been shown to occur outside the BAF and lamin binding regions, indicating that the recruitment and localization of emerin in the nuclear envelope is complicated and may require an unknown third partner within the inner nuclear membrane (Lee *et al.*, 2001; Berk *et al.*, 2013).

It is now evident that other than the INM, emerin localizes within the cell membrane especially in heart and skeletal muscles (Cartegni *et al.*, 1997) as part of the focal adhesion system and also promotes the differentiation of myoblasts (Frock *et al.*, 2006). The localization of emerin in the cell membrane (Vaughan *et al.*, 2001; Berk *et al.*, 2013) points to its novel role in attaching the

membrane to the cytoskeleton (Cartegni *et al.*, 1997; Berk *et al.*, 2013). In lamin A-C mutant cells, characterized by mislocalization of emerin, an over-expression of emerin rescues the nuclear translocation of megakaryoblastic leukaemia 1 (MKL1) promoting actin polymerization in the cytoskeleton (Ho *et al.*, 2013). MKL1 is a transcription factor of vital importance in cardiac muscles which coordinates actin polymerization via an MKL-serum response factor (SRF) signaling. In lamin mutant cells, over-expression of emerin is required to promote the polymerization (Holaska *et al.*, 2004) of globular actin normally attached to MKL1 (Ho *et al.*, 2013) which increases its mobility in the structure of the cytoskeleton (Ho *et al.*, 2013). The implicated emerin is thought to have mislocalized from the INM as a result of the mutant lamin phenotype, which further indicates the dependency of INM proteins on each other (Guo *et al.*, 2014) for their retention and localization (Hirano *et al.*, 2005; Holaska, 2008). Besides binding actin, emerin has been shown to bind β-tubulin and could possibly be involved in regulating the position of the centrosome (Berk *et al.*, 2013). Table 1 gives a summary of the various proteins that have been shown to interact with emerin.

Table 1: Binding partners of emerin

	Partner	Affinity	Reference
High Affinity	Nesprin-1α	4 nM	Mislow et al., 2002
	GCL	30 nM	Holaska et al., 2002
	Lamin A	40 nM	Holaska et al., 2002
	Btf	100 nM	Haraguchi et al., 2004
	Lmo7	125 nM	Holaska et al., 2006
	BAF	200 nM	Holaska et al., 2002
	F-actin	300-500 nM	Holaska et al., 2004
Low Aff.	HDAC3	7.3 uM	Demmerle et al., 2012
Not Meas.	YT521b	?	Wilkinson et al., 2003
	MAN1	?	Mansharamani & Wilson, 2005
	Nesprin-2	?	Zhang et al., 2005
	Nuclear myosin IC	?	Holaska & Wilson, 2005
	β-catenin	?	Markiewicz et al., 2006
	β-tubulin	?	Salpingidou et al., 2007
	SUN1	?	Haque et al., 2009
	SUN2	?	Haque et al., 2009

Summary of known binding partners of emerin whose binding affinities have been established (Berk *et al.*, 2013).

The interaction between emerin and other components of the NE and the chromatin is directed by a cell cycle dependent phosphorylation mechanism (Holaska *et al.*, 2004; Hirano *et al.*, 2005; Hatch and Hetzer, 2014). For instance, the dissociation of emerin from the DNA bridging protein BAF (Holaska, 2008) has been shown to occur following phosphorylation of emerin at the Ser^{175} site (Hirano *et al.*, 2005). Similarly, phosphorylation of emerin reduces its binding to actin and lamin A-C (Hatch and Hetzer, 2014). It is now confirmed that phosphorylation of emerin occurs in four serine residue regions and one threonine residue that are found within the region of binding with other proteins (Hirano *et al.*, 2005). The phosphorylation is enhanced by the activation of various kinases such as cyclic dependent kinases (Pfaller and Newport, 1995;

Hirano *et al.*, 2005; Xue and Funabiki, 2014), protein kinase A and C (PKA& PKC) (Hatch and Hetzer, 2014) and the mitogen activated protein kinases (MAPK) pathway (Berk *et al.*, 2013) which are activated at the onset of mitosis (Terasaki *et al.*, 2001) and at interphase (Berk *et al.*, 2013).

The role of emerin in gene regulation

Besides the structural hypothesis in causing disease, mutations in the structure of emerin have been shown to impair gene regulation processes (Lammerding *et al.*, 2005) which are feared to result in improper muscle regeneration (Koch and Holaska, 2014). This is likely to occur because emerin has been shown to be associated with various transcription factors such as, the germ cell less (GCL) and the apoptosis inducer BCL associated transcription factor (Btf) (Bengtsson and Wilson, 2004; Berk *et al.*, 2013). Emerin interacts directly and sequesters Btf in muscle cells and it is believed that deficiency in emerin in muscle cells results in apoptosis (Bengtsson and Wilson, 2004). In addition, emerin has been reported to be required for the activation of genes responsible for responding to mechanical pressure such as MyoD via its interaction with the Lim domain only-7 (LMO7), a transcription factor that is responsible for regulating myoblast differentiation (Dedeic *et al.*, 2011). Previously, Melcon, (2006) reported that deficiencies in emerin result in the deregulation of retinoblastoma (RB), another gene responsible for controlling muscle regeneration.

Emerin has also been shown to be responsible for regulating the Wnt signaling pathway by binding to transcription factors such as β-catenin, and studies in emerin deficient fibroblasts reveal an abnormal elevation of β-catenin within the nucleus (Berk *et al.*, 2013). Berk *et al.* (2013) further indicates that deficiencies in emerin in mouse cardiac muscles result in the

deregulation of genes controlled by the mitogen-activated protein kinases (MAPK) and the transforming growth factor beta (TGF-β) pathways. These pathways are important for the regulation of the differentiation and regeneration of muscle tissues and have been associated with the observed muscle degeneration in EDMD (Koch and Holaska, 2014).

The role of emerin in disease

The X-linked form of EDMD is caused by mutations in the structure of emerin, while the autosomal dominant form results from mutations in lamins (Lammerding *et al.*, 2005; Koch and Holaska, 2014). EDMD is characterized by the wasting of skeletal and cardiac muscles that occurs during early life and progresses into a severe condition that results in cardiac arrest and sudden death (Astejada *et al.*, 2007). Patients are normally fitted with pacemakers following early detection to avoid the risk of sudden death (Koch and Holaska, 2014). Tissues obtained from EDMD patients indicate various forms of myopathy such as variations in the size of muscle fibres, deformation of the nuclear structure as revealed by transmission electron microscopy (TEM), and necrosis (Astejada *et al.*, 2007). Because of the variations in the symptoms, early diagnosis is based on the immunodetection of emerin via immunohistochemistry staining and gene sequencing (Koch and Holaska, 2014).

The occurrence of the X-linked form of EDMD has been associated with mutations at positions 54, 95 and 183 in emerin (Figure 2). It is thought that most alterations in these positions are nonsense mutations which yield a soluble form of emerin that is incapable of effectively localizing at the nuclear periphery (Lammerding *et al.*, 2005). The autosomal dominant form of EDMD is thought to result from missense mutations in the *LMNA* gene (Fairley, 2002) that not only result in the misfolding and the mislocalization of type A lamins, but also result in the

mislocalization of other lamin-associated proteins including emerin (Lammerding *et al.*, 2005). Most cells exhibiting mutations in the structure of lamins would thus depict a phenotype similar to that observed in emerin deficient cells, and this explains the expected disease severity in lamin deficient patient samples (Lammerding *et al.*, 2005; Muntoni *et al.*, 2006; Astejada *et al.*, 2007).

It remains surprising that mutations in such proteins that are ubiquitously expressed would result in such a tissue specific disease condition (Hutchison *et al.*, 2001; Fairley *et al.*, 2002). However with regard to their role in regulating the nuclear structure, it is hypothesized that mutations in both emerin and lamin A-C amount to the disruption of the nuclear structure which becomes impaired in response to mechanical stress (Hutchison *et al.*, 2001; Lammerding *et al.*, 2005; Holaska and Wilson, 2007). This explains the presentation of muscle and cardiac defects observed in EDMD. In addition, the two proteins have been shown to be involved in gene regulation where they bind to various transcription regulators including regulators of differentiation and regeneration of muscle related genes (Koch and Holaska, 2014). Cells lacking lamins and emerin are thus characterized by abnormalities in the nuclear shape coupled with impaired response to mechanical stress and inefficient gene regulation (Hutchison *et al.*, 2001; Lammerding *et al.*, 2005).

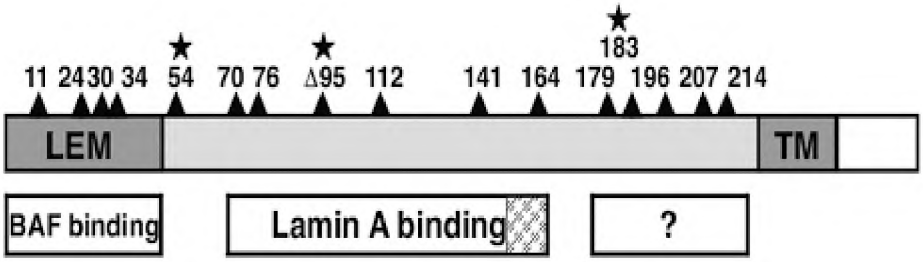

Figure 2: Schematic illustration of the location of mutations in emerin in X-linked EDMD
The amino acid positions marked with triangles and stars indicate the positions in the structure of the EMD protein that are mutated in the event of X-linked EDMD. Next to the lamin A binding region is an actin binding domain highlighted in grey. The region marked with a question mark

indicates a location next to the transmembrane (TM) domain whose binding partners are yet to be identified (Lee *et al*., 2001).

Emerin deficiencies and the nuclear envelope in cancers

Cancer cells are characterized by a deformed nuclear morphology compared to normal cells, which occurs as a result of a poorly reconstituted nuclear envelope (Zink *et al*., 2004). The architecture of the NE is highly determined by the interaction between the nuclear lamina and the INM proteins (Liu, 2003) which guide the assembly and disassembly of the NE during mitosis (Guttinger *et al*., 2009). Figure 3 illustrates the common differences in the morphology of the NE between normal and cancer cells.

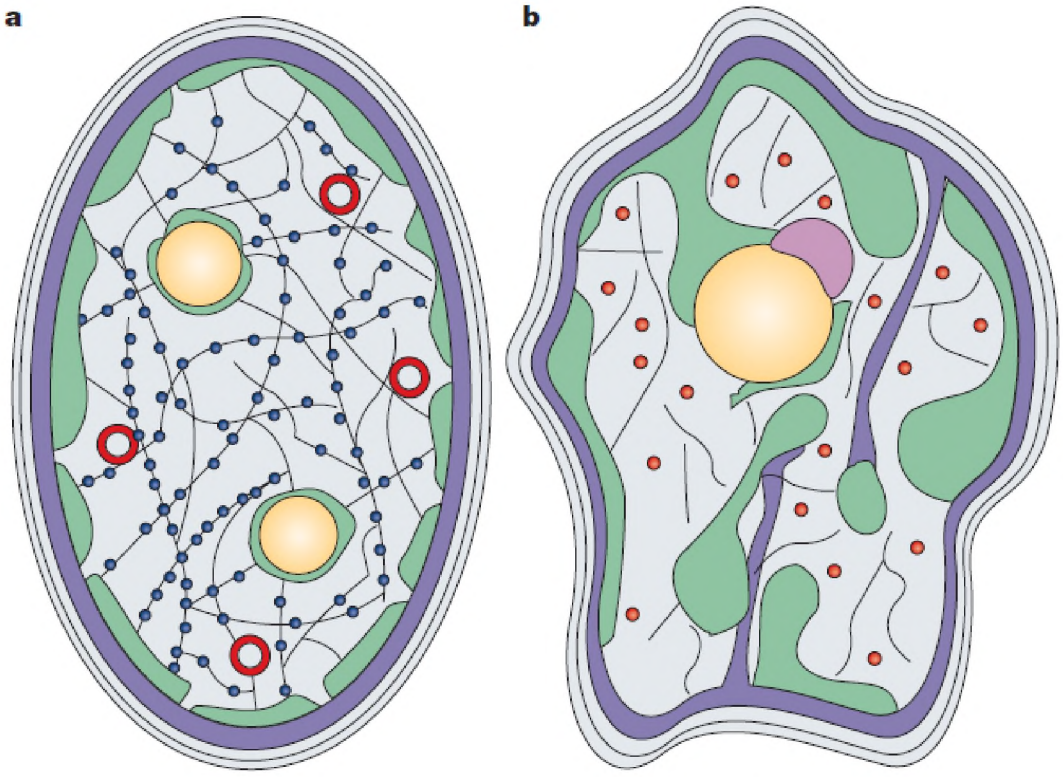

Figure 3: Differences in nuclear structure between a normal and a cancer cell
(a) Depicts the structure of a normal nucleus characterized by a distinct nuclear lamina depicted in purple and a close to round/oval shape. The lamina is correctly tethered to the chromatin constituting the heterochromatin labeled green which allows for ideal metabolism and

localization of molecules such as p53. (b) A number of changes common to certain types of tumour cells are depicted, for instance, the nuclei is enlarged and irregular in shape while some nuclear molecules such as the promyelocytic leukaemia (PML) body indicated in red are mislocalized (Zink *et al.*, 2004).

The structure and morphology of the nuclear membrane is an ideal prognostic indicator in the assessment of various types of cancer, for example, the commonly used Papanicolaou test (also referred to as the PAP smear test) in cervical cancer is based on the morphology of the nucleus (Zink *et al.*, 2004; Capo-chichi *et al.*, 2011). In most mammals, deformation of the nuclear morphology occurs as a result of mutations or suppression of structural proteins in the nuclear envelope such as emerin (Capo-chichi *et al.*, 2011). A common characteristic of certain cancers especially, ovarian and cervical cancers in females is aneuploidy, a condition characterized by an abnormal number of chromosomes in a cell (Zink *et al.*, 2004; Guttinger *et al.*, 2009; Capo-chichi *et al.*, 2011; Xue and Funabiki, 2014). This condition occurs as a result of the arrest of mitosis and the subsequent abrogation of chromosome segregation (Guttinger *et al.*, 2009; Capo-chichi *et al.*, 2011; Xue and Funabiki, 2014). Studies indicate that an increase in mitotic arrest following suppression of emerin increases the occurrence of aneuploidy which has been shown to cause activities such as mutations in the tumour suppressor protein p53 which is common in ovarian cancer at high grade (Capo-chichi *et al.*, 2011).

Besides causing aneuploidy, suppression of nuclear envelope proteins such as lamins and emerin (Rowat *et al.*, 2006) is associated with nuclear lamina fragility (Rowat *et al.*, 2006) and disruption of the NE which has been implicated in the loss of compartmentalization and the subsequent mislocalization of nuclear components (Hatch and Hetzer, 2014). For instance, the collapse of the NE following disruption in the lamina and the INM proteins causes the mislocalization of proteins such as promyelocytic leukemia (PML) (Zink *et al.*, 2004) which is

involved in tumour suppression and genome stability (Shen *et al.*, 2006). Leukemic cells are characterized by mislocalized PML bodies and some anticancer drugs have been shown to correct malignant phenotypes by reassembling PML bodies (Zink *et al.*, 2004).

Protein folding by the molecular chaperone machinery

Protein folding refers to a physical process where unstructured polypeptide chains fold into tertiary structures characterized by a three dimensional conformation (Fink, 1999; Clark, 2004; Li *et al.*, 2012b). The latter is also referred to as a native protein conformation and was previously thought to be determined solely by the amino acid sequences of a protein (Fink, 1999; Lin and Rye, 2006; Hartl *et al.*, 2011) before discovery of protein folding pathways (Fink, 1999; Zuehlke and Johnson, 2012). However, most of the initially discovered folding pathways could not clearly elucidate the mechanisms involved in protein folding under various physiological conditions in the cell, because they only focused on an isolated polypeptide chain (Clark, 2004; Hartl *et al.*, 2011). It is now evident that on exiting the ribosome, proteins are subjected to numerous protein-protein interactions (PPI) besides interacting with various macromolecules such as ribonucleic acids (RNA) (Hartl *et al.*, 2011). Some of these interactions are unspecific and may result in protein misfolding and aggregation (van den Berg *et al.*, 2000; Hartl *et al.*, 2011). In order to overcome the accumulation of misfolded and aggregated proteins, cells have evolved various mechanisms to help in ensuring proper protein folding and refolding (Lin and Rye, 2006; Hartl *et al.*, 2011). A key component of the implicated machinery is the molecular chaperone cycle which was first discovered in the study of nuclear proteins in the assembly of the nucleosome (Laskey *et al.*, 1978; Li, 2011). A molecular chaperone refers to a protein that interacts with other proteins in their unfolded or nascent conformation enabling them to attain a

native conformation by preventing misfolding and aggregation (Li *et al.*, 2012a) but does not occur in the final protein structure (Hartl *et al.*, 2011; Li *et al.*, 2012a).

Some molecular chaperones are members of the heat shock protein superfamily, which are elevated on exposure to heat or stress in the cell (Gething and Sambrook, 1992; Feder and Hofmann, 1999; Odunuga *et al.*, 2004). The proteins that depend on the molecular chaperone machinery for their folding, activation, translocation across membranes and even degradation are frequently referred to as clients (Zuehlke and Johnson, 2012) of the chaperone machinery (Li *et al.*, 2012a). This distinguishes them from co-chaperones, which are a group of accessory proteins that help in the recruitment, presentation and stabilization of the binding between the client proteins and the chaperones (Li *et al.*, 2012a). Numerous protein families have been implicated in the molecular chaperone cycle but this study revolves around only two of these chaperones; the heat shock proteins (Hsp70 and Hsp90) in relation to the Hsp70/Hsp90 organizing protein (Hop).

Hsp90 is a highly conserved chaperone protein involved in the folding and activation of various proteins in the cell (Zuehlke and Johnson, 2012). It exists in two isoforms within the cytoplasm, Hsp90α is induced under stress but is not essential in the mouse (Grad *et al.*, 2010), while Hsp90β is an essential gene and is constitutively expressed (Voss, 1999). It is also evident that Hsp90 translocates into the nucleus (Li *et al.*, 2012a) besides co-precipitating with its client proteins. Other isoforms of Hsp90 such as the tumor necrosis factor type 1 receptor-associated protein (TRAP1) are found in the mitochondrion (Altieri *et al.*, 2012) while the 94kDa glucose regulated protein (Grp94) is in the ER (Li *et al.*, 2012a; Zuehlke and Johnson, 2012). Among the client proteins of the Hsp90 chaperone are steroid hormone receptors, protein kinases and

nuclear proteins (Li *et al.*, 2012a; Zuehlke and Johnson, 2012). The structure of Hsp90 consists of an N-terminal domain which contains an ATP binding site, a middle domain for interaction with co-chaperones, and clients and the C-terminal domain which binds various co-chaperones containing tetratricopeptide repeats (TPR), including the Hsp70/Hsp90 organizing protein (Hop) (Zuehlke and Johnson, 2012). Like Hsp90, there are various isoforms of Hsp70 localizing in different organelles, for instance the glucose regulated protein (Grp78) localizes in the ER (Li, 2011). Hsp70 also contains three structural domains, which include the ATPase domain at the N-terminus, the substrate binding domain and a C-terminal domain (Shonhai *et al.*, 2007). However, unlike Hsp90, Hsp70 interacts predominantly with nascent client proteins, a subset of which are transferred via Hop to the Hsp90 chaperone to achieve full maturation and activation (Li, 2011).

The Hsp70/Hsp90 molecular chaperone complex

It is believed that the Hsp70/Hsp90 chaperone machinery depends on the activity of various co-chaperones that come in at distinct phases of the cycle in order to regulate substrate binding specificity (Schmidt *et al.*, 2015). In this chaperone complex, clients first interact with Hsp70/Hsp40 before being handed over to Hsp90 via Hop. The role of Hsp40 in this early complex is to catalyze the formation of complexes between clients and Hsp70 (Schmidt *et al.*, 2015). Since Hsp90, unlike Hsp70, does not interact with clients in their unfolded or nascent confirmation (Li *et al.*, 2011), the role of Hsp70 in this early complex is to assist in presenting the client in a partially folded state to Hsp90 (Wandinger *et al.*, 2008), while Hop serves to tether Hsp70 to Hsp90 in order to allow for client transfer (Li, 2011). The interaction of the clients and the Hsp90 chaperone machinery is thought to be modulated by an ATPase activity which shifts the conformation of the Hsp90 dimer between an open and closed conformation (Wandinger *et*

al., 2008). Formation of the early complex between Hsp70-Hop-Hsp90 is thought to occur in the open conformation, where the binding of Hop inhibits the ATPase activity of Hsp70 and Hsp90 (Wandinger *et al.*, 2008). The cycle then progresses upon binding of other co-chaperones such as the peptidyl-propyl isomerases (PPIases) (Schmidt *et al.*, 2015) which also bind to the C-terminus of Hsp90 owing to possession of a TPR domain (Wandinger *et al.*, 2008). The binding of other co-chaperones such as p23 not only displaces Hsp70 and Hop from the complex, but also fosters the formation of the closed confirmation that is ATP hydrolysable (Wandinger *et al.*, 2008). p23 is an ATPase inactivating co-chaperone that is believed to trigger client transfer to Hsp90 for further processing (Lorenz *et al.*, 2014; Schmidt *et al.*, 2015). Upon the binding of the activator of Hsp90 ATPase (Aha1), ATP hydrolysis ensues and the client is finally released from Hsp90 to allow for another chaperoning cycle (Wandinger *et al.*, 2008).

The HSP70/HSP90 organizing protein (Hop)

The Hsp70/Hsp90 organizing protein (Hop) also referred to as the stress inducible phosphoprotein 1 (STIP1) or p60 (Lee *et al.*, 2012; Chao *et al.*, 2013) is a protein that belongs to the molecular chaperone machinery (Odunuga *et al.*, 2004; Carrigan *et al.*, 2005). Hop does not have any chaperone activity of its own (Scheufler *et al.*, 2000) and is therefore commonly described as a co-chaperone of the two major heat shock proteins Hsp70 and Hsp90 (Caplan, 2003; Gitau *et al.*, 2011). Hop is involved in recruiting and binding client proteins to Hsp70 and Hsp90 besides tethering Hsp70 to Hsp90 during protein folding and activation (Scheufler *et al.*, 2000; Caplan, 2003; Carrigan *et al.*, 2005; Calderwood, 2013; Baindur-Hudson *et al.*, 2015).

The structure of Hop contains nine tetratricopeptide repeats (TPR) normally clustered into three TPR domains (TPR1, TPR2A and TPR2B) (Scheufler *et al.*, 2000; Flom *et al.*, 2007; Onuoha *et*

al., 2008; Gitau *et al.*, 2011) (Figure 4) which have distinct roles in binding the chaperone complex. TPR1 and TPR2B bind to HSP70 while TPR2A binds to Hsp90 (Scheufler *et al.*, 2000; Odunuga *et al.*, 2004; Carrigan *et al.*, 2005; Rohl *et al.*, 2015; Schmidt *et al.*, 2015). In addition, Hop contains two DP domains that are rich in Asp and Pro and form alpha helical rich structures of largely undefined function. Hop and the chaperone machinery mainly operates within the cytoplasm (Bredemeyer *et al.*, 2006) but it is now evident that Hop also finds its way into the nucleus via an NLS in a cell cycle dependent manner (Longshaw *et al.*, 2004; Odunuga *et al.*, 2004; Gitau *et al.*, 2011). According to Longshaw *et al.*, (2004), inhibition of the phosphorylation of Hop by CDK2 prolongs its accumulation in the nucleus, while activation of phosphorylation leads to an exit of Hop. Despite the fact that the role of Hop in the cellular machinery has been demonstrated in cell migration, activation of oncogenes, cell signaling and signal transduction besides transcription regulation (Onuoha *et al.*, 2008; Gitau *et al.*, 2011; Calderwood, 2013), it remains unclear if the roles of Hop in the nucleus are similar to the roles in the cytoplasm (Longshaw *et al.*, 2004).

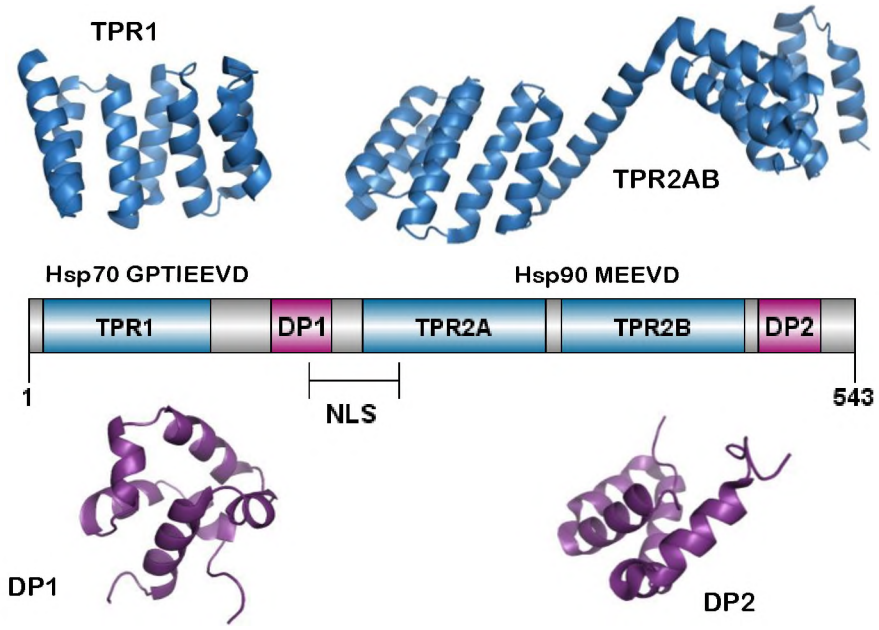

Figure 4: Schematic illustration of the functional domains of Hop
The TPR domains are the primary binding sites on Hop for the EEVD sequences of Hsp70 and Hsp90. The functions of the DP1 and DP2 domains are poorly defined (Baindur-Hudson *et al.*, 2015).

Hop has been shown to interact with various client proteins of the Hsp90 chaperone machinery by recruiting and presenting them for proper folding and activation (Onuoha *et al.*, 2008). Among the key client proteins that interact with Hop are signal transduction components such as the signal transducer and activator of transcription (Stat3) (Bradley *et al.*, 2012), involved in triggering pluripotency in embryonic stem cells (Longshaw *et al.*, 2009). In cell migration, Hop has been shown to be involved in moderating pseudopodia formation via its interaction with globular and filamentous actin and the latter increases the migration and invasiveness of tumour cell lines (Willmer *et al.*, 2013). Hop is also implicated in the interaction and activation of steroid receptors (Heinlein and Chang, 2001; Elbi *et al.*, 2004; Carrigan *et al.*, 2005; Onuoha *et*

al., 2008; Calderwood, 2013) which have been associated with tumour progression in breast and prostate cancer (Bhola *et al.*, 2013).

Besides the above interactions and its role as a co-chaperone, Hop has been shown to function as a surface ligand via interactions with the prion protein (PrP^c) which enhances the differentiation of neurons (Zanata *et al.*, 2002). The cellular prior protein is a ubiquitously expressed protein that is thought to be involved in regulating numerous biological functions including neuronal differentiation and the observed interaction with Hop confers neuroprotection and neuritogenesis in the brain (Lopes *et al.*, 2005). This interaction is thought to occur via activation of the cAMP and MAPK activity (Lopes *et al.*, 2005) and studies indicate that the observed interaction also promotes the proliferation of gliomas (Lopes *et al.*, 2014) in the central nervous system (CNS) but does not enhance the proliferation of normal glia (Erlich *et al.*, 2007).

Hop as a potential drug target

There has been a concentration on the potential of major chaperones such as Hsp90 as drug targets and little on the role of associated co-chaperones. However, in the recent past, there have been attempts to explore the therapeutic potential of co-chaperones such as Hop by targeting their interaction with Hsp70 and Hsp90 (Blair *et al.*, 2014; Edkins, 2016). Compounds such as sansalvamide A (San-A-amide) have been developed and tested for their ability to interrupt the binding of C-terminal Hsp90 binding co-chaperones such as Hop. However, these compounds result in undesired effects owing to domain similarities among various C-terminal binding co-chaperones (Cortajarena *et al.*, 2008; Blair *et al.*, 2014). Previously, Cortajarena *et al.*, (2008) demonstrated the potential of the use of TPR peptides against the Hsp90 C-terminal in deregulating the expression of HER2 in breast cancer, while Horibe *et al.*, (2011) demonstrated

the potential of an anti-TPR2A inhibitor as a therapeutic agent against a variety of cancers *in vitro*. Unlike the previous approaches, the anti-TPR2A peptide was shown to specifically inhibit the interaction between Hsp90 and Hop with minimal interference on other chaperone mediated interactions hence offering a promising anti-cancer therapy (Horibe *et al.*, 2011).

Hop has been shown to assist in the regulation of biological functions independent of Hsp90 (Song and Masison, 2005; Edkins, 2016) and the need to specifically target Hop independent of the interaction with Hsp70 and Hsp90 can therefore not be ignored. The potential of Hop as a drug target remains an interesting venture especially in diseases such as Alzheimer's where the depletion of Hop has been shown to result into an increase in the expression of Tau, a protein responsible for causing the disease condition (Blair *et al.*, 2014). Studies in cancer cell lines have demonstrated that depletion of Hop affects vital tumour related processes including invasion, migration and proliferation (Edkins, 2016). With the recent demonstration of having chaperone related functions independent of Hsp90 owing to the possession of its own ATPase activity (Yamamoto *et al.*, 2014; Edkins, 2016), it becomes increasingly important to continually pursue the therapeutic potential of Hop.

Problem statement/knowledge gap

Previous data from a global proteomics analysis conducted in our laboratory demonstrated a greater than two fold reduction in the levels of the nuclear membrane protein emerin when Hop protein levels were depleted using RNA interference (Wingate, 2016). Hop has been shown to be actively involved in recruiting and presenting client proteins to the Hsp90 chaperone machinery (Caplan, 2003) but nothing is currently known about its involvement with emerin function, despite the fact that both Hop and emerin have been shown to localize in the nucleus in a cell

cycle dependent manner (Longshaw *et al.*, 2004; Berk *et al.*, 2013). Although the localization of Hop in the nucleus relies on the NLS (Longshaw *et al.*, 2004; Odunuga *et al.*, 2004), the mechanisms involved in the localization of emerin remain unclear (Lee *et al.*, 2001). It is interesting that both emerin (Haraguchi *et al.*, 2004; Hirano *et al.*, 2005) and Hop (Longshaw *et al.*, 2004) are phosphorylated by cell cycle dependent kinases during mitosis and following depolymerization, emerin exits into the ER membrane (Webster *et al.*, 2009) and may subsequently mislocalize into the cytoplasm (Ho *et al.*, 2013). Hop also exits the nucleus on activation of phosphorylation by similar kinases (Longshaw *et al.*, 2004) and makes a return to the cytoplasm. It is possible that Hop is also involved in the activation of nuclear lamina and INM proteins, especially emerin, and subsequently determining their interaction and affecting the nuclear architecture.

There is no literature indicating a direct interaction between emerin and Hop despite the fact that both emerin and Hop share binding partners and subsequently influence similar functions. For instance, within the cytoplasm, emerin (Berk *et al.*, 2013; Ho *et al.*, 2013) and Hop both bind actin and tubulin (Li *et al.*, 2012b; Willmer *et al.*, 2013). It is therefore possible that Hop maybe involved in regulating the activation and translocation of emerin by colocalizing with emerin in the nucleus and cytoplasm and, because of the role of emerin in the NE, it becomes important to establish the possible mechanism of interaction with Hop which may likely influence its presence in the INM.

Despite the fact that emerin is recruited in the INM by BAF at the core region and retained by lamins, the mechanisms involved in the translocation, localization and retention of emerin in the INM and the cytoplasm remain unclear (Lee *et al.*, 2001). However, because emerin and Hop

both localize in the nucleus and the cytoplasm and subsequently undergo phosphorylation in a cell cycle dependent manner (Longshaw *et al.*, 2004; Hirano *et al.*, 2005) in addition to both binding actin and tubulin (Berk *et al.*, 2013; Ho *et al.*, 2013; Willmer *et al.*, 2013), it is possible that there could be an interaction between the two proteins. This study sought to determine the likely interaction between emerin and Hop and subsequently establish the effect of this interaction on the localization of emerin and its partner proteins and on the architecture of the NE.

Hypothesis

Hop interacts with emerin and regulates its function and/or localization thereby influencing the architecture of the nucleus.

Objectives

1. Analysis of the interaction between Hop and emerin in cell lines.
2. To determine the effect of HOP knockdown on the localization and function of emerin.
3. Analysis of the effect of Hop knockdown on nuclear architecture and function.

Chapter 2: Materials and methods

Materials

The general reagents used were supplied by Sigma Aldrich (USA) or SAARCHEM (Merck). Primary and secondary antibodies were purchased from Abcam [Hop (Ab56873), emerin (Ab56996), the HA tag (Ab9110), Lamin A-C (EPR4100)]. We used alpha tubulin (Ab7291) and histone (H3) (Ab1791) as our loading control for whole cell lysates and nuclear and cytoplasmic isolates respectively while GAPDH (EPR6256) was used as a loading control for whole cell lysates alone. All primary antibodies were used at a dilution of 1:1000 unless otherwise stated, while the species specific secondary antibodies were used at a dilution of 1:5000 unless otherwise stated. Antibodies used for assessment of the nucleus and nuclear associated marker proteins were supplied in the Nucleus and Nuclear Envelope-Associated Marker Proteins Antibody Sampler Kit (catalogue number 12784) from Cell Signaling Technology. A detailed description of all the antibodies used in this study is provided in the appendix (Table 2). Phosphate-buffered saline (PBS) (10 mM Na_3PO_4, 2.68 mM KCl and 140 mM NaCl), CelLytic-M lysis buffer (C3228, Sigma Aldrich), 1x mammalian protease inhibitor (P8340, Sigma Aldrich) and nocodazole (M1404, Sigma Aldrich) were purchased from Sigma Aldrich. The endotoxin free maxiprep kit (cat no 12362) was purchased from Qiagen (Netherlands). The pcDNA3.1-HA-Hop plasmid is a mammalian expression vector that contains the sequence for full length Hop with an N-terminal hemagglutinin (HA) tag. This plasmid was designed in house and synthesized by Genscript. The pcDNA3.1-HA-HSP90 mammalian expression plasmid was a gift from William Sessa (Addgene plasmid # 22487) and contains the sequence of the HSP90β with an N-terminal HA tag, which is also referred to as wild type HSP90. The plasmid encoding a green fluorescent tagged (GFP) emerin pEGFP-C1 (637) was a gift from Eric Schirmer

(Addgene plasmid # 61993). The HA co-immunoprecipitation kit (Cat no 26180) was purchased from Pierce/Thermo Scientific, while the GFP magnetic beads containing a green fluorescent tagged (GFP) single domain monoclonal antibody (ab193983) were purchased from Abcam. The inducible TRIPZ shRNA plasmid against human emerin was from Open Biosystems. The lentiviral packaging plasmids psPAX2 and pMD2.G and the human embryonic kidney cells (HEK293T) were kind donations from Professor Marco Weinberg, Witwatersrand University and Professor Sharon Prince, University of Cape Town, respectively. The MCF-7 (HTB-22) and the MDA-MB- 231 (HTB-26) breast cancer cells were purchased from the American Type Culture Collection (ATCC). Reagents used in cell culture such as Dulbecco's Modified Eagle's Medium (DMEM), Trypsin-EDTA, antibiotics (Penicillin, amphoteracin, and streptomycin) were supplied by Gibco Life technologies (USA). Reagents such as minimal essential medium (MEM) (Cat no 7145), L-Glutamine (Cat no 7513) were supplied by Sigma Aldrich (USA) while foetal bovine serum (FBS) (cat no 181H was supplied by BioWest (USA). The culture vessels and all the plastic ware used in tissue culture work were supplied by Nest Biotechnology. The Leibovitz's L-15 cell culture medium and the reduced serum medium (Opti-MEM) and the phosphate-buffered saline (PBS) tablets were purchased from Gibco^{TM} Life Technonologies (USA). Other tissue culture reagents including puromycin dihydrochloride, G418 disulfate salt, doxycycline hyclate and sodium pyruvate were supplied by Sigma-Aldrich (USA). The protein loading dyes; the prestained broad range protein molecular weight marker and the unstained broad range markers were supplied by Thermo Scientific (USA). The QCM ^{TM} 24 well migration assay chambers (Merck Cat. No. ECM 508) were purchased from Merck (USA).

Methods

Routine culture of mammalian cell lines

Human embryonic kidney cell line (HEK293T) stably transfected with TRIPZ plasmids encoding small hairpin ribonucleic acid (shRNA) against Hop (henceforth referred to as HEK293T-shHOP), emerin (henceforth referred to as HEK293T-shEMD) or a non-targeting control (henceforth referred to as HEK293T-shNT) (Contu, 2014) were cultured in Dulbecco's modified Eagle's medium (DMEM) with 10% (v/v) fetal bovine serum (FBS), 100 U/ml Penicillin-Streptomycin-Amphotericin (PSA), 1 mM Sodium pyruvate, 0.1 mM non-essential amino acids, 500 µg/ml G418, 2 µg/ml puromycin and grown in 9% CO_2 at 37°C. Wild type HEK293T cells were cultured in the same medium, except without the addition of puromycin. The MCF7 breast cancer cell line stably transfected with TRIPZ plasmids encoding shRNA against Hop (henceforth referred to as MCF7-shHOP) or a non-targeting control (MCF7-shNT) were cultured in DMEM containing 10% (v/v) fetal bovine serum (FBS), and 2 µg/ml puromycin and grown in 9% CO_2 at 37°C. The MDA-MB-231 breast cancer cell line stably transfected with TRIPZ plasmids encoding shRNA against Hop (henceforth referred to as MDA-shHOP) or a non-targeting control (MDA-shNT) were cultured in Leibovitz's L-15 medium containing 10% (v/v) fetal bovine serum (FBS), 100 U/ml PSA, and 2 µg/ml puromycin and grown at 37°C without additional CO_2.

Generation of the HEK393T cell line stably transfected with emerin specific shRNA using lentiviral particles

HEK293T cells were seeded at a concentration of $2x10^4$ cells/ml in a 6 well plate and left to adhere overnight. Following overnight incubation, the cells were transfected with a lentiviral packaging system consisting of the psPAX2 packaging vector at a concentration of 450 ng/well,

the pMD2.G lentiviral capsid vector at a concentration of 50 ng/well (Sterrenberg, 2015) and 500 ng/well of the EMD TRIPZ shRNA plasmid DNA in X-treme gene HP transfection reagent. Filter sterilized viral particle supernatants obtained using 0.45 µm filters 48 hours after transfection were used to transduce HEK293T cells seeded a day prior at a concentration of $2x10^4$ cells per ml as described by Sterrenberg (2015). The transduced cells were incubated at 37°C in 9% CO_2 for 48 hours before selection of colonies with puromycin at a concentration of 2 µg/ml. Five weeks after selection of positively transduced colonies, confirmation of the transduction was achieved via induction of the expression of the emerin shRNA by addition of 1 µg/ml of doxycycline to the growth medium with daily replenishment for 24-96 hours. The cells were harvested for analysis by removal of the medium, followed by a brief rinse with Phosphate-buffered saline (PBS) (10 mM Na_3PO_4, 2.68 mM KCl and 140 mM NaCl) and subsequent scraping of monolayer into CelLytic-M lysis buffer containing 1x mammalian protease inhibitor and incubated for 15 minutes at 4°C to allow for lysis. The lysates were cleared by centrifugation at 500 x *g* for 15 minutes at 4°C and the concentration of protein in the lysates was quantified by absorbance at 280 nm on a Nanodrop 2000 spectrophotometer. Following confirmation of depletion of emerin by Western blot analyses, the stable cell cultures were expanded in larger culture vessels using culture medium supplemented with puromycin for further propagation of the emerin shRNA cell line (henceforth referred to as HEK293T-shEMD).

Depletion of Hop and emerin by RNA interference

HEK293T-shHop, HEK293T-shEMD and HEK293T-shNT together with the MCF7-shHop and the MCF7-shNT and the MDA-shHop and the MDA-shNT cell lines were seeded at $1x10^6$ cells/ml and allowed to adhere overnight. The shRNA construct is a tet-on expression vector and the expression of the Hop-specific, EMD-specific and control shRNA was induced by addition of

1 µg/ml doxycycline to the complete growth medium. The doxycycline was replenished daily for 24-96 hours and the cells harvested for analysis by rinsing with PBS and scraping of the monolayers into CelLytic -M as previously described. The lysates were cleared by centrifugation at 500 x *g* for 15 minutes at 4°C, the protein concentration quantified using absorbance at 280 nm on a Nanodrop 2000 spectrophotometer and stored at -20 °C until analysis.

Treatment of cells with protoesomal/lysosomal inhibitors

HEK293T-shHOP, HEK293T-shEMD and HEK293T-shNT cell lines were seeded at $1x10^6$ cells/ml and allowed to adhere overnight before expression of the Hop-specific, EMD-specific and control shRNA was induced by addition of 1 µg/ml doxycycline to the complete growth medium. The doxycycline was replenished daily for 24-72 hours and the cells were then treated with 1 µg/ml of MG132 (proteasomal inhibitor) or 10 µg/ml of chloroquine (lysosomal inhibitor) and allowed to grow for another 24 hours. The cells were harvested as previously described and the effect of the proteosomal or lysosomal inhibitor on protein expression determined by Western blot analysis.

Sodium Dodecyl Sulphate Polyacrylamide Gel Electrophoresis (SDS-PAGE)

Cell lysates were resolved by discontinuous Sodium Dodecyl Sulphate Polyacrylamide gel electrophoresis (SDS-PAGE) using a 12 % (v/v) resolving gel (1.5 M Tris-HCl, pH 8.8) and a 4% (v/v) stacking gel (0.5M Tris-HCl, pH 6.8) as outlined by Laemmli (1970). The samples were mixed with 5x SDS sample buffer [0.05 M Tris-HCL, 5% (v/v) β-mercaptoethanol, 10% (v/v) glycerol 2% (w/v) SDS and 1% (w/v) Bromophenol blue], boiled for 5 mins and an equal amount of protein per well (50 µg) resolved at 120 V in 1X SDS running buffer [0.25 mM Tris-HCl, 1% (w/v) SDS, 192 mM Glycine].

Chemiluminescence-based Western blot analysis

The resolved proteins in the SDS-PAGE were transferred to a nitrocellulose membrane previously soaked in 1x Western transfer buffer [13 mM Tris-HCl, 20% (v/v) methanol, 100 mM glycine] and laid on soaked filter papers according to manufacturer's instructions (Santa Cruiz) in the Semi Dry Western transfer system (SD 20 Semi Dry, Lasec, SA). Transfer of proteins to the nitrocellulose membrane was achieved by application of 400 mA for 50 minutes and was confirmed by Ponceau staining of the membrane [0.5% (w/v) Ponceau S, 1% (v/v) glacial acetic acid]. The membrane with the bound proteins was incubated in 1% (w/v) non-fat dry milk powder in Tris -Buffered Saline (TBS) (50 mM Tris-HCl, pH 7.5, 150 mM NaCl) at room temperature for 45 minutes with rocking to allow for blocking of non-specific binding sites. The blocked membrane was incubated overnight at 4°C in primary antibody diluted in 1% (w/v) non-fat dry milk powder in TBS according to manufacturer's guidelines. The membrane was subjected to 4 washes at 10 minute intervals using TBS containing 0.1% (v/v) Tween 20 (TBS-T) with shaking at room temperature. Species specific secondary antibody coupled to a horseradish peroxide enzyme (HRP) diluted in 1% (w/v) non-fat dry milk in TBS was added to the membrane and incubated at room temperature for 45 minutes. The membrane was washed with 4 rinses at 10 minute intervals using TBS-T followed by chemiluminescent based detection using the enhanced clarity substrate (Biorad) on the XRS Chemidoc (Biorad) apparatus.

Preparation of endotoxin free plasmid DNA

The pcDNA3.1-HA-HOP, pcDNA3.1-HA-HSP90, TRIPZ EMD shRNA, and the emerin pEGFP-C1 plasmids were transformed into chemically competent *Escherichia coli* (*E.coli*) DHα5 cells and the mixture plated on 2X YT agar plates (2.5 g/L yeast extract, 5 g/L NaCl and 5 g/L tryptone) with 100 µg/mL ampicillin and incubated at 37°C for 18 hours to allow for growth

of colonies. Following confirmation of transformation, single colonies were inoculated in 5 mL of high salt Luria broth (LB) medium (10 g/L Tryptone, 5 g/L yeast extract, 10 g/L NaCl) with 100 µg/mL ampicillin and incubated overnight at 37ºC with shaking. A volume of 250 µl from the overnight 5 mL culture was used to inoculate 250 mL flasks of high salt LB medium containing 100 µg/mL of ampicillin and the flasks incubated at 37 ºC overnight with shaking. Extraction of endotoxin free plasmid DNA was achieved using the endotoxin free Maxiprep kit according to manufacturer's guidelines. The eluted DNA was quantified by absorbance at 260 nm on a Nanodrop 2000 spectrophotometer and stored at -20 ºC until use.

Transfection of mammalian cells with DNA

Human embryonic kidney cells (HEK293T) cultured as previously described were seeded at a concentration $1x10^4$ cells/ml in a 24 well plate and allowed to adhere overnight. Transfection mixtures containing 0.5 µg of each DNA plasmid in either 0.5 or 1 µl of Xtremegene HP transfection reagent (for 1:1 or 1:2 transfection ratios, respectively) in 100 µl of serum free Opti-MEM according to manufacturer's instructions were introduced into the appropriate wells. Untransfected cells were included as a control for each transfected DNA construct. Following incubation for 48 hours at 37ºC in 9% CO_2, cells were harvested and lysates prepared in 200 µl CelLytic M buffer as previously described and stored at -20ºC following protein quantification until required for analysis. Equal amounts of protein (50 µg) were analyzed by SDS-PAGE and Western blot analysis for protein expression. The same procedure was used for larger scale transfections of HEK293T cells in 10 cm dishes, with the exception that a cell density of $1x10^6$ cells/ml and a 1:1 dilution of plasmid DNA (10 µg) and (10 µl) of transfection reagent in 1000 µl of Opti-MEM was used. Following lysis with 600 µl of CelLytic-M, an aliquot from the

transfected and the untransfected whole cell lysates (50µl) was prepared for SDS-PAGE and Western blot analysis, and the remaining lysates used in co-immunoprecipitation reactions.

Co-immunoprecipitation of protein complexes from transfected mammalian cell lysates

Co-immunoprecipitation (IP) studies using HA co-IP kits either from Pierce or Sigma-Aldrich were conducted on lysates prepared from HEK293T cells that remained untransfected or were transfected with mammalian expression plasmids encoding HA-tagged proteins. The anti-HA antibody agarose slurry (20 µl) was added to a spin column containing 600 µl of cell lysate prepared in CelLytic-M and incubated overnight at 4 °C with shaking. Thereafter, the column was washed 3 times for 15 second intervals with filter sterilized TBS-T and bound proteins eluted from the column using 5x non reducing sample buffer provided in the kit with subsequent boiling at 100 °C for 5 minutes and centrifugation at 500 x *g* for 15 seconds at 4°C. The eluted samples were stored at -20°C until required for SDS-PAGE and Western blot analysis for co-immunoprecipitated complexes. Prior to the SDS-PAGE, 5% (v/v) β-mercaptoethanol was added to the samples and boiled.

Immunoprecipitation using the anti-GFP magnetic beads was performed on lysates made from HEK293T cells that remained untransfected or were transfected with a mammalian expression plasmid encoding a GFP-tagged emerin. The anti-GFP magnetic beads (25µl) were combined with 300µl of the cell lysate made in CelLytic-M and incubated at 4°C with gentle agitation for one hour. The tubes were placed on a magnetic rack for 5 seconds and the supernatant removed followed by four washes with ice cold wash buffer containing 50 mM Tris-HCL (pH 7.5) 150 mM NaCl and 0.05% (v/v) NP-40. The magnetic beads were resuspended in 20µl of 5X SDS sample buffer [0.05 M Tris-HCL, 5% (v/v) β-mercaptoethanol, 10% (v/v) glycerol 2% (w/v)

SDS and 1% (w/v) Bromophenol blue] and boiled for 5 minutes. To recover the immunoprecipitated proteins, the tubes were placed on the magnetic rack for 5 seconds to isolate the beads and the sample buffer containing the proteins collected in a sterile tube and stored at -20°C until required for SDS-PAGE and Western blot analysis for co-immunoprecipitated complexes.

Immunofluorescence analysis and confocal microscopy

The subcellullar localization of proteins in HEK293T-shEMD, HEK293T-shHop and HEK293T-shNT cell lines alongside the wild type HEK293T cells was assessed by indirect immunofluorescence staining and confocal microscopy. Cells were seeded on sterile coverslips at a concentration of $1x10^4$ cells/ml and shRNA expression in the HEK293T-shEMD, HEK293T-shHop and HEK293T-shNT cell lines induced for 96 hours with 1 µg/ml doxycycline with daily reprenishing before being fixed in ice-cold methanol for 1 minute following a brief rinse with sterile PBS. Cells were permeabilised using 0.1% (v/v) Triton-X100 in PBS for 10 minutes and then blocked in 1% (w/v) bovine serum albumin (BSA) in TBS-T for 45 minutes at room temperature. Cells were incubated with 300 µl of 0.1% (w/v) BSA in TBS-T (BSA/TBS-T) containing primary antibodies (1 in 100 dilution) overnight at 4°C, after which, the coverslips were washed 3 times with 500 µl 0.1% (w/v) BSA/TBS-T for 5 minutes each wash. Species-specific fluorescently labeled secondary antibodies (diluted at 1 in 500) were added in 500 µl of 0.1% (w/v) BSA/ TBS-T and incubated in the dark at room temperature for at least 1 hour. Thereafter, coverslips were washed 3 times with 500 µl 0.1% (w/v) BSA/TBS-T for 5 minutes each wash. A final wash with sterile distilled water containing 1 µg/ml Hoechst 33342 was used to stain the nucleus. The coverslips were mounted on to microscope slides using DAKO mounting medium, and the edges sealed with nail varnish and left to dry. The cells were

examined by confocal microscopy using the Zeiss LSM 780 confocal microscope and analyzed with ZEN software.

Isolation of nuclei using the EZ nuclei isolation kit

HEK293T-shEMD, HEK293T-shHop and HEK293T-shNT cell lines were seeded as previously described and left to adhere overnight. The wild type HEK293T cells were seeded in a similar manner except without inclusion of puromycin and doxycycline. Induction of the shRNA in the HEK293T-shEMD, HEK293T-shHop and HEK293T-shNT cell lines with 1 μg/ml doxycycline was initiated for 96 hours and the cells harvested by scraping into EZ lysis buffer following removal of medium and a brief rinse with PBS. A cytoplasmic fraction was obtained following centrifugation at 500 x *g* for 5 minutes at 4ºC using the EZ nuclei isolation kit (Sigma) according to manufacturer's guidelines. Intact nuclei (Watson, 2000) were isolated in the last centrifugation step at 500 x *g* for 5 minutes at 4ºC and resuspended in nuclei storage buffer provided in the kit. The protein concentration in the nuclei and cytoplasmic fractions was quantified using absorbance at 280 nm on a Nanodrop 2000 spectrophotometer and kept at -20ºC before SDS-PAGE and Western blotting.

Cell cycle synchronization using Nocodazole

HEK293T-shEMD, HEK293T-shHop and HEK293T-shNT cell lines were seeded on sterile coverslips at a concentration of $1x10^4$ cells/ml and left to adhere overnight. Induction of the shRNA expression with 1 μg/ml doxycycline was initiated for 96 hours with daily replenishment of doxycycline. After 96 hours, the cells were treated with 10 μg/ml of Nocodazole and incubated for 12 hours before removal of medium, a brief rinse with PBS and processing of cells for immunofluorescence and confocal microscopy as previously described. The cells were

examined by confocal microscopy using the Zeiss LSM 780 confocal microscope and analyzed with ZEN software.

Transmission electron microscopy assessment of nuclear structure

HEK293T-shEMD, HEK293T-shHop and HEK293T-shNT cell lines were seeded and left to adhere overnight. Induction of the shRNA with 1 μg/ml doxycycline was initiated for 96 hours with daily replenishment of doxycycline. The cells were harvested by removal of the medium, a brief rinse with PBS and trypsinization in 0.05% (v/v) Trypsin/EDTA solution. A portion of cells (50 μl) lysed in CelLytic-M buffer was prepared for SDS-PAGE and Western blotting to confirm the levels of Hop and emerin. The rest of the cells were centrifuged for 5 minutes at 500 x *g* at 4°C and following removal of the supernatant, the pellet was resuspended in PBS and centrifuged for 5 minutes at 500 x *g*. The supernatant was removed to leave a dry pellet that was immediately washed in fixing buffer (0.1 M Na cacodylate, 0.1 M sucrose, 2 mM $CaCl_2$, 2 mM $MgCl_2$ pH 7.4) and incubated at room temperature for 1 hour in fixing buffer made with 3% (w/v) paraformaldehyde and 2% (w/v) glutaraldehyde. Thereafter, the samples were fixed with 1% (w/v) tannic acid in fixing buffer at room temperature for 30 minutes after a wash in fixing buffer alone. Following two washes with fixing buffer, the samples were further fixed for 40 minutes with 1% (v/v) osmium tetroxide at room temperature and washed twice with fixing buffer. A final wash was done with sterile water followed by dehydration of the samples in ascending series of concentrations of ethanol [30% (v/v), 50% (v/v), 70% (v/v), 90% (v/v), 2 x 100%] for 10 minutes in each concentration at room temperature. The samples were incubated for 10 minutes in propylene oxide and ethanol (1:1) and infiltrated with propylene oxide in Spurr's resin (1:1) for 2 hours, followed by an overnight incubation in fresh resin at room temperature. The fixed blocks were introduced to fresh resin and cured overnight at 60°C. The

cured samples were sliced into thin sections using a diamond knife on a microtome and stained with one drop of uranyl acetate [7.5% (v/v) in distilled water] on each section for 5 minutes followed by a further staining in 3 % (v/v) lead citrate (Krysko *et al.*, 2008) and images acquired using a Zeiss Libra 120 transmission electron microscope. The size of the nucleus from the HEK293-shNT cells and the HEK293T-shHop cells and from the HEK293-shNT cells and the HEK293T-shEMD cells were compared using Image J and the mean area of the nucleus was compared using an unpaired t-test in Graph pad prism 5.

Cell migration and long term survival assay

Assessment of cell migration and long term survival was achieved via slight modification of the QCM^{TM} 24 well cell migration assay and the conventional clonogenic assay (Yang, 2012). HEK293T-shEMD, HEK293T-shHop and HEK293T-shNT cell lines were cultured and the expression of the Hop, emerin and the non-targeting shRNA induced for 96 hours as described above. Cells were harvested by removal of the medium, a brief rinse with PBS and trypsinization in 0.05% (v/v) Trypsin/EDTA solution. The cell suspension was centrifuged at 500 x *g* for 5 minutes at 4ºC and, following removal of the supernatant, and the pellet was resuspended in fresh medium at a concentration of $1x10^6$ cells per mL. To proceed with the migration assay, we prepared a cell suspension at $0.5x10^6$ cells per mL in DMEM culture medium without FBS and added 500µL of this suspension into the QCM ^{TM} 24 well migration assay upper chambers made of 8 µm pore sized inserts according to the Boyden chamber principle. We added 500µL of complete HEK293T culture medium to the bottom of the chamber and incubated the plate for 24 hours at 37ºC in 9% CO_2. After the 24 hours incubation, we carefully removed the medium from the top and bottom side of the chambers. Cells from the upper chamber and those that had migrated to the underside of the transwell membrane were collected by trypsinization and

counted. The cells collected from the bottom and top of the chambers were seeded into the long term clonogenic assay at a concentration of 2.5 $x10^3$ cells in 6 well plates and allowed to grow for up to 13 days in complete medium without doxycycline. The cells were supplied with fresh medium after every 3 days of incubation at 37°C in 9% $C0_2$. Long term survival was assessed following fixation of the cells with 3:1 of methanol and acetic acid and stained with 0.5% crystal violet and the numbers of colonies formed compared using a one way ANOVA in Graph pad prism 5 at a P value of <0.05.

Statistical analysis and reproducibility

Statistical significance was assessed using Student t-tests and one way ANOVA in Excel or Graphpad prism 5 and a P value of <0.05 was deemed significant. All the results are a representative of triplicate independent experiments unless otherwise stated.

Chapter 3: Results

Generation of a stable emerin shRNA cell line (HEK293T-shEMD)

Our global proteomics analysis indicated that the nuclear envelope protein emerin was down regulated to greater than 2 fold in Hop depleted HEK293T cell lysates. In order to link the effects of Hop to emerin depletion in cells, we first developed a stable cell line for the RNAi-mediated depletion of emerin in HEK293T cells. Equivalent stable cell lines for the expression of Hop specific or control shRNA expression had been generated as part of a previous study. We used a lentiviral delivery system to introduce the emerin shRNA plasmid into cells. Viral particles carrying the emerin specific shRNA were used to transduce HEK293T cells and stable transformants selected for using puromycin. Before the start of selection with puromycin (Figure 5A), all the cells appeared healthy and were adhered to the bottom of the culture dish. At 5 days after the start of puromycin selection (Figure 5B), the majority of the cells appeared to be floating in the culture medium with only a small proportion adhering to the bottom of the culture dish. Following removal of the floating cells, the surviving clones were expanded under continued selection with puromycin every 48 hours to generate the HEK293T-shEMD cell line (Figure 5C). In Figure 5D, we used Western blot analysis to confirm the effect of the expression of the shRNA against emerin on the protein levels of emerin and Hop on lysates made from the HEK293T-shEMD cell line and the control HEK293T-shNT (generated as part of a previous study) that had been induced for expression of the shRNA for 96 hours using doxycycline. When we probed for Hop, we observed a minimal decrease in the band intensity within the lane containing the shEMD sample compared to the control lane (shNT). In contrast, when we probed for emerin, we only observed a band within the lane containing the shNT sample and none within the lane containing the shEMD sample. We then probed for GAPDH which served as our

loading control. Taken together, this suggested that the expression of the shRNA against emerin resulted in the depletion of emerin but only had a minimal effect on the levels of Hop. These data confirmed that we had successfully generated a stable cell line in which protein levels of emerin could be depleted by RNAi upon doxycycline treatment.

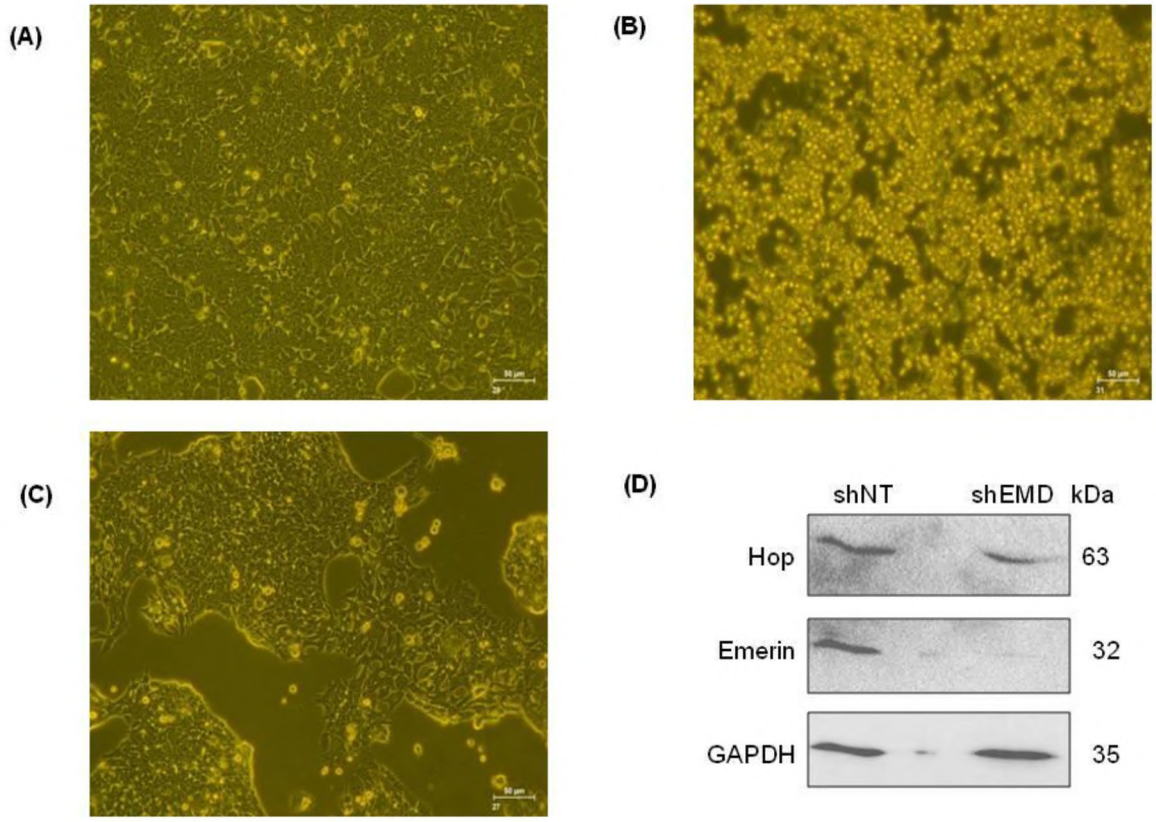

Figure 5: Generation of the HEK293T-shEMD stable cell line
A lentiviral delivery system was used to introduce the EMD shRNA plasmid into HEK293T cells. Following transduction of cells, selection of positively transduced colonies was initiated using puromycin and images obtained prior to the start of the selection (A), 5 days post selection (B) and 15 days post selection (C). In (D) lysates from HEK293T-shEMD (shEMD) and HEK293T-shNT (shNT) cells that had been induced with doxycycline for expression of shRNA for 96 hours were resolved by SDS-PAGE with subsequent Western blotting for detection of the levels of Hop, emerin and GAPDH.

Depletion and over-expression of Hop results in the depletion of emerin protein levels

After generating our HEK293T-shHop cell line, we wanted to confirm the results of the global proteomics analysis that suggested the down regulation of emerin following depletion of Hop. We used Western blot analysis of lysates prepared from HEK293T-shHop and the control HEK293T-shNT cells, as well as MCF7-shHop and the MCF7-shNT and MDA-shHop and the MDA-shNT cell lines, that had all been induced for expression of shRNA for 96 hours to confirm the effect of the depletion of Hop on the expression of emerin (Figure 6). Using an antibody against Hop, we noted a reduction in the Hop band intensity in the lane containing the HEK293T-shHop lysate (Figure 6A, lane shHop) compared to the HEK293T-shNT control (Figure 6A, lane shNT) sample at the same exposure. We observed reduced levels of emerin in the Hop depleted lysate, compared to the control lysate. When we probed with GAPDH, we observed even band intensities in the lanes containing the HEK293T-shHop (shHop) and the HEK293T-shNT (shNT) sample. The reduced Hop band intensity in the lane containing the HEK293T-shHop sample relative to the control indicated the depletion of Hop following induction of the expression of the Hop-specific shRNA, while the reduction in the emerin band in the same sample suggested a decrease in the expression of emerin following the depletion of Hop. The staining for GAPDH was used as our loading control. The same trend was observed across the two other cell lines: MCF7-shHop and the MCF7-shNT (Figure 6B) and the MDA-shHOP and the MDA-shNT cell lines (Figure 6C) showing that the expression of the Hop specific shRNA results in the depletion of Hop and also diminishes emerin protein levels in multiple different cell lines (Figure 6B and C). Beside each figure is a densitometry analysis of the western blot indicating a reduction in the levels of emerin in Hop depleted cells.

We next tested the effect of the depletion of emerin on the protein levels of Hop in HEK293T-shEMD and HEK293T-shNT cells that had been induced for shRNA expression for 96 hours (Figure 6D). We observed a substantially reduced emerin band intensity in the lane containing a lysate from the HEK293T-shEMD cells (Figure 6D, lane shEMD) compared to the lane containing a lysate from the HEK293T-shNT control (Figure 6D, lane shNT). There was a minor decrease in the Hop band intensity in the emerin depleted lysate (Figure 6D, shEMD) compared to the lane containing the control lysate (Figure 6D, shNT). The band intensities for GAPDH were used as our protein loading control. The observed difference in the band intensity suggested that the expression of the shRNA against emerin resulted in the depletion of emerin protein levels but only had a minimal effect on the Hop protein levels. Beside this Western blot is a densitometry analysis of the levels of Hop and emerin indicating a reduction in the expression of emerin and not Hop on the expression of the shRNA against emerin.

We subsequently checked the effect of over-expressing Hop on the levels of emerin using lysates made from HEK293T cells transfected for 24 to 96 hours with the pcDNA3.1-HA-Hop plasmid (Figure 6E). An antibody against Hop was used to detect the endogenous and recombinant HA-Hop, while the recombinant HA-Hop was detected using an antibody against the HA tag. At 96 hours, we noted an increase in the Hop and HA-Hop band intensities compared to the earlier time points (24 to 72 hours). The same membrane was probed for emerin and a decrease in the band intensity was observed at 96 hours post transfection compared to the other time points, which correlated with the increased levels of HA-Hop at the same time point. The lane containing a lysate from cells that remained untransfected (UN) had Hop and emerin band intensities that were similar to the bands observed at 24-72 hours. The band intensities for GAPDH (loading control) were uniform in all lanes. The untransfected sample further served as

a control for transfection and distinguished HA-Hop from endogenous Hop. The observed decrease in the band intensity for emerin at the same time point as the maximal expression of HA-Hop suggested that the over-expression of Hop also resulted in the depletion of emerin. Beside this figure is a densitometry analysis of the levels of Hop and emerin at 96 hours where emerin is significantly reduced at this time when Hop is over expressed compared to at 0 hrs.

Depletion of Hop via shRNA results into the depletion of subcellullar levels of emerin

We next used the EZ- nuclei isolation kit to isolate an intact nuclei that is thought to be devoid of cytoplasmic contamination and the nuclear envelope (Watson, 2000) from the HEK293T-shHop, and the control HEK293-shNT cells that had been induced for shRNA expression. On probing for Hop, the isolated cytoplasmic fraction had a reduced band intensity in the lane containing the HEK293T-shHop fraction (Figure 7A, Cytoplasm, lane shHop) compared to the lane containing the control HEK293T-shNT cytoplasmic fraction (Figure 7A, Cytoplasm, lane shNT). In the nuclei fraction, the control HEK293T-shNT showed a low intensity band for Hop, while the HEK293T-shHop did not show any bands at the predicted molecular weight for Hop (Figure 7A, Nucleus, lanes shHop and lane shNT). On probing for α-tubulin, the cytoplasmic fraction from both lysates had uniform band intensities (Figure 7A, cytoplasm, lanes shHop and shNT) while the nuclei from both the HEK293T-shHop and the control HEK293T-shNT did not show any bands (Figure 7B, Nucleus, lanes shHop and shNT).

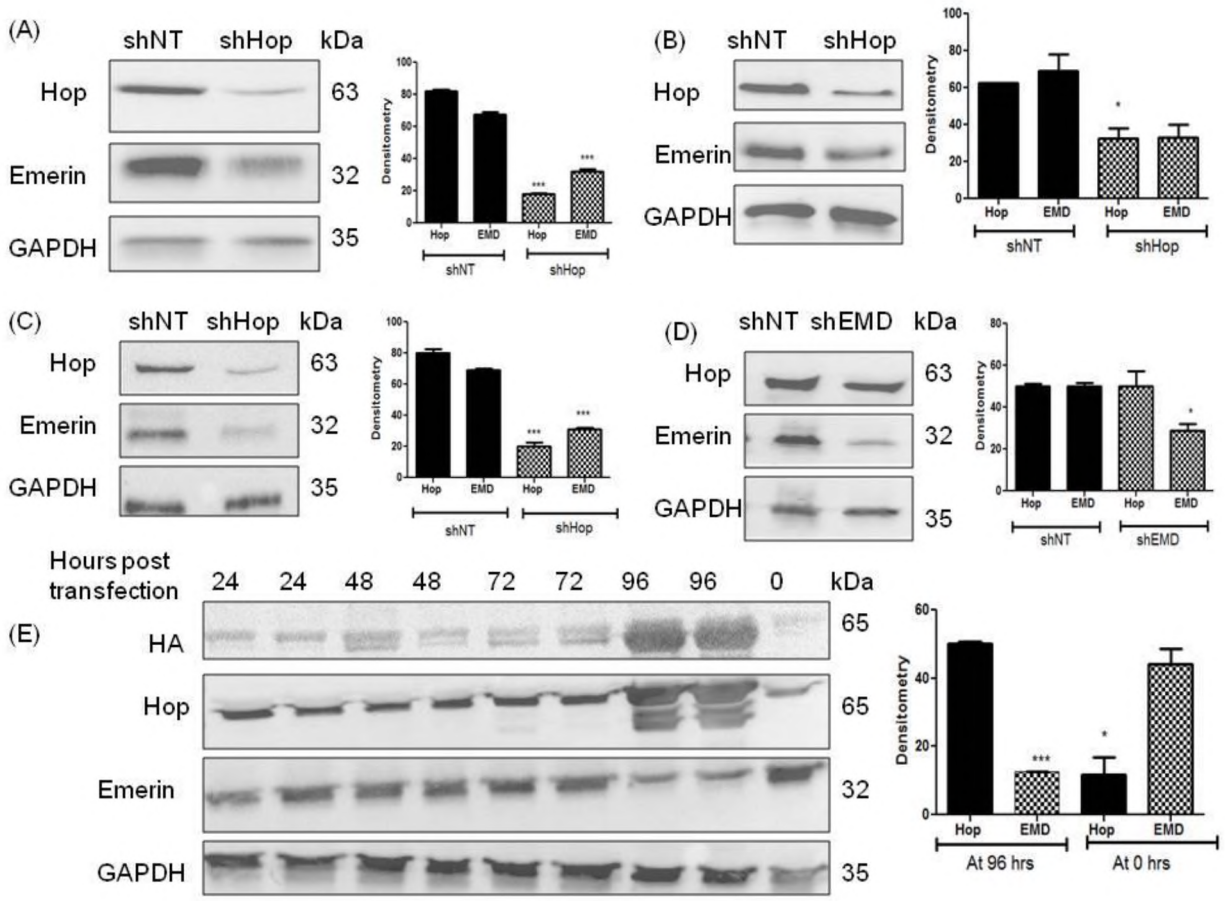

Figure 6 : Effect of the depletion and over expression of Hop on the levels of emerin
Lysates from (A) HEK293T-shHop (shHop) and HEK293T-shNT (shNT), (B) MCF7-shHop and MCF7-shNT, (C) MDA-shHop and the MDA-shNT and (D) HEK293T-shEMD (shEMD) and HEK293T-shNT (shNT) cell lines that had been induced for expression of shRNA for 96 hours were resolved by SDS-PAGE with subsequent Western blotting for detection of the levels of Hop, emerin and GAPDH. (E) Lysates from HEK293T cells that had been transfected with HA-Hop for different time points (24 to 96 hours) and a control that remained untransfected (UN) were resolved by SDS-PAGE followed by Western blotting for detection of the expression of HA-Hop, Hop, and emerin. The expression of GAPDH was used as a protein loading control in all cases. Beside each Western blot is a graph showing the average densitometry analysis of the levels of Hop and emerin. The data shown are representative of results obtained from 3 independent experiments. Statistical significance was assessed by comparison to the control samples where * indicates $p<0.05$, *** indicates $p<0.001$.

The same membrane was probed for emerin and the cytoplasmic fraction had a reduced band intensity in the lane containing the cytoplasmic portion from the HEK293T-shHop lysate (Figure 7A, cytoplasm, lane shHop) compared to the lane containing a cytoplasmic portion from the

HEK293T-shNT lysate (Figure 7A, cytoplasm, lane shNT). However, the nuclei from both the HEK293T-shHop lysate and the HEK293T-shNT lysate had uniform band intensities at the predicted molecular weight for emerin (Figure 7A, Nucleus, lanes shHop and shNT). The emerin staining observed from these isolates appears as double bands which is likely to be a result of different posttranslational modification. On probing for histone H3, the cytoplasmic fraction did not show any bands at the predicted molecular weight, but the nuclei from both the HEK293T-shHop lysate and the HEK293T-shNT lysate had bands of equal intensity (Figure 7A, Nucleus, lanes shHop and shNT).

The reduction in the band intensities in the lane containing both the cytoplasmic and nuclear fractions from the HEK293T-shHop lysate compared to the lane containing the control on probing for Hop indicates the depletion of Hop within both the cytoplasm and nucleus following expression of the Hop-specific shRNA. The uniform band intensities in the cytoplasmic portion from both the HEK293T-shHop lysate and the HEK293T-shNT lysate on probing for tubulin suggests the successful isolation of a cytoplasmic fraction; while the absence of bands corresponding to tubulin in lanes containing nuclei from the HEK293T-shHop lysate and the HEK293T-shNT lysate suggests lack of contamination of the nuclei with cytoplasmic material. The reduced band intensity on probing for emerin in the Hop depleted cytoplasmic portion correlates with the depletion of Hop in the same lane; while the enrichment of emerin in the nuclei from both the HEK293T-shHop lysate and the HEK293T-shNT lysate suggests the presence of emerin in the nucleoplasm. The absence of bands corresponding to histone H3 in the cytoplasmic fraction suggested the purity of the isolated cytoplasmic fraction while the even band intensities in the lanes containing nuclei from the HEK293T-shHop lysate and the

HEK293T-shNT lysate suggests equal protein loading in the two lanes (Figure 7A, Nuclei, lanes shHop and sh NT) and the successful isolation of nuclei.

We similarly isolated nuclei and cytoplasmic fractions using the EZ kit from HEK293T-shEMD cells and the control HEK293T-shNT (Figure 7B) and probed for the same proteins as reported above. On probing for Hop, the HEK293T-shEMD cytoplasmic fraction had a slightly reduced band intensity (Figure 7B, cytoplasm, lane shEMD) compared to the lane containing cytoplasmic material from the HEK293T-shNT control (Figure 7B, cytoplasm, lane shNT). The lanes containing nuclei from both the HEK293T-shEMD lysate the HEK293T-shNT control (Figure 7B, nuclei, lanes shEMD and shNT) had low levels of Hop at the same exposure which was similar to what was observed in the HEK293T-shNT nuclei isolates in Figure 7A. Like in Figure 7A, tubulin was only detected in the cytoplasmic fraction with the presence of bands of uniform intensity at the predicted molecular weight. However, on probing for emerin, unlike in Figure 7A, there was a reduction in the emerin band intensity within the lanes containing the cytoplasmic fraction (Figure 7B, cytoplasm, lane shEMD) and the nuclear fraction (Figure 7B, nuclei, lane shEMD) from the HEK293T-shEMD lysate compared to the control HEK293T-shNT (Figure 7B, cytoplasm and nuclei; lane shNT). On probing for histone H3, we observed bands of equal intensity within the lanes containing nuclei fraction from both the HEK293T-shEMD and the control HEK293T-shNT lysates (Figure 7B, nuclei, lanes shEMD and shNT) while the cytoplasmic fraction did not show any histone H3 bands at the predicted molecular weight.

The reduction in the band intensity within the lane containing a cytoplasmic portion from the HEK293T-shEMD lysate compared to the control on probing for Hop suggests the slight

depletion of Hop in the cytoplasm following expression of the EMD shRNA. The even band intensities in the cytoplasm on probing for tubulin served as our protein loading control besides suggesting successful isolation of cytoplasmic material, while the absence of tubulin bands in the nuclei from both the HEK293T-shEMD and the HEK293T-shNT suggests the purity of the isolated nuclei. The reduction in the band intensity in the shEMD lane in both the cytoplasmic and nuclei portion on probing for emerin suggests the depletion of both nuclear and cytoplasmic emerin following expression of the EMD-shRNA while the even band intensity in the nuclei portion from both lysates on probing for histone H3 served as our protein loading control. The absence of bands corresponding to histone H3 in the cytoplasmic fraction suggests the purity of the isolated cytoplasmic portion. Beneath each figure is the densitometry analysis of the levels of Hop and emerin in the cytoplasmic fraction (CT) depicting a significant reduction in the levels of emerin in the Hop depleted cytoplasmic portion and vice versa.

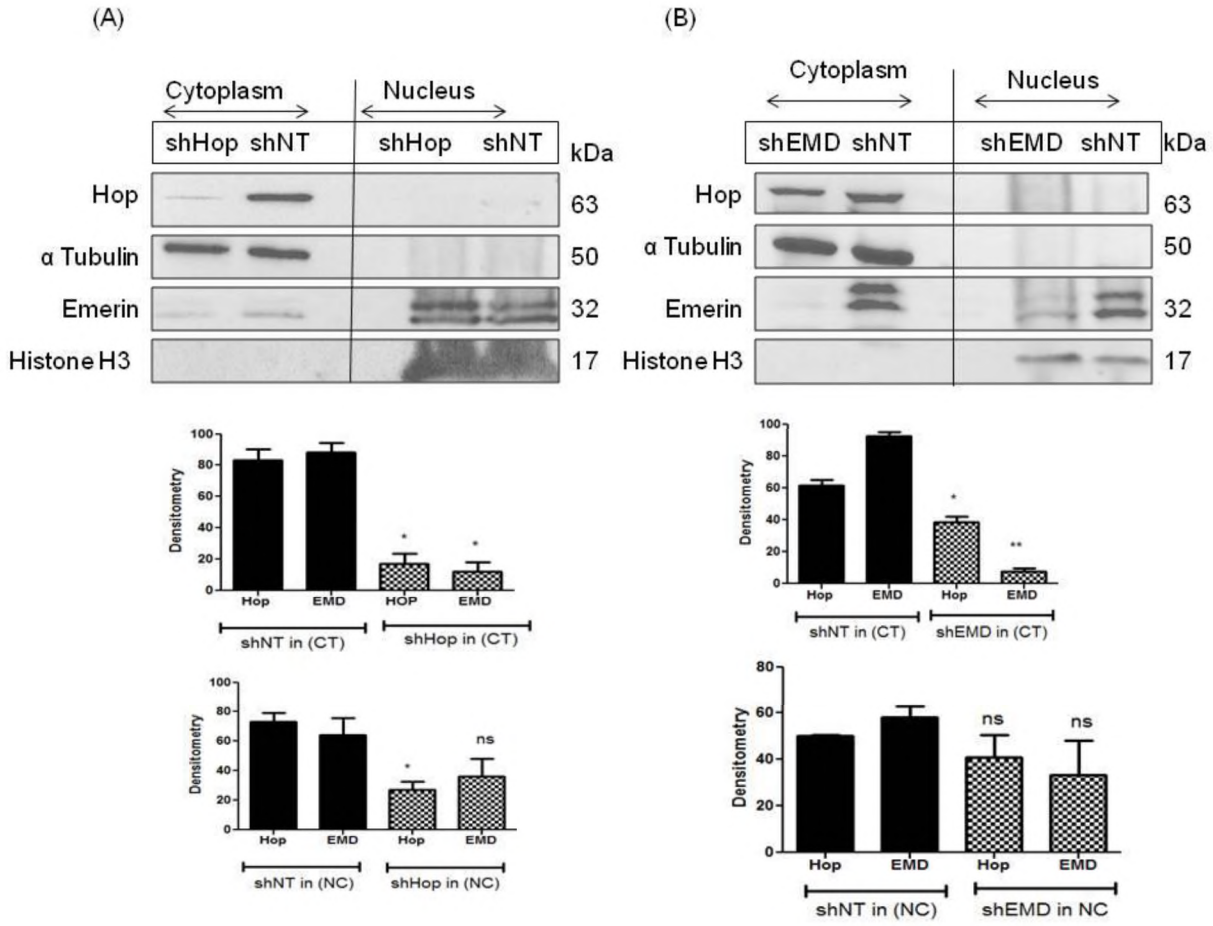

Figure 7: Western blot assessment of the effect of Hop depletion on the subcellullar levels of emerin

Figure 7A represents isolates from the HEK293T-shHop (shHop) and the control HEK293T-shNT (shNT) lysates isolated using the EZ nuclei isolation kit while 7B represents similar isolates from the HEK293T-shEMD (shEMD) and the control HEK293T-shNT lysates. Beneath each Western blot is a densitometry analysis of the levels of Hop and emerin from the cytoplasmic fractions (CT) and the nuclear fractions (NC) where (**) indicatesi a p value of < 0.01 while (*) indicates a p value of < 0.05 and ns indicates that the differences are not significant. These images are a representative of results obtained from 3 independent experiments in each case.

Depletion of Hop targets emerin for degradation

Having observed a reduction in the protein levels of emerin following depletion of Hop, we wanted to determine the mechanism by which emerin was being depleted. To establish if the

depletion of Hop induced the degradation of emerin via the proteasomal degradation pathway, we induced expression of the shRNA in HEK293T-shHop, HEK293T-shEMD and the control HEK293T-shNT cells for 72 hours and subsequently treated the cells with 10 μM of the proteasomal inhibitor (MG132) and continued the incubation for another 24 hours. Although incubation with MG132 can be toxic to cells could subsequently alter degradation, we obtained lysates and conducted a Western blot analysis using antibodies against Hop, emerin and alpha tubulin (as a loading control) (Figure 8A). The lanes containing lysates from the HEK293T-shHop cells [with and without MG132 (shHop)] had reduced Hop band intensities compared to the lanes containing the HEK293T-shNT lysates [with and without MG132 (shNT)] and lanes containing the HEK293T-shEMD lysates [with and without MG132 (shEMD)], which confirmed the depletion of Hop via expression of the Hop specific shRNA. However, on probing for emerin, the lane containing the HEK293T-shHop lysate that had been treated with the proteasome inhibitor (shHop) had an increased band intensity compared to the rest of the lanes at the same exposure. The lanes containing lysates from the HEK293T-shEMD [with and without MG132 (shEMD)] did not have any bands at the predicted molecular weight of emerin suggesting depletion of emerin following expression of the shEMD specific RNA. A probe with alpha tubulin depicted bands of equal intensity across all lanes which serves as our protein loading control since tubulin is a member of the cytoskeleton network whose members are known to be resistant to degradation (Song *et al.*, 1997). The increased emerin band intensity in the lane containing the lysate from the HEK293T-shHop sample that had been treated with the proteasomal inhibitor (shHop) compared to the other lanes suggested that the depletion of Hop resulted in degradation of emerin via the proteasome and that the effect could be reversed on treating cells with a proteasome inhibitor.

Similarly, we determined if the depletion of Hop induced the degradation of emerin via the lysosomal degradation pathway (Figure 8B). We induced expression of the shRNA in HEK293T-shHop, HEK293T-shEMD and the control HEK293T-shNT cells for 72 hours and subsequently treated the cells with 100 μM chloroquine and continued the incubation for another 24 hours. We obtained lysates and conducted a Western blot analysis using antibodies against Hop, emerin and alpha tubulin (as a loading control) (Figure 8B). The lanes containing lysates from the HEK293T-shHop cells [with and without chloroquine (shHop)] had reduced Hop band intensities compared to the lanes containing the HEK293T-shNT lysates [with and without chloroquine (shNT)] and lanes containing the HEK293T-shEMD lysates [with and without chloroquine (shEMD)], which confirmed the depletion of Hop via expression of the Hop specific shRNA. However, on probing for emerin, the lane containing the HEK293T-shHop lysate that had been treated with chloroquine (shHop) had an increased band intensity compared to the lane containing the HEK293T-shHop lysate that had not been treated with chloroquine at the same exposure. The lanes containing lysates from the HEK293T-shEMD [with and without chloroquine (shEMD)] had reduced band intensities compared to the lanes containing the HEK293T-shNT lysates [with and without chloroquine (shNT)] at the predicted molecular weight of emerin suggesting depletion of emerin following expression of the shEMD specific RNA. The increased emerin band intensity in the lane containing the lysate from the HEK293T-shHop sample that had been treated with the chloroquine (shHop) compared to the untreated sample suggested that the depletion of Hop resulted in degradation of emerin via the lysosomal degradation pathway.

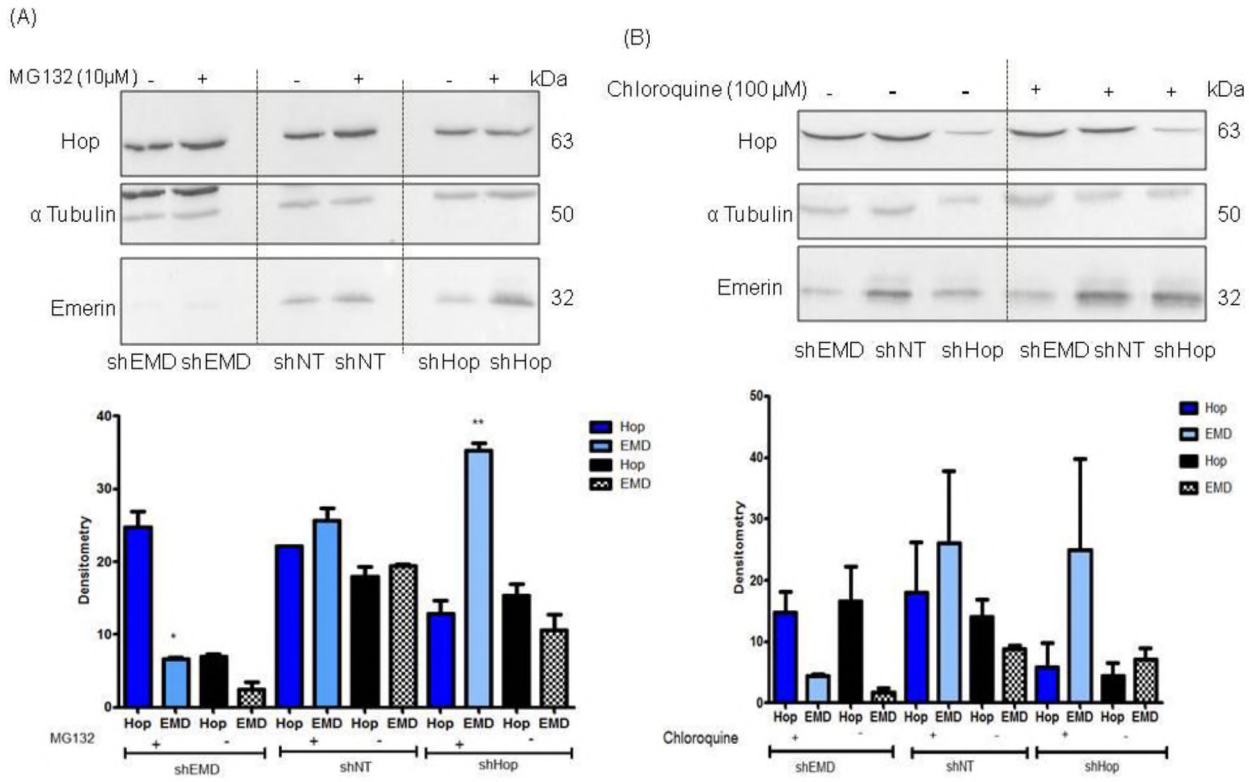

Figure 8: Depletion of Hop via shRNA targets emerin for proteasomal and lysosomal degradation:

(A) Lysates from HEK293T-shHop, HEK293T-shEMD, and HEK293T-shNT cell lines that had been induced for expression of shRNA for 72 hours then treated with 10 μM MG132 and incubated for another 24 hours. (B) Lysates from HEK293T-shHop, HEK293T-shEMD, and HEK293T-shNT cell lines that had been induced for expression of shRNA for 72 hours then treated with chloroquine and incubated for another 24 hours. In both cases, lysates were resolved by SDS-PAGE with subsequent Western blotting for detection of the levels of Hop, emerin and alpha tubulin. - denotes the sample that was induced for shRNA expression but not treated with inhibitor, while + denotes that the sample was induced for expression of the shRNA and later treated with the inhibitor, beside each Western blot is a densitometry analysis where (**) indicates a p value of <0.01 while (*) indicates a p value <0.05. These images are a representative of results obtained from 3 independent experiments.

Knockdown of Hop results in the mislocalization of emerin and *vice versa*

We used immunofluorescence staining and confocal microscopy to assess the impact of the depletion of Hop on emerin localization and *vice versa* (Figure 9). The Hop staining pattern was predominantly in the cytoplasm and appeared bright in the HEK293T-shNT cells (Figure 9A, upper panel, red) and brighter in the HEK293T-shEMD cells (Figure 9A, middle panel, red) compared to the HEK293T-shHOP cells. In the HEK293T-shEMD cells there was increased Hop staining within the nucleus which suggested the mislocalization of Hop following the depletion of emerin. In the HEK293T-shHop cells (Figure 9A, bottom panel, red) the staining for Hop was of a lower intensity compared to the HEK293T-shNT control which is consistent with the loss of Hop protein levels observed in Western blot assays.

The emerin staining in the HEK293T-shNT cells (Figure 9B, upper panel, green) was observed in the cytoplasm and in a ring around the nuclear periphery which represents the NE. The emerin staining in the HEK293T-shEMD cells (Figure 9B, middle panel, green) was of a lower intensity compared to the staining in the HEK293T-shNT cells which is consistent with the loss of emerin observed in Western blot assays. In the HEK293T-shHop cells, the emerin staining appeared brighter and more diffuse in both the cytoplasm and the nucleus without the distinct nuclear periphery staining (Figure 9B, bottom panel, green) which suggested the mislocalization of emerin following the depletion of Hop.

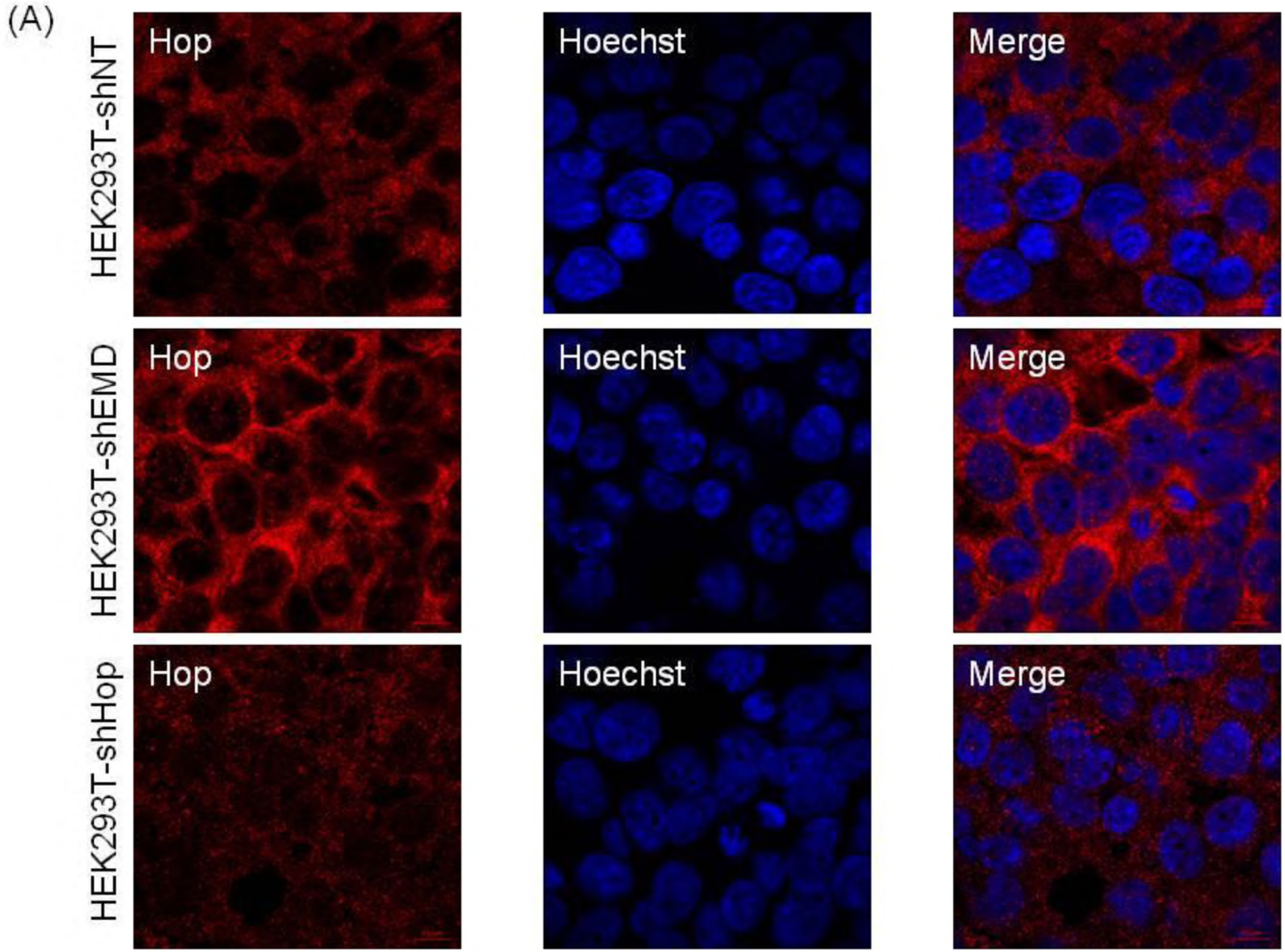
(A)
HEK293T-shNT
HEK293T-shEMD
HEK293T-shHop
Hop
Hoechst
Merge
Hop
Hoechst
Merge
Hop
Hoechst
Merge

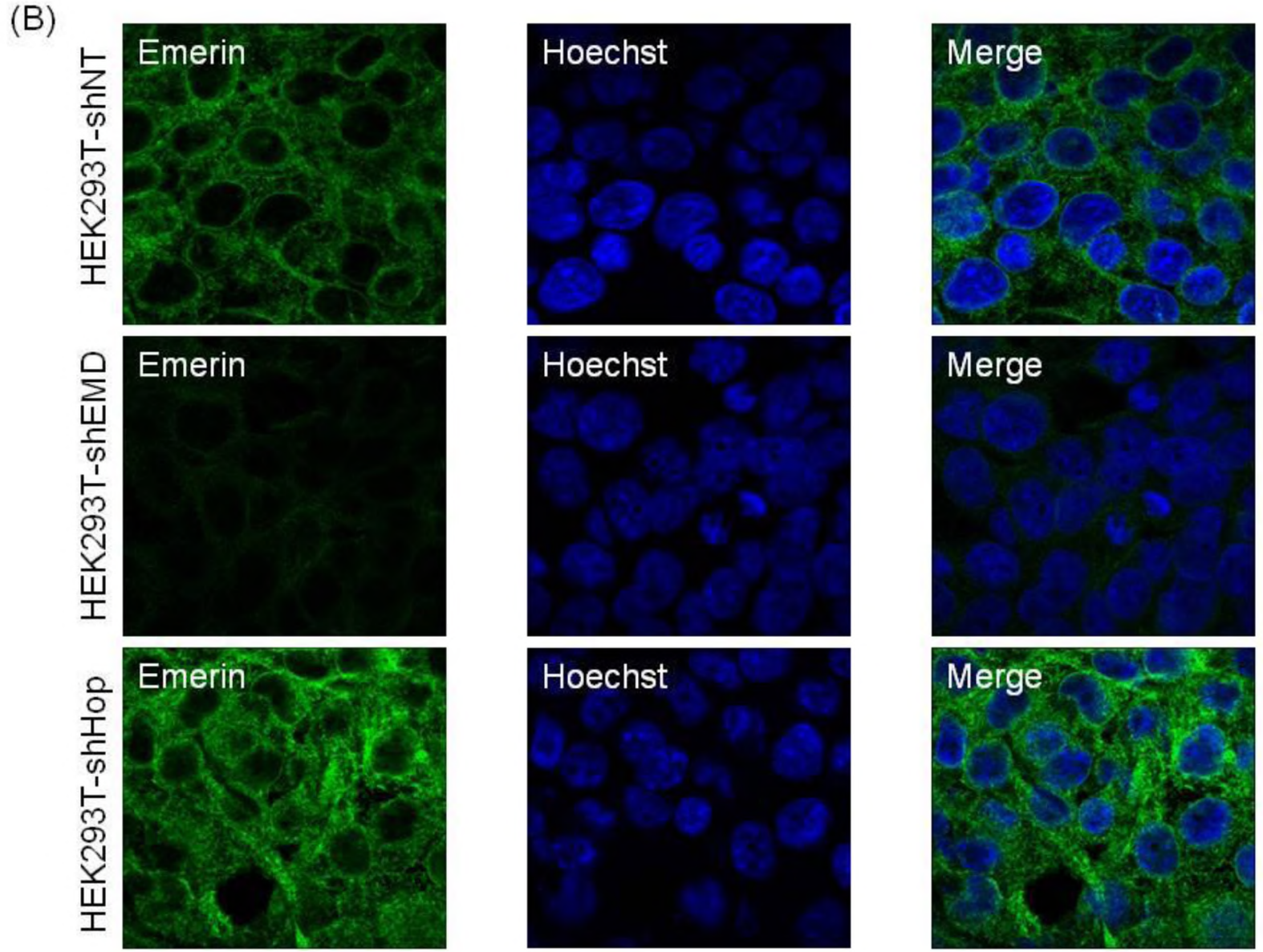
(B)
HEK293T-shNT
HEK293T-shEMD
HEK293T-shHop
Emerin
Hoechst
Merge
Emerin
Hoechst
Merge
Emerin
Hoechst
Merge

Figure 9: Immunofluorescence staining and confocal microscopy analysis of the effect of the depletion of Hop on the localization of emerin and *vice versa*

HEK293T-shNT, HEK293T-shEMD and HEK293T-shHop cells were induced for shRNA expression for 96 hours and stained for Hop (red) in (A) and emerin (green) in (B). The nucleus is stained blue with Hoechst 33342 (1 µg/ml). The images were acquired on the Zeiss LSM 780 confocal microscope (scale bar 10µm). These images are a representative of results obtained from 3 independent experimen

Effect of Hop depletion on emerin binding partners

We used antibodies provided in the Nucleus and Nuclear Envelope-Associated Marker Proteins Antibody Sampler Kit to assess the effect of the depletion of Hop and emerin on other nuclear associated proteins using nuclear isolates obtained using the EZ kit. When we tested for the effect of the depletion of both Hop and emerin on lamin A-C proteins, we observed increased band intensities in the lanes containing nuclei from the HEK293T-shHop and the HEK293T-shEMD (Figure 10, lanes shHop and shEMD) cells compared to the lane containing nuclei from the control HEK293T-shNT (Figure 10, lane shNT) cells. The observed increase in the band intensity at the predicted molecular weight for lamin A-C in the lanes containing nuclei from the HEK293T-shHop and the HEK293T-shEMD lysates compared to the control HEK293T-shNT suggests an increase in the expression of lamin A-C in the nucleus following the depletion of emerin. The levels of histone H3 were used as our protein loading control. Beside the Western blot is a densitometry analysis indicating a significant increase in the expression of lamin A-C especially in the HEK293T-shEMD lysates compared to the HEK293T-shNT control.

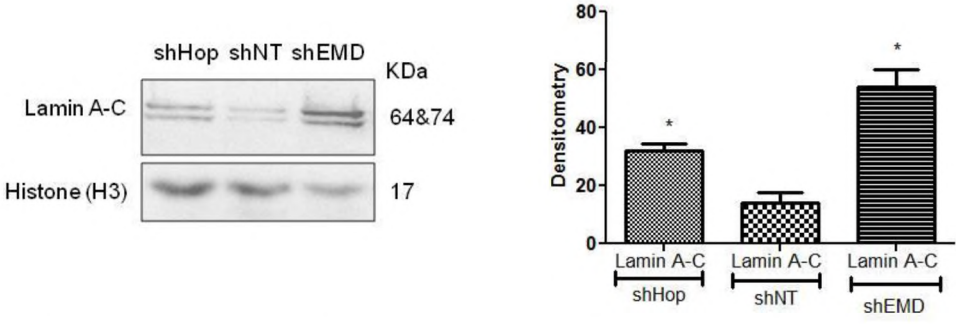

Figure 10: Western blot analysis of the effect of the depletion of Hop and emerin on the expression of lamin A-C

Nuclear fractions from HEK293T-shHop (shHop), HEK293T-shEMD (shEMD) and the control HEK293T-shNT (shNT) cells were resolved by SDS-PAGE and probed for lamin A-C. Beside the Western blot is a densitometry analysis of the levels of lamin A-C across the 3 samples where * indicates p value of <0.05. This image is a representative of results obtained from 3 independent experiments.

We further used immunofluorescence staining and confocal microscopy to assess the impact of the depletion of Hop and emerin on the localization lamin A-C and tubulin that both bind emerin (Hale *et al.*, 2008). In Figure 11A, the lamin A-C staining appeared to demarcate a ring around the nucleus in the HEK293T-shNT cells (Figure 11A, upper panel, red), which is consistent with the location of the nuclear lamina (Towbin *et al.*, 2013), while the staining in the HEK293T-shEMD cells (Figure 9A, middle panel, red) and the HEK293T-shHop cells (Figure 11A, bottom panel, red) appeared brighter compared to the staining in the HEK293T-shNT cells with an increased staining within the nucleus, rather than just at the periphery. This suggested an increase in the expression of lamin A-C following the depletion of emerin in both the HEK293T-shHop and the HEK293T-shEMD cells which correlates with the results obtained in the Western blot.

The tubulin staining in the HEK293T-shNT cells (Figure 11B, top panel, green) appeared to be confined within the cytoplasm, while the staining in the HEK293T-shEMD cells (Figure 11B, middle panel, green) appeared dull suggesting a mislocalizaton of tubulin following emerin depletion. The tubulin staining in the HEK293T-shHop cells appeared as a filamentous staining within the cytoplasm (Figure 11B, bottom panel, green) suggesting a mislocalization of tubulin in these cells. These data are not unexpected as both Hop and emerin bind tubulin (Hale *et al.*, 2008; Li *et al.*, 2012b)

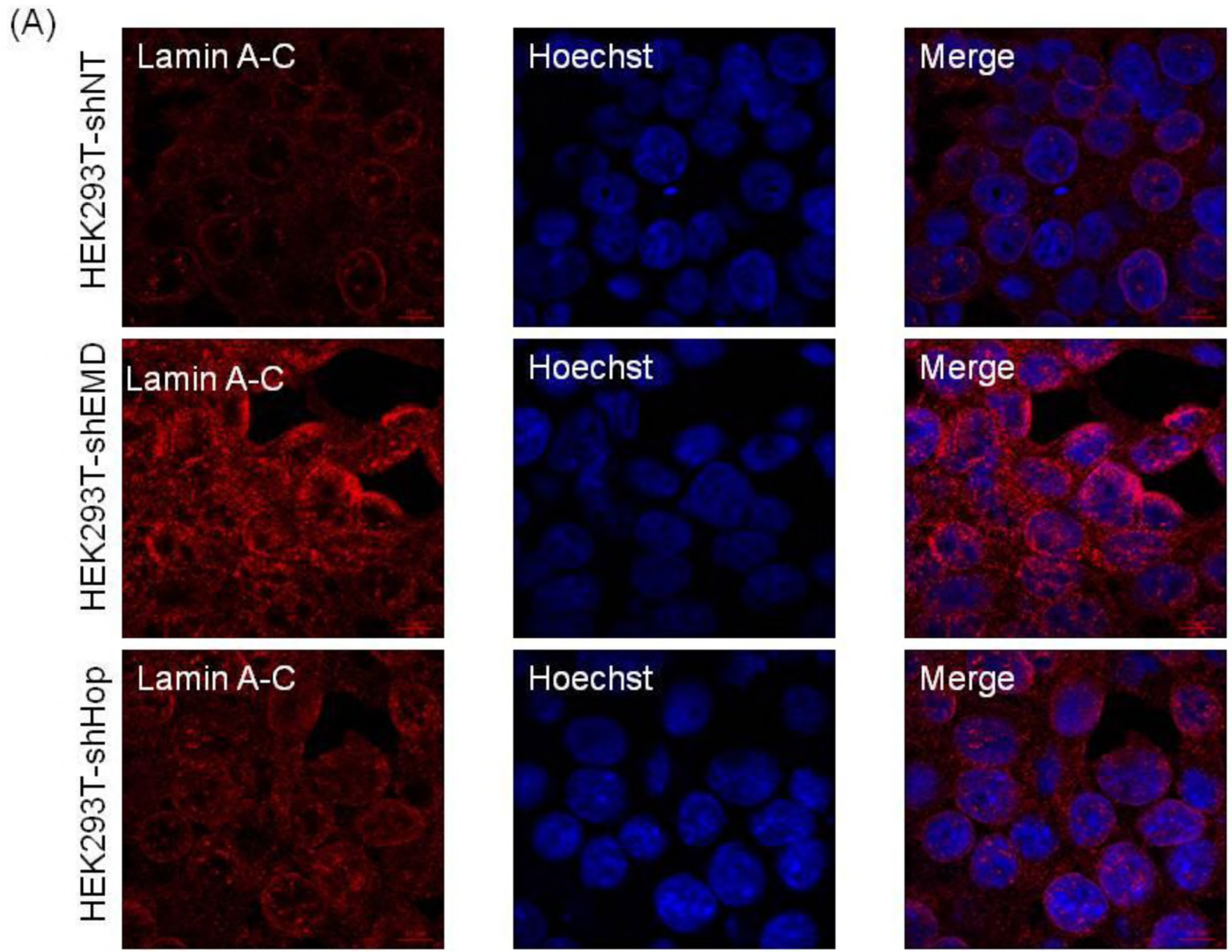
(A)
HEK293T-shNT
Lamin A-C
Hoechst
Merge
HEK293T-shEMD
Lamin A-C
Hoechst
Merge
HEK293T-shHop
Lamin A-C
Hoechst
Merge

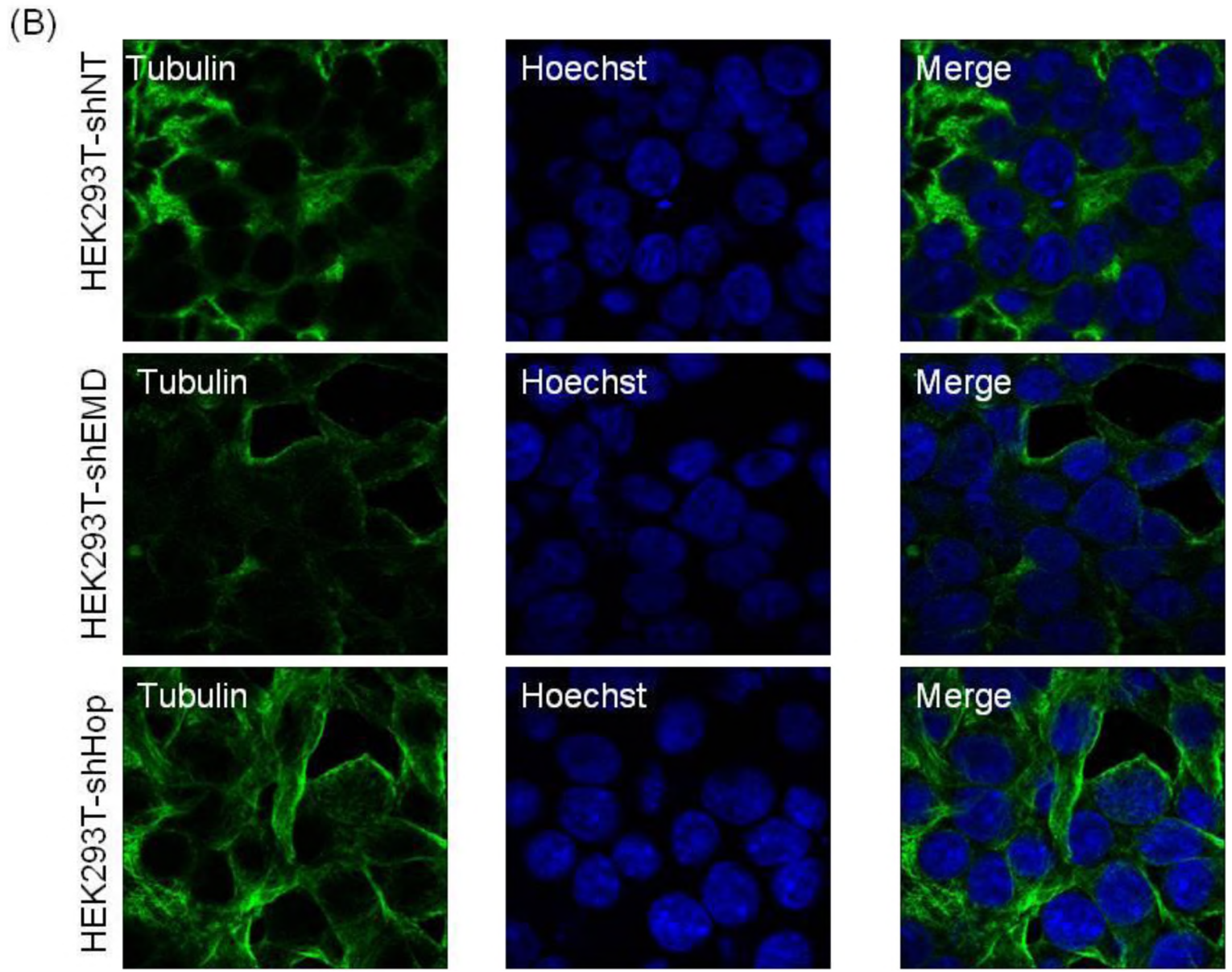
(B)
HEK293T-shNT
Tubulin
Hoechst
Merge
HEK293T-shEMD
Tubulin
Hoechst
Merge
HEK293T-shHop
Tubulin
Hoechst
Merge

Figure 11: Immunofluorescence staining and confocal microscopy analysis of the effect of the depletion of Hop and emerin on expression and localization of emerin binding partners

HEK293T-shNT, HEK293T-shEMD and HEK293T-shHop cells were induced for shRNA expression for 96 hours and co-stained for lamin A-C (red) in (A) and tubulin (green) in (B). The nucleus is stained blue with Hoechst 33342 (1 µg/ml). The images were acquired on the Zeiss LSM 780 confocal microscope (scale bar 10µm). These images are a representative of results obtained from 3 independent experiments.

The depletion of Hop and emerin results into the mislocalization of emerin binding partners in mitotic cells

We synchronised HEK293T-shNT, HEK293T-shEMD and HEK293T-shHop cells that had been induced for shRNA expression for 96 hours with 10μg/ml of nocodazole for 12 hours prior to determining the effect on lamin A-C and tubulin. This treatment was aimed at arresting cells in mitosis by interfering with the polymerization of microtubules before releasing them into the G1 phase. In Figure 12A, the lamin A-C staining in the HEK293T-shNT cells (Figure 12A, top panel, red) was predominantly in the cell cortex in both mitotic and non-mitotic cells (Figure 12A, top panel, arrows) while the staining in the HEK293T-shEMD (middle panel) and HEK293T-shHop (bottom panel) cells was observed in the cell cortex and nucleus in non-mitotic cells (Figure 12A, middle and bottom panels, arrows) and in distinct red punctae that localized to the edges of the nucleus in mitotic cells (Figure 12A, middle and bottom panel, arrows). The staining in the HEK293T-shNT cells is consistent with the expected localization of lamin A-C following the depolymerization of microtubules via nocodazole treatment (Qi *et al.*, 2016) while the staining in the HEK293T-shEMD and HEK293T-shHop cells suggested an increase in the expression of lamin A-C in the absence of emerin. The staining for alpha tubulin in the HEK293T-shNT cells (Figure 12B top panel, green, arrow) was predominantly in the cell cortex and appeared similar to the lamin A-C staining observed in Figure 12A. In the HEK293T-shEMD and HEK293T-shHop cells, the tubulin staining appeared brighter compared to the staining in the HEK293T-shNT cells and was observed in both the cell cortex and within the nucleus (Figure 12B, middle and bottom panels, arrows) which suggested the mislocalization of tubulin.

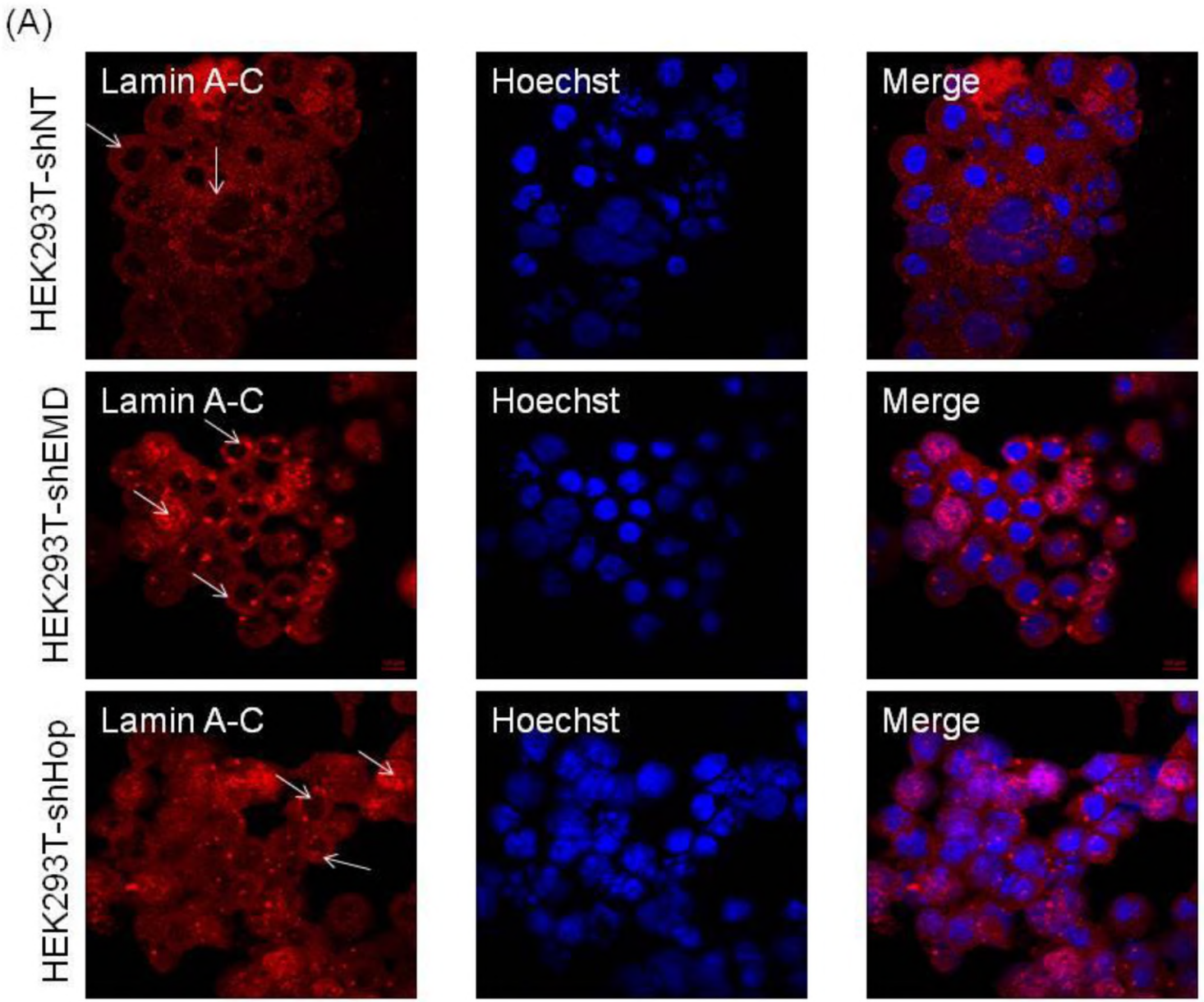
(A)
HEK293T-shNT
HEK293T-shEMD
HEK293T-shHop
Lamin A-C
Hoechst
Merge
Lamin A-C
Hoechst
Merge
Lamin A-C
Hoechst
Merge

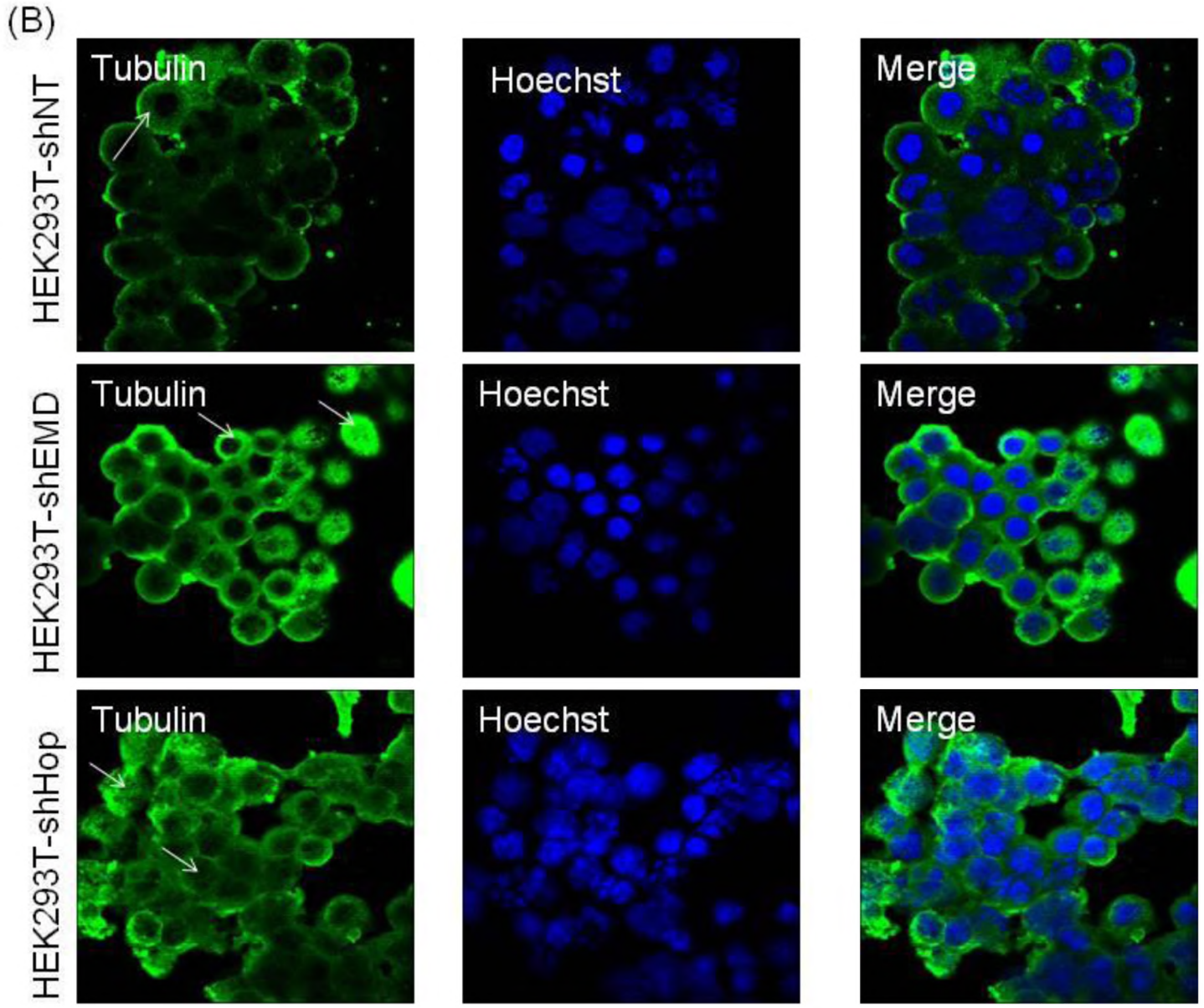
(B)
HEK293T-shNT
HEK293T-shEMD
HEK293T-shHop
Tubulin
Hoechst
Merge
Tubulin
Hoechst
Merge
Tubulin
Hoechst
Merge

Figure 12: Immunofluorescence staining and confocal microscopy analysis of the effect of Nocodazole on the expression and localization of emerin binding partners following the depletion of Hop and emerin

HEK293T-shNT, HEK293T-shEMD and HEK293T-shHop cells were induced for shRNA expression for 96 hours then treated with nocodazole for 12 hours and co-stained for lamin A-C (red) in (A) and tubulin (green) in (B). The nucleus is stained blue with Hoechst 33342 (1 µg/ml). The arrow heads illustrate the staining in the cell cortex and within the nucleus. The images were acquired on the Zeiss LSM 780 confocal microscope (scale bar 10µm). These images are a representative of results obtained from 3 independent experiments.

Hop and emerin colocalize in cells

Having determined that Hop depletion resulted in degradation and mislocalization of emerin, we next wanted to establish if Hop and emerin might interact. We first used immunofluorescence staining coupled with confocal microscopy to assess the localization of Hop and emerin in HEK293T cells (Figure 13). Emerin expression was detected in the cytoplasm but was also concentrated in perinuclear staining that represents the nuclear envelope. Hop was expressed throughout the cytoplasm and in the nucleus. In some cases, punctae nuclear Hop staining was observed (Figure 13A, arrow). A merge of the emerin and Hop channel suggested colocalization of the two signals, particularly in the perinuclear region. The colour scattergram indicated a linear relationship between the red and green pixels which is indicative of pixel-on-pixel colocalization. Using Pearson's correlation coefficient analysis, we also observed a good colocalization between Hop and emerin ($Rr = 0.721 \pm 0.049$).

To confirm that Hop and emerin are located in the same organelles, we subsequently performed a nuclear and cytoplasmic fractionation in HEK293T cells followed by Western blot analysis of the protein levels (Figure 13B). The alpha tubulin detection depicted a band within the lane containing the cytoplasmic fraction (CT) and not in the lane containing the nuclear fraction (NC). A probe with histone H3 depicted a band at the predicted molecular weight within the lane containing the nuclear fraction (NC) and not in the lane containing the cytoplasmic fraction. Taken together, the tubulin and histone profiles suggested the successful separation of the nuclear and cytoplasmic fraction and the lack of contamination of the cytoplasmic fraction with nuclear material (and *vice versa*). When we probed for Hop, we observed bands at the predicted molecular weight in lane containing both the nuclear (NC) and the lane containing the cytoplasmic (CT) fraction, although the band corresponding to nuclear Hop was of a lower

intensity compared to the cytoplasmic Hop band. This suggested that the isolated nuclei has a lower concentration of Hop compared to the cytoplasm.

On probing for emerin, we observed a band at the predicated molecular weight within the lane containing a nuclear fraction (NC) which suggested that emerin and Hop (also observed in the same lane) can both localize in the nucleus. The lack of a band corresponding to the predicted molecular weight of emerin in the cytoplasmic fraction suggested the low concentration of emerin in the isolated cytoplasmic fraction. Taken together, these data suggest that Hop and emerin colocalized in HEK293T cells, which suggested that an interaction between the two proteins in cells would be possible. Beneath this Western blot is a densitometry analysis depicting the levels of Hop and emerin from the nuclear fractions where the levels of emerin are significantly high compared to the levels of Hop.

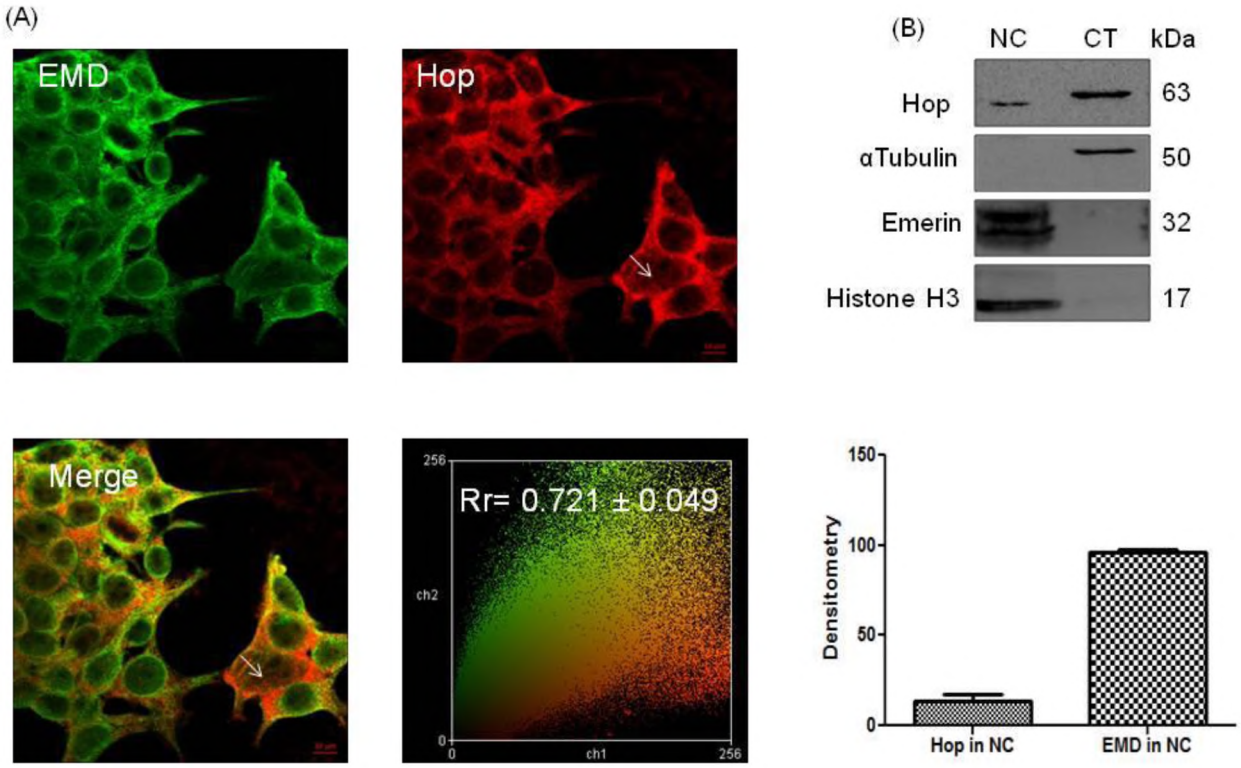

Figure 13: Hop and emerin colocalise in cells

(A) HEK293T cells were seeded on coverslips and stained for Hop (red) and emerin (green) and images acquired on the Zeiss LSM 780 confocal microscope (scale bar 10µm). The arrow head illustrates the Hop staining within the nucleus. (B) Western blot analysis of a nuclear and a cytoplasmic fractions from HEK293T cells with subsequent detection of the levels of Hop and emerin and beneath it is a densitometry analysis of the levels of Hop and emerin from the nuclear (NC) fractions. These images are a representative of results obtained from 3 independent experiments.

Hop and emerin are in a common complex

In order to determine if Hop is part of the emerin interactome, we first performed an immunoprecipitation using GFP magnetic beads from lysates transfected for 48 hours with a GFP-emerin plasmid or untransfected control lysates (Figure 14A). Using Western blotting, we observed bands corresponding to the predicted molecular weights of lamin A-C, Hop, GFP-emerin and histone H3 in the lane containing the immunoprecipitate from the GFP-emerin transfected lysate and no bands in the lane containing an immunoprecipitate from the untransfected control. The lack of bands in the lane containing the immunoprecipitate from the untransfected lysate suggested lack of unspecific binding. We did not observe any band corresponding to the predicted molecular weight of Hsp90 in the lane containing the immunoprecipitate from the GFP-emerin transfected lysate. These data suggested that lamin A-C, Hop and histone H3 are in a common complex with emerin and that Hsp90 is not required for the formation of this complex.

We next performed HA-co-immunoprecipitation from lysates made from HEK293T cells transfected with the pcDNA3.1-HA-Hop plasmid for 48 hours. Lysates from HEK293T cells that remained untransfected were included as a control. Western blot analysis indicated bands corresponding to the predicted molecular weights of Hsp90, HA-Hop and emerin in the lane containing the immunoprecipitate from the pcDNA3.1-HA-Hop transfected lysate and no bands corresponding to the predicted molecular weight of lamin A-C (Figure 14B). The lane containing the immunoprecipitate from the untransfected lysate did not show any bands. The absence of bands in the lane containing the immunoprecipitate from the untransfected lysate indicates the lack of non-specific protein binding to the HA-agarose column. The absence of bands corresponding to the predicted molecular weight of lamin A-C in the lane containing an

immunoprecipitate from the transfected sample suggested that lamin A-C does not form a complex with Hop. The presence of bands at the predicted molecular weight of Hsp90, HA-Hop and emerin suggests that emerin and Hsp90 form complexes with Hop.

We confirmed if Hsp90 was required for the complex formed between Hop and emerin using lysates from HEK293T cells transfected with the pcDNA3.1-HA-HSP90 plasmid for 48 hours and treated as above (Figure 14C). The lane containing the immunoprecipitate from the pcDNA3.1-HA-Hsp90 transfected lysate had bands corresponding to HA-Hsp90 and Hop, but did not show any emerin band. The lane containing the immunoprecipitate from the untransfected lysate did not show any bands, which suggested lack of non-specific binding to the HA-agarose column. The presence of a HA-Hsp90 band in the immunoprecipitate from the pcDNA3.1-HA-Hsp90 transfected lysate indicated that the immunoprecipitation protocol was successful. The presence of a Hop band in the same lane indicated that Hop was isolated in a complex with Hsp90 while the absence of a band corresponding to emerin in the HA-Hsp90 immunoprecipitate suggested that Hsp90 is not required for Hop to interact with emerin. These data correlate with the lack of Hsp90 observed in the emerin immunoprecipitates (Figure 14A).

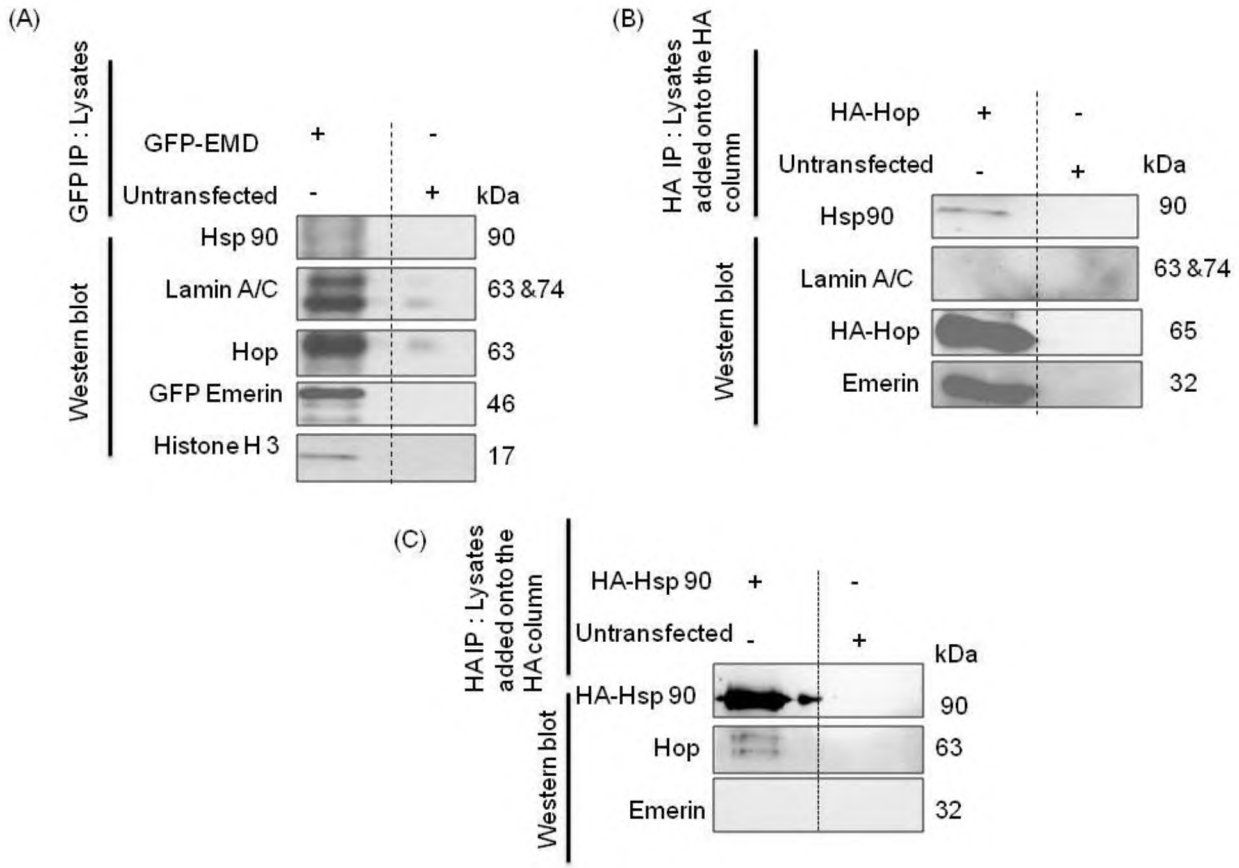

Figure 14: Analysis of the interaction between Hop and emerin via immunoprecipitation
(A) Lysates from HEK293T cells transfected with the GFP-emerin plasmid and subsequently immunoprecipitated alongside an untransfected control using GFP magnetic beads were resolved by SDS-PAGE followed by Western blot analysis of expected protein complex. (B) Lysates from HEK293T cells transfected with the pcDNA3.1-HA-HOP plasmid and subsequently immunoprecipitated alongside an untransfected control using a HA co-immunoprecipitation kit were resolved by SDS-PAGE followed by Western blot analysis of expected protein complex. The same procedure was used in (C) to detect complex formation following transfection of HEK293T cells with the pcDNA3.1-HA-HSP90 plasmid. (-) denotes absence of treatment while (+) denotes presence of indicated treatment. The data shown are representative of results obtained from 3 independent experiments.

Knockdown of Hop distorts the shape of the nucleus and reduces nuclear size

Given that emerin is a component of the nuclear envelope, we next determined whether the depletion of Hop and or emerin had any effect on the nuclear structure using transmission electron microscopy (TEM). We induced the expression of shRNA in the HEK293T-shHop, HEK293T-shEMD and the control HEK293T-shNT for 96 hours and confirmed the effect on protein expression in a Western blot before proceeding to perform TEM. In Figure 15 below, (A) depicts a Western blot on lysates obtained HEK293T-shHop cells and the control HEK293T-shNT cells, while (B) depicts a Western blot on lysates obtained from HEK293T-shEMD cells and the control HEK293T-shHop cells. These data confirmed a depletion of Hop and emerin in induced HEK293T-shHop cell lysates (Figure 15A) and in induced HEK293T-shEMD lysates (Figure 12B) compared to the control HEK293T-shNT lysates (Figure 15A and B).

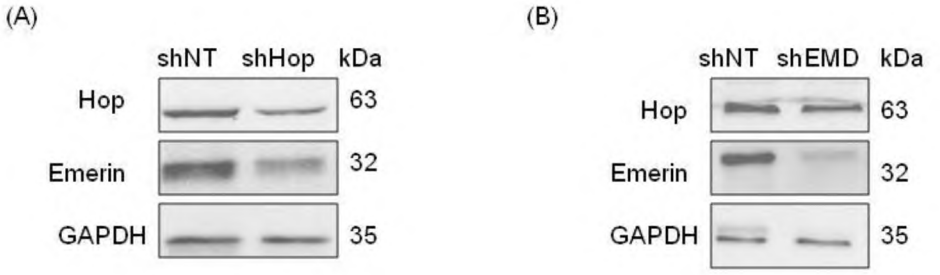

Figure 15 : Confirmation of the depletion of Hop and emerin levels prior to TEM
HEK293T-shHop and HEK293T-shNT (A) and HEK293T-shEMD and the control HEK293T-shNT (B) were induced for expression of shRNA for 96 hours and the effect on protein levels of Hop and emerin analyzed using a Western blot. These images are a representative of results obtained from 3 independent experiments.

We proceeded to analyze the cell samples by TEM and subsequently compared the nuclear shape and size of the acquired images. In Figure 16 below, (A) depicts images from the HEK293T-shNT cells (upper panel), the HEK293T-shEMD cells (middle panel) and the HEK293T-shHop cells (bottom panel). The nuclear structure in the HEK293-shNT cells (Figure 16A, upper panel) was characterized by a smooth nuclear margin with a round or oval shape which is close to the morphology of a normal nucleus (Bussolati *et al.*, 2008; Webster *et al.*, 2009; D'Arrigo *et al.*, 2010), while the structure of the nucleus in the HEK293T-shEMD cells and the HEK293T-shHop cells (Figure 16A, middle and bottom panel) were characterized by invagination in the nuclear margin and an irregular shape.

We subsequently compared the size of the nucleus from the HEK293-shNT cells and the HEK293T-shHop cells (Figure 16B) and from the HEK293-shNT cells and the HEK293T-shEMD cells (Figure 16C) using Image J. The mean area of the nucleus was compared using an unpaired t-test in Graph pad prism 5. The data is depicted using the mean ±SD at a P value of <0.05, in a sample size of 20 nuclei in each arm. In B, the nuclei from the HEK293-shNT cells had a higher mean ± SD compared to the nuclei from the HEK293T-shHop cells and the difference was statistically significant (P value = **0.0148**). Similarly in C, the nuclei from the HEK293-shNT cells had a higher mean ± SD compared to the nuclei from the HEK293T-shEMD cells and the difference was statistically significant (P value = **0.0001**). The results obtained indicated that the depletion of either Hop or emerin affects the nuclear shape and size in a similar manner. This suggested that the effects of Hop depletion on the nuclear morphology are due to the associated loss in emerin.

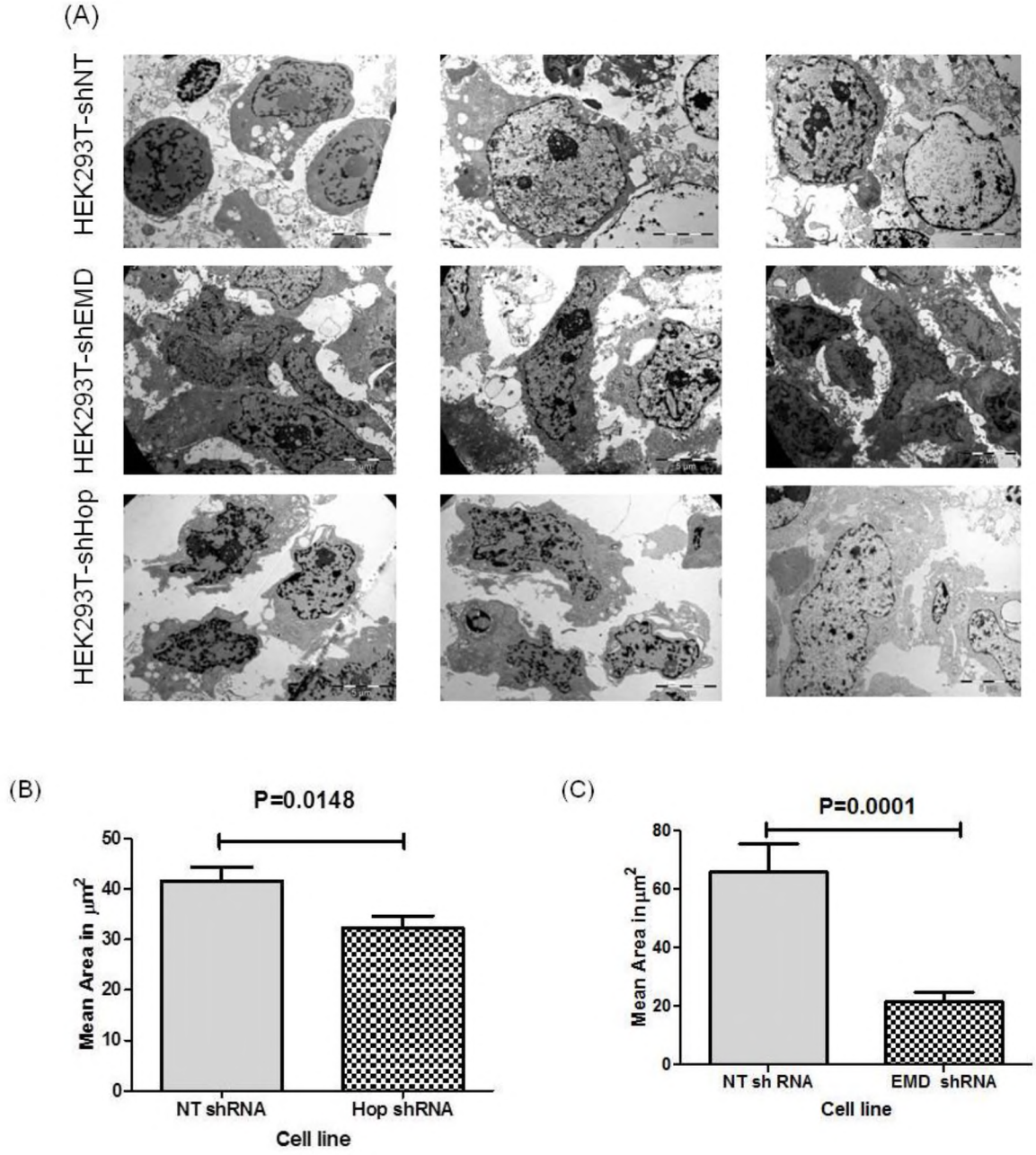

Figure 16 : Comparison of the nuclear structure and size following TEM
HEK293T-shNT, HEK293T-shEMD and HEK293T-shHop cells (A) were induced for expression of shRNA and the effect on the structure on the nucleus determined following image acquisition by TEM. The 3 images in each panel represent 3 independent replicates. The sizes of the nucleus from (B) HEK293T-shHop and HEK293T-shNT cells and (C) HEK293T-shEMD and the control HEK293T-shNT cells were determined in Image J and the mean area compared using an unpaired t-test in Graphpad prism 5. These data are a representative of results obtained from 3 independent experiments.

Depletion of Hop and emerin increases long term survival after transwell migration

In order to assess the effect of changes in nuclear structure on cell survival, we designed an experiment to analyze the effects of mechanical stress on the nucleus. We predicted that transwell migration would necessitate the restriction of the nucleus through pores and would result in cells displaying the effects of nuclear fragility in the Hop and emerin depleted backgrounds. Following induction of the expression of the shRNA in the HEK293T-shHop, HEK293T-shEMD and the HEK293-shNT cells, we assessed the effect on the transwell migration and the long term survival of cells using a combination of the QCM^{TM} 24 well transwell migration assay and the clonogenic assay (Yang, 2012). In Figure 17A, cells that had migrated through the pores and those that had not migrated (cells obtained from the top side of the chamber inserts) were seeded at an equal density in 6 well plates and allowed to grow for same period of time (13 days). On harvesting and staining the cells, we noted that migrated cells showed a reduced long term survival compared to cells obtained from the upper chamber (non-migrated cells) for all three cell lines. However, we observed that the wells containing cells that did not migrate through the pores did not depict any differences in the ability to grow in long term culture across the three cell lines (Figure 17A top panel). In contrast, HEK293T-shHop, and the HEK293T-shEMD cells showed greater long term survival than the HEK293T-shNT cells following passage through the pores as evidenced by their ability to form more colonies (Figure 17A bottom panel). These data suggested that the Hop and emerin depleted cells were more capable of survival as single colonies in culture compared to the HEK293T-shNT cells but only after transwell migration. Cells that did not pass through the pores remained equally unaffected by the changes in the growth conditions. We did a particle analysis of the colonies formed for triplicate assays using ImageJ and the results obtained suggested that the cells that did not pass

through the pores were equally unaffected (Figure 17B) by the growth conditions while the HEK293T-shHop, and the HEK293T-shEMD (Figure 17C) cells formed more colonies compared to the HEK293T-shNT cells following transwell migration. The mean number of colonies formed was compared using a one way ANOVA in Graph pad prism 5 at a P value of <0.05. These data suggested that depletion of Hop and emerin increases the ability of cells to survive in single colonies.

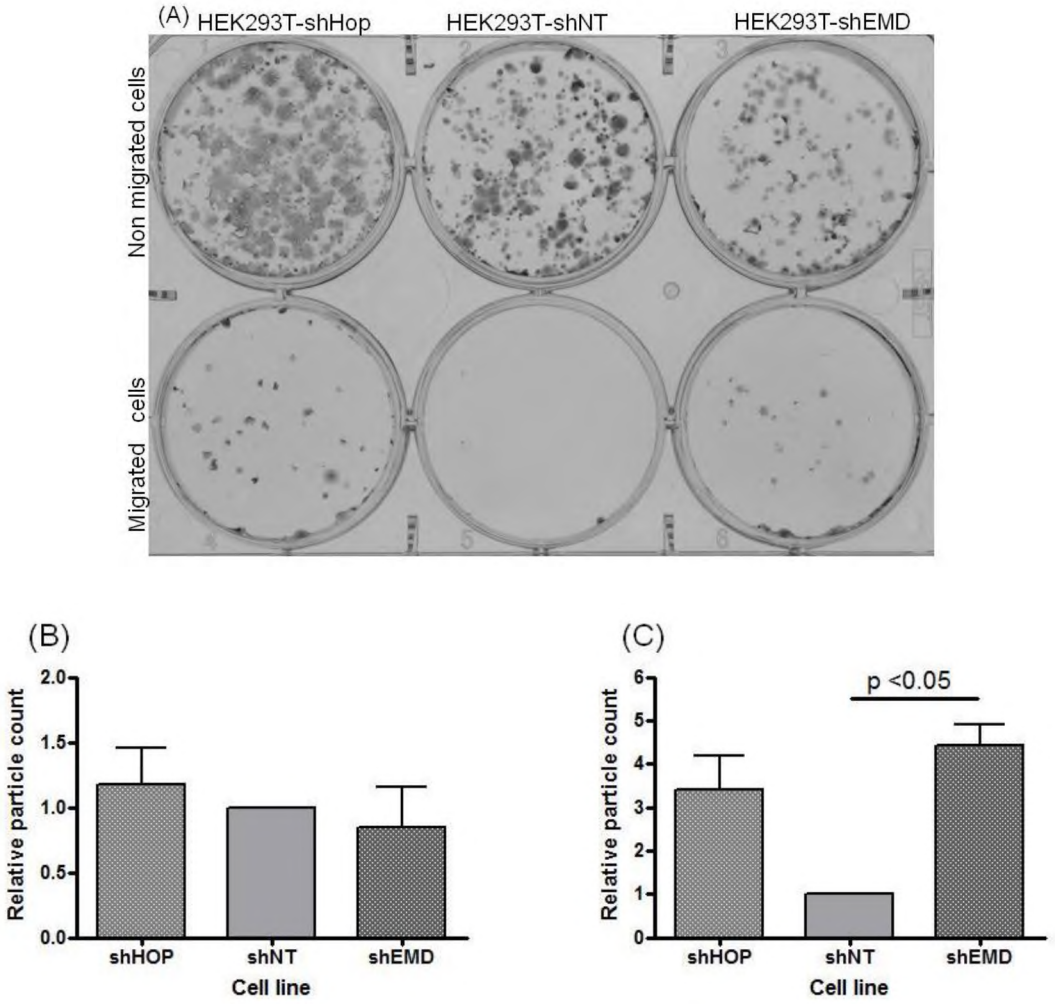

Figure 17: Assessment of the effect of the depletion of Hop and emerin on the long term survival of cells

(A) Clonogenic assay of HEK239T-shHop, HEK293T-shEMD and HEK293T-shNT cells before (top panel) and after (bottom panel) migration through the pores of a transwell migration chamber. (B) and (C) Quantification of triplicate clonogenic assay using particle analysis in ImageJ. The numbers of colonies were normalized to the HEK293T-shNT control, which was

taken as 1 and statistical significance compared using a one way ANOVA in Graphpad prism. These images are a representative of results obtained from 3 independent experiments.

Chapter 4: Discussion and conclusions

A proteomics study previously done in our lab indicated that emerin was one of the proteins that was downregulated to greater than 2 fold when Hop was knocked down using Hop specific shRNA (Wingate, 2016). Our study tested the hypothesis that Hop interacts with emerin and regulates its function and/or localization, thereby influencing the structure of the nuclear envelope. The results obtained suggest that the knockdown of Hop via shRNA and the over expression of Hop both result in the depletion of emerin at 96 hours. Subcellullar fractionation revealed that depletion of Hop affects the cytoplasmic and nuclear levels of emerin while analysis of the effect of the depletion of Hop on the localization of emerin via immunoflourescence staining and confocal microscopy indicated that the depletion of Hop results in the mislocalization of emerin. Treatment of cells with MG-132 and chloroquine indicated that the expression of the Hop specific shRNA targets emerin for degradation via both the proteasomal and lysosomal degradation pathways. We further established that Hop and emerin colocalize in cells suggesting that they might associate with each other. Using immunoprecipitation analysis, it was confirmed that Hop and emerin interact in a common complex that is independent of the expression of Hsp90. Assessment of nuclear structure using transmission electron microscopy confirmed that loss of Hop and emerin results in the deformation of the nuclear structure coupled with a reduction in the nuclear size and an increase in the expression of the nuclear protein lamin A-C. In addition, we also established that the depletion of Hop and emerin results in an increase in long term survival, but only after transwell migration. Taken together, our data suggest that loss of Hop may influence nuclear structure through the loss of emerin. We propose that Hop acts as a scaffold to organize emerin and

maintain its stability, thereby supporting the structure of the nucleus. There is currently no literature that indicates the possibility of Hop interacting with emerin and our study thus provides, to the best of our knowledge, the first report on the interaction between Hop and emerin and the effect on the nuclear structure. We hypothesize that Hop interacts with emerin complexes as a scaffold to stabilize it and ensure its correct localization and function.

The depletion or inhibition of Hop has previously been shown to result in the depletion of cellular proteins other than emerin. For example, siRNA mediated depletion of Hop in breast cancer cells depleted RhoC protein levels (Willmer *et al.*, 2013) while in pancreatic cancers, Hop depletion via siRNA reduced tumour invasiveness by depleting levels of the matrix metalloproteinases-2 (MMP-2) (Walsh *et al.*, 2011). Depletion of Hop has been shown to inhibit response to cellular stress via depleting levels of the PrP^{C} (Beraldo *et al.*, 2013). Limited studies on the over expression of Hop in mouse models have demonstrated that Hop over expression regulates the expression of Hsp90 chaperone by increasing its expression and secretion without affecting the levels of its clients (Ferretti, 2015). However, the loss of emerin upon depletion of Hop is interesting as the interaction of the two proteins is independent of Hsp90, while many of the other proteins depleted when Hop levels are reduced are Hsp90 client proteins. This may be due to a bias towards the study of Hsp90 clients in the context of Hop inhibition or depletion, but it does demonstrate that it is possible that Hop stabilizes both Hsp90 client proteins and proteins independent of Hsp90.

Our study is also the first to demonstrate that the knockdown and the overexpression of Hop can both reduce the expression of another protein. It is possible to obtain the same phenotype following the knockdown and the over expression of a gene especially if the steady-state levels

of a particular protein are affected by an increase in the rate of degradation (Prelich, 2012). It has also been demonstrated that for proteins that occur in a multi-complex, over expression of one protein can interfere with the complex by triggering a competition for shared binding partners which disrupts the stoichiometry (Prelich, 2012). For instance in a study with histones, the over expression of H3 or H2A has been shown to result in defective gene expression that can only be rescued by co-over expression of all the implicated histones a mechanism that restores the stoichiometry (Prelich, 2012). Besides competition for binding partners, overexpression of a protein can also result in the inhibition or activation of another protein by rendering it inactive or active. For example, in yeast, inactivation of protein phosphatases following over expression of the stress-activated kinase results in inhibition of Cdc25 (Prelich, 2012). The same mechanism has been reported in the case of the serine/threonine protein kinase 1 (SRPK1) regulation of the expression of protein kinase B (Akt), where depletion of SRPK1 results in the activation of Akt by hindering its association with the PH domain and leucine rich repeat protein phosphatase 1 (PHLPP1) and over expression of SRPK1 sequesters PHLPP1 and enhances the activation of Akt (Wang *et al*., 2014).

Our data also fits the hypothesis that Hop is serving as a scaffold protein that tethers emerin at the nuclear envelope. The depletion of emerin following Hop knockdown and overexpression is typical of canonical tethering by scaffold proteins and resembles the mechanism exhibited by Ste5 a scaffold protein of the MAPK pathway in yeast (Good *et al*., 2011) and Ras GTPase activating like protein 1 (IQGAP1) a scaffold protein for the epidermal growth factor (EGF) (Sacks, 2006) where over expression and knockdown of the scaffold proteins attenuate the implicated pathway. Our confocal microscopy and subcellullar fractionation data confirmed that Hop and emerin colocalize in the nucleus, further supporting the hypothesis that Hop is serving

as a scaffold protein since scaffold proteins have been shown to localize with their clients and are likely to interact with them (Sacks, 2006).

Unc-45, another TPR containing co-chaperone of Hsp90, has been shown to result in the depletion of myosin protein levels following its overexpression and knockdown via shRNA (Gunawan *et al.*, 2013). In the study, the authors indicate that Unc-45 chaperones the folding and maturation of myosin and thus a knockdown of the expression of Unc-45 would result in the misfolding of myosin, while an over expression of Unc-45 would result into the over stabilization of myosin. These two effects were shown to both increase the susceptibility of myosin to degradation (Gunawan *et al.*, 2013; Lee *et al.*, 2014). Ni *et al.*, (2011) further indicate that an excess and an absence of the chaperone activity of Unc-45 both result into the depletion of myosin. We therefore suspect that Hop may be influencing the expression of emerin in a manner similar to the observed effects of Unc-45 on myosin, or that Hop may be tethering emerin at the nuclear envelope owing to its role as a scaffolding protein (Good *et al.*, 2011). Indeed, TPR domains, like those found in Hop and Unc-45, are known to be involved in multiple protein-protein interactions characteristic of scaffold proteins (Blatch and Lassle, 1999). However, this observation is also interesting due to the recent publication suggesting that Hop has ATPase activity and therefore may have independent chaperone activity (Yamamoto *et al.*, 2014; Baindur-Hudson *et al.*, 2015).

Unlike in the case of Unc-45 and myosin where myosin was shown to bind both Unc-45 and Hsp90 (Lee *et al.*, 2014), in our study we confirmed that Hop and emerin interact in a complex that is independent of the expression of Hsp90. This suggested the involvement of Hop that was beyond the Hsp90 chaperone. However, despite having its own chaperone activity (Gunawan *et*

al., 2013), a crystal structure analysis of Unc45 later revealed that it serves as a scaffold protein that presents Hsp90 to myosin to allow for complete folding of myosin (Lee *et al.*, 2014). The degradation of myosin following the knockdown or over expression of Unc-45 (Gunawan *et al.*, 2013; Lee *et al.*, 2014) matches the observed degradation of emerin following the depletion of Hop in our study suggesting that hop may be influencing the expression of emerin in a manner similar to the observed effects of Unc-45 on myosin.

It is also typical of scaffold proteins to influence the subcellular localization of their client proteins (Sacks, 2006) besides regulating their interaction with other proteins (Good *et al.*, 2011). Our subcellular fractionation data suggested that the expression of the Hop specific shRNA results in the depletion of subcellular levels of emerin. Emerin was depleted in the nuclear envelope and the cytoplasm although it appears in the cytoplasmic fraction because the isolation protocol removes the nuclear envelope with the cytoplasmic fraction (Watson, 2000). Data from our immunfluorescence staining with confocal microscopy suggested that the expression of the Hop specific shRNA resulted in the mislocalization of emerin. The observed mislocalization of emerin was similar to the trend observed in cells expressing an emerin mutant that lacks the transmembrane domain (Fairley *et al.*, 2002). The transmembrane domain in emerin is thought to be essential for its correct localization at the INM and Fairley *et al.*, (2002) established that deletion of this domain not only results into the mislocalization of emerin but was also associated with a redistribution of lamin A-C, coupled with deformation in the structure of the nucleus (Fairley *et al.*, 2002) which also resembles the effects observed in this study. However in this case, we predict that Hop is required not only to stabilize the protein levels of emerin, but also to tether it to the nuclear envelope.

In our study, Hop was found to occur in a common complex with emerin in which other proteins such as histone H3 and lamin A-C were also involved. This supports the hypothesis that it is a scaffold protein interacting with emerin in a multi-complex consisting of other nuclear associated proteins. Given that Hop and emerin are in a multi-complex with numerous other partners, it would be important to establish the effect of over expressing emerin on the stoichiometry of Hop-emerin interactions to determine if the effects on emerin following the overexpression and knockdown of Hop are as a result of the interference with the stoichoimetry ratio as expected of protein scaffolding (Sacks, 2006; Prelich, 2012). However, it is typical of scaffold proteins involved in multi-complex protein-protein interactions to exhibit what is termed as a biphasic effect whereby increasing the concentration of the scaffold results in a surplus of partner proteins in the complex which amounts into inhibition of interaction or formation of incomplete complexes (Good *et al.*, 2011).

The interaction between Hop and emerin is supported by the observed changes in the expression and localization of emerin binding partners following depletion of Hop. This suggested an interference with the stoichoimetry ratio which is typical of interactions guided by scaffold proteins (Good *et al.*, 2011). Our subcellullar fractionation and immunofluorescence staining data indicated that loss of both Hop and emerin results in an increase in the expression of the nuclear envelope protein lamin A-C. Emerin and lamin A-C are functionally linked (Hutchison *et al.*, 2001). The mechanisms involved in the emergence of EDMD have been associated with impairment of gene regulation and defects in the nuclear structure following mutations in both emerin and lamin A-C (Hutchison *et al.*, 2001; Lammerding *et al.*, 2005; Koch and Holaska, 2014). In disease conditions, loss of emerin yields a recessive EDMD condition, while loss of lamin A-C results into an autosomal dominant EDMD condition (Lammerding *et al.*, 2005; Koch

and Holaska, 2014). Cells deficient in emerin have been shown to exhibit a redistribution of lamin A-C (Fairley *et al.*, 2002). This suggests that emerin and lamins control similar functions and their expression levels may dictate observed disease outcomes (Holaska and Wilson, 2007). We speculate that the observed increase in the expression of lamin A-C in the Hop and emerin depleted cells is a compensation for the loss of emerin in these cells. Emerin and lamin proteins have been shown to rely on each other for their correct localization in the nuclear envelope (Vaughan *et al.*, 2001; Fairley *et al.*, 2002; Guo *et al.*, 2014) and studies indicate that over expression of emerin can rescue defects associated with loss of lamins (Holaska *et al.*, 2004), while loss of emerin has been shown to be associated with a compensatory effect in the expression of other nuclear envelope proteins (Liu *et al.*, 2003). We therefore hypothesize that the increase in the expression of lamin A-C is serving to compensate for the loss of emerin in the HEK293T-shHop and HEK293T-shEMD cells and may be caused due to interference with the stoichoimetry within the Hop-emerin multi-complex. The compensatory upregulation of lamin A-C in response to emerin loss may also partly explain why a more severe phenotype is not observed in the cells, despite the changes in the structure of the nucleus observed. Tubulin, another protein that interacts with both Hop and emerin (Salpingidou *et al.*, 2007; Li *et al.*, 2012b), was shown to be mislocalized in our Hop and emerin depleted cells, which further supports the hypothesis that the observed effects are as a result of the interference with the stoichoimetry within the Hop-emerin multi-complex.

The loss of emerin (either by shRNA or via Hop depletion) resulted in distortions in the nuclear structure but otherwise did not exhibit a severe growth phenotype. Aside from the proposed upregulation of lamin A-C, we speculate that this may also be due to the fact that the fragility of the emerin-depleted nuclear envelope is only manifested when the cells are under mechanical

stress. Emerin and lamin A-C have been shown to control the nuclear structure dynamics via regulating response to mechanical stress besides controlling gene transcription processes (Qi *et al.*, 2016). Indeed, this is consistent with EDMD, where the diseased phenotype is only observed in cell types that encounter mechanical stress, such as muscle and cardiac cells (Hutchison *et al.*, 2001). We therefore attempted to test the long term survival of cells after subjecting the nucleus to a form of mechanical stress. We used transwell migration with an 8 μm pore size that would require the nucleus to be restricted during passage of the cells through the membrane. Our data suggested that the Hop and emerin depleted cells exhibit increased long term survival compared to the wild type cells, but only after migration across the transwell membrane. Cells that had not migrated showed similar levels of long term survival irrespective of the levels of emerin. This response was unexpected. However, cells depleted of NE proteins have been shown to exhibit better survival compared to controls and this was associated with an increase in DNA repair mechanisms following the induced damage on the nucleus (Raab *et al.*, 2016). In another study on the effect of the depletion of emerin on cell proliferation, it was established that the interaction of emerin and GCL represses the transcription of the E2F-DP3 genes whose expression is important for cells to enter into the synthesis phase (S-Phase) and cells depleted in emerin were shown to be highly proliferative (Koch and Holaska, 2014). Qi *et al.*, (2016) also demonstrated that depletion of emerin renders cells more proliferative and migratory owing to the deformation of the nucleus. Taking into account the findings from these studies, our data suggested that the increased migration and the long term survival of our Hop and emerin depleted cells after transwell migration is as a result of the interference with the nuclear structure and gene expression following depletion of emerin. However, to further understand the mechanism involved in the long term survival of our cells, it would be important for further

studies to establish if the levels of DNA repair proteins such as the endosomal sorting complex required for transport iii (ESCRT iii) and the GCL implicated in proliferation are affected in the Hop and emerin depleted cells via Western blots. In addition, it would be important to assess other cell cycle parameters that might be affected following the depletion of emerin using assays such as DNA staining and assessment of chromosome stability.

Conclusion

From the findings in this study, we suggest that Hop is serving as a scaffold protein that tethers emerin at the nuclear envelope and that the effects of the depletion of Hop on the nuclear structure are directly due to loss of emerin. This interaction does not require Hsp90. To further understand if Hop is independently stabilizing emerin, it will be important for future studies to determine the involvement of Hsp70 in the complex formed between Hop and emerin. Because changes in the expression of emerin have been associated with the emergence of EDMD, the results obtained in our study also suggest a possible and previously undescribed role of Hop in this disease and it therefore remains important to assess the levels of Hop in samples obtained from EDMD patients to validate this hypothesis. This may also imply that emerin levels may be affected in other disease conditions that have been shown to be determined by the expression of Hop such as Alzheimer's and cancers.

Chapter 5: References

Altieri, D.C., Stein, G.S., Lian, J.B. and Languino, L.R. (2012) TRAP-1, the mitochondrial Hsp90. Biochim Biophys Acta 1823, 767-73.

Astejada, M.N., Goto, K., Nagano, A., Ura, S., Noguchi, S., Nonaka, I., Nishino, I. and Hayashi, Y.K. (2007) Emerinopathy and laminopathy clinical, pathological and molecular features of muscular dystrophy with nuclear envelopathy in Japan. Acta Myol 26, 159-64.

Baindur-Hudson, S., Edkins, A.L. and Blatch, G.L. (2015) Hsp70/Hsp90 organising protein (hop): beyond interactions with chaperones and prion proteins. Subcell Biochem 78, 69-90.

Bengtsson, L. and Wilson, K.L. (2004) Multiple and surprising new functions for emerin, a nuclear membrane protein. Curr Opin Cell Biol 16, 73-9.

Beraldo, F.H., Soares, I.N., Goncalves, D.F., Fan, J., Thomas, A.A., Santos, T.G., Mohammad, A.H., Roffe, M., Calder, M.D., Nikolova, S., Hajj, G.N., Guimaraes, A.L., Massensini, A.R., Welch, I., Betts, D.H., Gros, R., Drangova, M., Watson, A.J., Bartha, R., Prado, V.F., Martins, V.R. and Prado, M.A. (2013) Stress-inducible phosphoprotein 1 has unique cochaperone activity during development and regulates cellular response to ischemia via the prion protein. FASEB J 27, 3594-607.

Berk, J.M., Tifft, K.E. and Wilson, K.L. (2013) The nuclear envelope LEM-domain protein emerin. Nucleus 4, 298-314.

Bhola, N.E., Balko, J.M., Dugger, T.C., Kuba, M.G., Sanchez, V., Sanders, M., Stanford, J., Cook, R.S. and Arteaga, C.L. (2013) TGF-beta inhibition enhances chemotherapy action against triple-negative breast cancer. J Clin Invest 123, 1348-58.

Blair, L.J., Sabbagh, J.J. and Dickey, C.A. (2014) Targeting Hsp90 and its co-chaperones to treat Alzheimer's disease. Expert Opin Ther Targets 18, 1219-32.

Blatch, G.L. and Lassle, M. (1999) The tetratricopeptide repeat: a structural motif mediating protein-protein interactions. Bioessays 21, 932-9.

Bradley, E., Bieberich, E., Mivechi, N.F., Tangpisuthipongsa, D. and Wang, G. (2012) Regulation of embryonic stem cell pluripotency by heat shock protein 90. Stem Cells 30, 1624-33.

Bredemeyer, A.J., Carrigan, P.E., Fehniger, T.A., Smith, D.F. and Ley, T.J. (2006) Hop cleavage and function in granzyme B-induced apoptosis. J Biol Chem 281, 37130-41.

Burke, B., Shanahan, C., Salina, D. and Crisp, M. (2005) Aspects of nuclear envelope dynamics in mitotic cells. Novartis Found Symp 264, 22-30; discussion 30-4, 227-30.

Bussolati, G., Marchio, C., Gaetano, L., Lupo, R. and Sapino, A. (2008) Pleomorphism of the nuclear envelope in breast cancer: a new approach to an old problem. J Cell Mol Med 12, 209-18.

Calderwood, S.K. (2013) Molecular cochaperones: tumor growth and cancer treatment. Scientifica (Cairo) 2013, 217513.

Caplan, A.J. (2003) What is a co-chaperone? Cell Stress Chaperones 8, 105-7.

Capo-chichi, C.D., Cai, K.Q., Simpkins, F., Ganjei-Azar, P., Godwin, A.K. and Xu, X.X. (2011) Nuclear envelope structural defects cause chromosomal numerical instability and aneuploidy in ovarian cancer. BMC Med 9, 28.

Carrigan, P.E., Riggs, D.L., Chinkers, M. and Smith, D.F. (2005) Functional comparison of human and Drosophila Hop reveals novel role in steroid receptor maturation. J Biol Chem 280, 8906-11.

Cartegni, L., di Barletta, M.R., Barresi, R., Squarzoni, S., Sabatelli, P., Maraldi, N., Mora, M., Di Blasi, C., Cornelio, F., Merlini, L., Villa, A., Cobianchi, F. and Toniolo, D. (1997) Heart-specific localization of emerin: new insights into Emery-Dreifuss muscular dystrophy. Hum Mol Genet 6, 2257-64.

Chao, A., Lai, C.H., Tsai, C.L., Hsueh, S., Hsueh, C., Lin, C.Y., Chou, H.H., Lin, Y.J., Chen, H.W., Chang, T.C. and Wang, T.H. (2013) Tumor stress-induced phosphoprotein1 (STIP1) as a prognostic biomarker in ovarian cancer. PLoS One 8, e57084.

Clark, P.L. (2004) Protein folding in the cell: reshaping the folding funnel. Trends Biochem Sci 29, 527-34.

Contu, L. (2014) The Effects of Extracellular and Intracellular Hop on Cell Migration Processes. In: Biochemistry and Microbiology, Vol. Masters. Rhodes University, Grahamstown.

Cortajarena, A.L., Yi, F. and Regan, L. (2008) Designed TPR modules as novel anticancer agents. ACS Chem Biol 3, 161-6.

D'Arrigo, C., Barboro, D., Galante, D. and Balbi, C. (2010) Transmission electron microscopy of the nuclear matrix and its proteins. Microscopy: Science, Technology, Applications and Education.

Dedeic, Z., Cetera, M., Cohen, T.V. and Holaska, J.M. (2011) Emerin inhibits Lmo7 binding to the Pax3 and MyoD promoters and expression of myoblast proliferation genes. J Cell Sci 124, 1691-702.

Edkins, A.L. (2016) Hsp90 Co-chaperones as Drug Targets in Cancer: Current Perspectives. Top Med Chem, 21-54.

Elbi, C., Walker, D.A., Romero, G., Sullivan, W.P., Toft, D.O., Hager, G.L. and DeFranco, D.B. (2004) Molecular chaperones function as steroid receptor nuclear mobility factors. Proc Natl Acad Sci U S A 101, 2876-81.

Erlich, R.B., Kahn, S.A., Lima, F.R., Muras, A.G., Martins, R.A., Linden, R., Chiarini, L.B., Martins, V.R. and Moura Neto, V. (2007) STI1 promotes glioma proliferation through MAPK and PI3K pathways. Glia 55, 1690-8.

Fairley, E., Riddell, A., . Ellis, J., and Kendrick-Jones, J.,. (2002) The cell cycle dependent mislocalisation of emerin may contribute to the Emery-Dreifuss muscular dystrophy phenotype. Cell science, 341-354.

Fairley, E.A., Riddell, A., Ellis, J.A. and Kendrick-Jones, J. (2002) The cell cycle dependent mislocalisation of emerin may contribute to the Emery-Dreifuss muscular dystrophy phenotype. J Cell Sci 115, 341-54.

Feder, M.E. and Hofmann, G.E. (1999) Heat-shock proteins, molecular chaperones, and the stress response: evolutionary and ecological physiology. Annu Rev Physiol 61, 243-82.

Ferretti, S., Beraldo, H., Fan, J., Silva, J., Martins, V., Prado, V., and Prado,M.,. (2015) The role of stress inducible phosphoprotein (stip1/sti1/hop) in astrocyte differentiation and neuronal protection against the toxicity of aβ1-42 peptide (aβos). In: 23rd Congress of the International Union for Biochemistry and Molecular Biology,44th Annual Meeting of the Brazilian Society for Biochemistry and Molecular Biology, Foz do Iguaçu, PR, Brazil.

Fichtman, B., Ramos, C., Rasala, B., Harel, A. and Forbes, D.J. (2010) Inner/Outer nuclear membrane fusion in nuclear pore assembly: biochemical demonstration and molecular analysis. Mol Biol Cell 21, 4197-211.

Fink, A.L. (1999) Chaperone-mediated protein folding. Physiol Rev 79, 425-49.

Flom, G., Behal, R.H., Rosen, L., Cole, D.G. and Johnson, J.L. (2007) Definition of the minimal fragments of Sti1 required for dimerization, interaction with Hsp70 and Hsp90 and in vivo functions. Biochem J 404, 159-67.

Frock, R.L., Kudlow, B.A., Evans, A.M., Jameson, S.A., Hauschka, S.D. and Kennedy, B.K. (2006) Lamin A/C and emerin are critical for skeletal muscle satellite cell differentiation. Genes Dev 20, 486-500.

Gething, M.J. and Sambrook, J. (1992) Protein folding in the cell. Nature 355, 33-45.

Gitau, G.W., Mandal, P., Blatch, G.L., Przyborski, J. and Shonhai, A. (2011) Characterisation of the Plasmodium falciparum Hsp70-Hsp90 organising protein (PfHop). Cell Stress Chaperones 17, 191-202.

Good, M.C., Zalatan, J.G. and Lim, W.A. (2011) Scaffold proteins: hubs for controlling the flow of cellular information. Science 332, 680-6.

Grad, I., Cederroth, C.R., Walicki, J., Grey, C., Barluenga, S., Winssinger, N., De Massy, B., Nef, S. and Picard, D. (2010) The molecular chaperone Hsp90alpha is required for meiotic progression of spermatocytes beyond pachytene in the mouse. PLoS One 5, e15770.

Gunawan, F., Arandjelovic, M. and Godt, D. (2013) The Maf factor Traffic jam both enables and inhibits collective cell migration in Drosophila oogenesis. Development 140, 2808-17.

Guo, Y., Kim, Y., Shimi, T., Goldman, R.D. and Zheng, Y. (2014) Concentration-dependent lamin assembly and its roles in the localization of other nuclear proteins. Mol Biol Cell 25, 1287-97.

Guttinger, S., Laurell, E. and Kutay, U. (2009) Orchestrating nuclear envelope disassembly and reassembly during mitosis. Nat Rev Mol Cell Biol 10, 178-91.

Hagen, C., Dent, K.C., Zeev-Ben-Mordehai, T., Grange, M., Bosse, J.B., Whittle, C., Klupp, B.G., Siebert, C.A., Vasishtan, D., Bauerlein, F.J., Cheleski, J., Werner, S., Guttmann, P., Rehbein, S., Henzler, K., Demmerle, J., Adler, B., Koszinowski, U., Schermelleh, L., Schneider, G., Enquist, L.W., Plitzko, J.M., Mettenleiter, T.C. and Grunewald, K. (2015) Structural Basis of Vesicle Formation at the Inner Nuclear Membrane. Cell 163, 1692-701.

Hale, C.M., Shrestha, A.L., Khatau, S.B., Stewart-Hutchinson, P.J., Hernandez, L., Stewart, C.L., Hodzic, D. and Wirtz, D. (2008) Dysfunctional connections between the nucleus and the actin and microtubule networks in laminopathic models. Biophys J 95, 5462-75.

Haraguchi, T., Holaska, J.M., Yamane, M., Koujin, T., Hashiguchi, N., Mori, C., Wilson, K.L. and Hiraoka, Y. (2004) Emerin binding to Btf, a death-promoting transcriptional repressor, is disrupted by a missense mutation that causes Emery-Dreifuss muscular dystrophy. Eur J Biochem 271, 1035-45.

Haraguchi, T., Koujin, T., Hayakawa, T., Kaneda, T., Tsutsumi, C., Imamoto, N., Akazawa, C., Sukegawa, J., Yoneda, Y. and Hiraoka, Y. (2000) Live fluorescence imaging reveals early recruitment of emerin, LBR, RanBP2, and Nup153 to reforming functional nuclear envelopes. J Cell Sci 113 (Pt 5), 779-94.

Haraguchi, T., Koujin, T., Segura-Totten, M., Lee, K.K., Matsuoka, Y., Yoneda, Y., Wilson, K.L. and Hiraoka, Y. (2001) BAF is required for emerin assembly into the reforming nuclear envelope. J Cell Sci 114, 4575-85.

Hartl, F.U., Bracher, A. and Hayer-Hartl, M. (2011) Molecular chaperones in protein folding and proteostasis. Nature 475, 324-32.

Hatch, E. and Hetzer, M. (2014) Breaching the nuclear envelope in development and disease. J Cell Biol 205, 133-41.

Heinlein, C.A. and Chang, C. (2001) Role of chaperones in nuclear translocation and transactivation of steroid receptors. Endocrine 14, 143-9.

Hetzer, M.W. (2010) The nuclear envelope. Cold Spring Harb Perspect Biol 2, a000539.

Hirano, Y., Segewa, M., Ouchi, F., Yamakawa, Y., Furakawa, J., Takeyasu, K. and Horigome, T. (2005) Dissociation of Emerin from Barrier-to-autointegration Factor is Regulated through Mitotic Phosphorylation of Emerin in a Xenopus Egg Cell-free System. Journal of Biological Chemistry 280, 39925-39933.

Ho, C.Y., Jaalouk, D.E., Vartiainen, M.K. and Lammerding, J. (2013) Lamin A/C and emerin regulate MKL1-SRF activity by modulating actin dynamics. Nature 497, 507-11.

Holaska, J.M. (2008) Emerin and the nuclear lamina in muscle and cardiac disease. Circ Res 103, 16-23.

Holaska, J.M., Kowalski, A.K. and Wilson, K.L. (2004) Emerin caps the pointed end of actin filaments: evidence for an actin cortical network at the nuclear inner membrane. PLoS Biol 2, E231.

Holaska, J.M. and Wilson, K.L. (2007) An emerin "proteome": purification of distinct emerin-containing complexes from HeLa cells suggests molecular basis for diverse roles including gene regulation, mRNA splicing, signaling, mechanosensing, and nuclear architecture. Biochemistry 46, 8897-908.

Horibe, T., Kohno, M., Haramoto, M., Ohara, K. and Kawakami, K. (2011) Designed hybrid TPR peptide targeting Hsp90 as a novel anticancer agent. J Transl Med 9, 8.

Hutchison, C.J., Alvarez-Reyes, M. and Vaughan, O.A. (2001) Lamins in disease: why do ubiquitously expressed nuclear envelope proteins give rise to tissue-specific disease phenotypes? J Cell Sci 114, 9-19.

Katta, S.S., Smoyer, C.J. and Jaspersen, S.L. (2014) Destination: inner nuclear membrane. Trends Cell Biol 24, 221-9.

Koch, A.J. and Holaska, J.M. (2014) Emerin in health and disease. Semin Cell Dev Biol 29, 95-106.

Krysko, D.V., Vanden Berghe, T., Parthoens, E., D'Herde, K. and Vandenabeele, P. (2008) Methods for distinguishing apoptotic from necrotic cells and measuring their clearance. Methods Enzymol 442, 307-41.

Lammerding, J., Hsiao, J., Schulze, P.C., Kozlov, S., Stewart, C.L. and Lee, R.T. (2005) Abnormal nuclear shape and impaired mechanotransduction in emerin-deficient cells. J Cell Biol 170, 781-91.

Laskey, R.A., Honda, B.M., Mills, A.D. and Finch, J.T. (1978) Nucleosomes are assembled by an acidic protein which binds histones and transfers them to DNA. Nature 275, 416-20.

Lee, C.F., Melkani, G.C. and Bernstein, S.I. (2014) The UNC-45 myosin chaperone: from worms to flies to vertebrates. Int Rev Cell Mol Biol 313, 103-44.

Lee, C.T., Graf, C., Mayer, F.J., Richter, S.M. and Mayer, M.P. (2012) Dynamics of the regulation of Hsp90 by the co-chaperone Sti1. EMBO J 31, 1518-28.

Lee, K.K., Haraguchi, T., Lee, R.S., Koujin, T., Hiraoka, Y. and Wilson, K.L. (2001) Distinct functional domains in emerin bind lamin A and DNA-bridging protein BAF. J Cell Sci 114, 4567-73.

Li, J., Buchner, J. Weinkauf, S. Sattler, M. . (2011) Co-chaperones Interactions in the HSP90 Chaperone Cycle. In: Department Chemie. Technische Universität München.

Li, J., Soroka, J. and Buchner, J. (2012a) The Hsp90 chaperone machinery: Conformational dynamics and regulation by co-chaperones. Biochimica et Biophysica Acta (BBA) - Molecular Cell Research 1823, 624-635.

Li, J., Sun, X., Wang, Z., Chen, L., Li, D., Zhou, J. and Liu, M. (2012b) Regulation of vascular endothelial cell polarization and migration by Hsp70/Hsp90-organizing protein. PLoS One 7, e36389.

Lin, Z. and Rye, H.S. (2006) GroEL-mediated protein folding: making the impossible, possible. Crit Rev Biochem Mol Biol 41, 211-39.

Liu, J., Lee, K.K., Segura-Totten, M., Neufeld, E., Wilson, K.L. and Gruenbaum, Y. (2003) MAN1 and emerin have overlapping function(s) essential for chromosome segregation and cell division in Caenorhabditis elegans. Proc Natl Acad Sci U S A 100, 4598-603.

Liu, J., Lee, K., Segura-Totten, M., Neufeld, E., Wilson, K., and Greunbaum, Y. (2003) MAN1 and Emerin have Overlapping Function(s) Essential for Chromosome Segregation and Cell Division in Caenorhabditis Elegans. PNAS 100, 4598-4603.

Longshaw, V.M., Baxter, M., Prewitz, M. and Blatch, G.L. (2009) Knockdown of the co-chaperone Hop promotes extranuclear accumulation of Stat3 in mouse embryonic stem cells. Eur J Cell Biol 88, 153-66.

Longshaw, V.M., Chapple, J.P., Balda, M.S., Cheetham, M.E. and Blatch, G.L. (2004) Nuclear translocation of the Hsp70/Hsp90 organizing protein mSTI1 is regulated by cell cycle kinases. J Cell Sci 117, 701-10.

Lopes, M.H., Hajj, G.N., Muras, A.G., Mancini, G.L., Castro, R.M., Ribeiro, K.C., Brentani, R.R., Linden, R. and Martins, V.R. (2005) Interaction of cellular prion and stress-inducible protein 1 promotes neuritogenesis and neuroprotection by distinct signaling pathways. J Neurosci 25, 11330-9.

Lopes, M.H., Santos, T.G., Rodrigues, B.R., Queiroz-Hazarbassanov, N., Cunha, I.W., Wasilewska-Sampaio, A.P., Costa-Silva, B., Marchi, F.A., Bleggi-Torres, L.F., Sanematsu, P.I., Suzuki, S.H., Oba-Shinjo, S.M., Marie, S.K., Toulmin, E., Hill, A.F. and Martins, V.R. (2014) Disruption of prion protein-HOP engagement impairs glioblastoma growth and cognitive decline and improves overall survival. Oncogene 34, 3305-14.

Lorenz, O.R., Freiburger, L., Rutz, D.A., Krause, M., Zierer, B.K., Alvira, S., Cuellar, J., Valpuesta, J.M., Madl, T., Sattler, M. and Buchner, J. (2014) Modulation of the Hsp90 chaperone cycle by a stringent client protein. Mol Cell 53, 941-53.

Lu, L., Ladinsky, M.S. and Kirchhausen, T. (2011) Formation of the postmitotic nuclear envelope from extended ER cisternae precedes nuclear pore assembly. J Cell Biol 194, 425-40.

Marshall, I.C. and Wilson, K.L. (1997) Nuclear envelope assembly after mitosis. Trends Cell Biol 7, 69-74.

Melcon, G., Kozlov, S., Cutler, D.A., Sullivan, T., Hernandez, L., Zhao, P., Mitchell, S., Nader, G., Bakay, M., Rottman, J.N., Hoffman, E.P. and Stewart, C.L. (2006) Loss of emerin at the nuclear envelope disrupts the Rb1/E2F and MyoD pathways during muscle regeneration. Hum Mol Genet 15, 637-51.

Muntoni, F., Bonne, G., Goldfarb, L.G., Mercuri, E., Piercy, R.J., Burke, M., Yaou, R.B., Richard, P., Recan, D., Shatunov, A., Sewry, C.A. and Brown, S.C. (2006) Disease severity in dominant Emery Dreifuss is increased by mutations in both emerin and desmin proteins. Brain 129, 1260-8.

Odunuga, O.O., Longshaw, V.M. and Blatch, G.L. (2004) Hop: more than an Hsp70/Hsp90 adaptor protein. Bioessays 26, 1058-68.

Onuoha, S.C., Coulstock, E.T., Grossmann, J.G. and Jackson, S.E. (2008) Structural studies on the co-chaperone Hop and its complexes with Hsp90. J Mol Biol 379, 732-44.

Pfaller, R. and Newport, J.W. (1995) Assembly/disassembly of the nuclear envelope membrane. Characterization of the membrane-chromatin interaction using partially purified regulatory enzymes. J Biol Chem 270, 19066-72.

Prelich, G. (2012) Gene overexpression: uses, mechanisms, and interpretation. Genetics 190, 841-54.

Qi, Y.X., Yao, Q.P., Huang, K., Shi, Q., Zhang, P., Wang, G.L., Han, Y., Bao, H., Wang, L., Li, H.P., Shen, B.R., Wang, Y., Chien, S. and Jiang, Z.L. (2016) Nuclear envelope proteins modulate proliferation of vascular smooth muscle cells during cyclic stretch application. Proc Natl Acad Sci U S A 113, 5293-8.

Raab, M., Gentili, M., de Belly, H., Thiam, H.R., Vargas, P., Jimenez, A.J., Lautenschlaeger, F., Voituriez, R., Lennon-Dumenil, A.M., Manel, N. and Piel, M. (2016) ESCRT III repairs nuclear envelope ruptures during cell migration to limit DNA damage and cell death. Science 352, 359-62.

Rohl, A., Tippel, F., Bender, E., Schmid, A.B., Richter, K., Madl, T. and Buchner, J. (2015) Hop/Sti1 phosphorylation inhibits its co-chaperone function. EMBO Rep 16, 240-9.

Rowat, A.C., Lammerding, J. and Ipsen, J.H. (2006) Mechanical properties of the cell nucleus and the effect of emerin deficiency. Biophys J 91, 4649-64.

Sacks, D.B. (2006) The role of scaffold proteins in MEK/ERK signalling. Biochem Soc Trans 34, 833-6.

Salpingidou, G., Smertenko, A., Hausmanowa-Petrucewicz, I., Hussey, P.J. and Hutchison, C.J. (2007) A novel role for the nuclear membrane protein emerin in association of the centrosome to the outer nuclear membrane. J Cell Biol 178, 897-904.

Scheufler, C., Brinker, A., Bourenkov, G., Pegoraro, S., Moroder, L., Bartunik, H., Hartl, F.U. and Moarefi, I. (2000) Structure of TPR domain-peptide complexes: critical elements in the assembly of the Hsp70-Hsp90 multichaperone machine. Cell 101, 199-210.

Schmidt, C., Beilsten-Edmands, V. and Robinson, C.V. (2015) The joining of the Hsp90 and Hsp70 chaperone cycles yields transient interactions and stable intermediates: insights from mass spectrometry. Oncotarget 6, 18276-81.

Shen, T.H., Lin, H.K., Scaglioni, P.P., Yung, T.M. and Pandolfi, P.P. (2006) The mechanisms of PML-nuclear body formation. Mol Cell 24, 331-9.

Shonhai, A., Boshoff, A. and Blatch, G.L. (2007) The structural and functional diversity of Hsp70 proteins from Plasmodium falciparum. Protein Sci 16, 1803-18.

Song, Q., Wei, T., Lees-Miller, S., Alnemri, E., Watters, D. and Lavin, M.F. (1997) Resistance of actin to cleavage during apoptosis. Proc Natl Acad Sci U S A 94, 157-62.

Song, Y. and Masison, D.C. (2005) Independent regulation of Hsp70 and Hsp90 chaperones by Hsp70/Hsp90-organizing protein Sti1 (Hop1). J Biol Chem 280, 34178-85.

Sterrenberg, J. (2015) Establishment of Human OCT4 as a Putative HSP90 Client Protein: A Case of HSP90 Chaperoning Pluripotency. In: Biochemistry, Vol. Doctorate. Rhodes University, Grahamstown.

Terasaki, M., Campagnola, P., Rolls, M.M., Stein, P.A., Ellenberg, J., Hinkle, B. and Slepchenko, B. (2001) A new model for nuclear envelope breakdown. Mol Biol Cell 12, 503-10.

Towbin, B.D., Gonzalez-Sandoval, A. and Gasser, S.M. (2013) Mechanisms of heterochromatin subnuclear localization. Trends Biochem Sci 38, 356-63.

Tsuchiya, Y., Hase, A., Ogawa, M., Yorifuji, H. and Arahata, K. (1999) Distinct regions specify the nuclear membrane targeting of emerin, the responsible protein for Emery-Dreifuss muscular dystrophy. Eur J Biochem 259, 859-65.

van den Berg, B., Wain, R., Dobson, C.M. and Ellis, R.J. (2000) Macromolecular crowding perturbs protein refolding kinetics: implications for folding inside the cell. EMBO J 19, 3870-5.

Vaughan, A., Alvarez-Reyes, M., Bridger, J.M., Broers, J.L., Ramaekers, F.C., Wehnert, M., Morris, G.E., Whitfield, W.G.F. and Hutchison, C.J. (2001) Both emerin and lamin C depend on lamin A for localization at the nuclear envelope. J Cell Sci 114, 2577-90.

Voss, A., Thomas, T., Gruss, and P.,. (1999) Mice lacking HSP90b fail to develop a placental labyrinth. Development 127, , 1-11

Walsh, N., Larkin, A., Swan, N., Conlon, K., Dowling, P., McDermott, R. and Clynes, M. (2011) RNAi knockdown of Hop (Hsp70/Hsp90 organising protein) decreases invasion via MMP-2 down regulation. Cancer Lett 306, 180-9.

Wandinger, S.K., Richter, K. and Buchner, J. (2008) The Hsp90 chaperone machinery. J Biol Chem 283, 18473-7.

Wang, P., Zhou, Z., Hu, A., Ponte de Albuquerque, C., Zhou, Y., Hong, L., Sierecki, E., Ajiro, M., Kruhlak, M., Harris, C., Guan, K.L., Zheng, Z.M., Newton, A.C., Sun, P., Zhou, H. and Fu, X.D. (2014) Both decreased and increased SRPK1 levels promote cancer by interfering with PHLPP-mediated dephosphorylation of Akt. Mol Cell 54, 378-91.

Watson, N., . (2000) Isolation and use of mammalian cell nuclei. Cell biology.

Webster, M., Witkin, K.L. and Cohen-Fix, O. (2009) Sizing up the nucleus: nuclear shape, size and nuclear-envelope assembly. J Cell Sci 122, 1477-86.

Willmer, T., Contu, L., Blatch, G.L. and Edkins, A.L. (2013) Knockdown of Hop downregulates RhoC expression, and decreases pseudopodia formation and migration in cancer cell lines. Cancer Lett 328, 252-60.

Wingate, I. (2016) Identification of potential novel roles for Hsp70/Hsp90 organising protein (Hop) using proteomic analysis in human cells. In: Biochemistry and Microbiology, Vol. Msc thesis. Rhodes, Grahamstown.

Wolff, N., Gilquin, B., Courchay, K., Callebaut, I., Worman, H.J. and Zinn-Justin, S. (2001) Structural analysis of emerin, an inner nuclear membrane protein mutated in X-linked Emery-Dreifuss muscular dystrophy. FEBS Lett 501, 171-6.

Worman, H.J. (2005) Components of the nuclear envelope and their role in human disease. Novartis Found Symp 264, 35-42; discussion 42-50, 227-30.

Xue, J.Z. and Funabiki, H. (2014) Nuclear assembly shaped by microtubule dynamics. Nucleus 5, 40-6.

Yamamoto, S., Subedi, G.P., Hanashima, S., Satoh, T., Otaka, M., Wakui, H., Sawada, K., Yokota, S., Yamaguchi, Y., Kubota, H. and Itoh, H. (2014) ATPase activity and ATP-dependent conformational change in the co-chaperone HSP70/HSP90-organizing protein (HOP). J Biol Chem 289, 9880-6.

Yang, X. (2012) Clonogenic Assay to Test Cancer Therapies. Bio-protocol 2.

Zanata, S.M., Lopes, M.H., Mercadante, A.F., Hajj, G.N., Chiarini, L.B., Nomizo, R., Freitas, A.R., Cabral, A.L., Lee, K.S., Juliano, M.A., de Oliveira, E., Jachieri, S.G., Burlingame, A., Huang, L., Linden, R.,

Brentani, R.R. and Martins, V.R. (2002) Stress-inducible protein 1 is a cell surface ligand for cellular prion that triggers neuroprotection. EMBO J 21, 3307-16.

Zink, D., Fischer, A.H. and Nickerson, J.A. (2004) Nuclear structure in cancer cells. Nat Rev Cancer 4, 677-87.

Zuehlke, A.D. and Johnson, J.L. (2012) Chaperoning the chaperone: a role for the co-chaperone Cpr7 in modulating Hsp90 function in Saccharomyces cerevisiae. Genetics 191, 805-14.

Chapter 6: Appendices

Table 2: Description of antibodies used

Antibody name	Species	Supplier	Catalogue number	Dilutions
Primary Antibodies				
Anti-human Lamin A-C	Rabbit	Abcam (UK)	(EPR4100)	WB: 1:1000
Anti-human Emerin	Mouse	Abcam	ab54996	WB: 1:1000
Anti-human GAPDH [EPR6256] – Loading Control (HRP)	Rabbit	Abcam	ab185059	WB: 1:1000
Anti-*Aequorea victoria* GFP (FL)	Rabbit	Santa Cruz Biotechnology	sc-8334	WB: 1:1000, IF: 1:100
Anti-HA tag (ChIP Grade)	Rabbit	Abcam	ab9110	WB: 1:1000
Anti-human Histone H3 – Nuclear Loading Control and ChIP Grade	Rabbit	Abcam	ab1791	WB: 1:10000
Anti-human Hsp90α (9D2)	Rat	Enzo Life Sciences (USA)	ADI-SPA-840-F	WB: 1:10000
Anti-human Hsp90β [5G4]	Mouse	Abcam	ab119833	WB: 1:1000
Anti-human Hsp90α/β (F-8)	Mouse	Santa Cruz Biotechnology	sc-13119	WB: 1:1000
Anti-human STIP1	Mouse	Abcam	ab56873	WB: 1:1000, IF: 1:100
Anti-human STIP1 [EPR6605]	Rabbit	Abcam	ab126724	WB: 1:1000
Anti- human αTubulin	Mouse	Abcam	Ab7291	WB: 1:1000
Secondary antibodies				
Anti-Rabbit IgG H&L (HRP)	Donkey	Abcam	ab16284	WB: 10000
Anti-Mouse IgG H&L (HRP)	Goat	Abcam	ab97023	WB: 1:5000
Anti-Mouse IgG H&L (DyLight® 550)	Donkey	Abcam	ab96876	IF: 1:500
Anti-Rabbit IgG H&L (DyLight® 488)	Donkey	Abcam	ab96891	IF: 1:500